2015

Vibration Control in High-Rise Buildings for Multi-Hazard

Srinivasa Adithya Sailesh Abburu
Louisiana State University and Agricultural and Mechanical College, saileshabburu@gmail.com

VIBRATION CONTROL IN HIGH-RISE BUILDINGS FOR MULTI-HAZARD

A Thesis

Submitted to the Graduate Faculty of the
Louisiana State University and
Agricultural and Mechanical College
in partial fulfillment of the
requirements for the degree of
Master of Science in Civil Engineering

in

The Department of Civil Engineering

by
Srinivasa Adithya Sailesh Abburu
B.Tech, Acharya Nagarjuna University, 2013
December 2015

Acknowledgments

I would never have been able to finish my dissertation without the guidance of my advisor, help from friends, and support from my family.

I would like to express my deepest gratitude to my advisor Dr. Aly Mousaad Aly, for his guidance, caring, patience, and for providing me with an excellent atmosphere for conducting research. You were there always when needed and guided me all the way till the end. I have learnt a lot of things discussing with you, which I have never dreamt off. Working with you helped me gain a lot of knowledge in high-rise buildings and vibrations in them and mitigation techniques. I would like to thank you once again for giving me the opportunity to work with you and for constantly supporting me.

I would like to express my gratitude to Dr. Steve Cai and Dr. Suresh Moorthy for their valuable suggestions and information in completing my research. I would like to thank Dr. Jim Wang and Dr. Rodney Henderson of plant, soil and environment department for helping me financially through my time at LSU.

I would also like to thank my parents, and my family for always supporting me and encouraging me in my bad and good times. Finally, my friends who was with me at all times and for being a part to my success.

Table of Contents

List of Tables

List of Figures

Abstract

Increasing population and migration of people to cities has led to the construction of high-rise buildings. High-rise buildings have received a renewed interest in many city business locations, where land is scarce, as per their economic, sustainability and other benefits. Taller and taller towers are being built everywhere in the world. However, the increased frequency of multi-hazard disasters makes it challenging to balance between a resilient and sustainable construction. As a saying, 'with new inventions come new problems'. High-rise buildings usually have issues with increased wind loads brought by, for instance, hurricanes, which can decrease their serviceability and cause failure of the structure. Although floor accelerations under wind loads are lower than those under earthquake loads, they occur for a relatively long time that raises comfort and serviceability issues. However, inter-story drifts under wind loads can raise security issues. The results presented in this thesis show that high-rise and slender buildings designed for wind may be safe under moderate earthquake loads, regarding the main force resisting system. Nevertheless, nonstructural components may present a significant percentage of loss exposure of buildings to earthquakes due to higher floor accelerations. Accordingly, the effect of earthquakes on tall buildings cannot be ignored. Damping devices are used to mitigate wind effects in tall buildings. These damping devices can also reduce the earthquake effects, but not to the full extent. In this thesis, the performance of a tuned mass damper (TMD) is studied under wind and earthquake loads (multi-hazard loading). A 76-story benchmark building is used in the analysis under multi-hazard loading. A new type of TMD called pounding tuned mass damper (PTMD) has growing importance in the reduction of earthquake effects. We adapt this PTMD for tall buildings and study its performance under multi-hazard loads, and compare it with a conventional TMD. In addition, the performance of viscous dampers in reducing earthquake effects is investigated. The

main objective of the current study was to further the understanding of the impact of multi-hazard loading, brought by wind and earthquakes, on the behavior of high-rise buildings, in order to apply such knowledge to design.

Chapter 1
Introduction

The increase in technology has led to the development of new construction materials and techniques. This made the concept of high-rise buildings possible, to meet the needs of people migrating into cities. The biggest problem with the high-rise buildings are the effects of the wind and earthquake, which can be termed multi-hazard. Both have significant effect on the safety and sustainability of the high-rise buildings. This has led to numerous studies about how wind and earthquake affects the buildings, what are the acceptable design limits, how they can be controlled to ensure durability of the structure. Before going to talk about countermeasures for this effect, in this chapter, we are going to learn about the mechanism of these multi-hazard on high-rise buildings.

Wind loads

The effect of wind on high-rise buildings differs to a great extent from small and medium structures. It is a phenomenon of great complexity due to many flow situations that occur when they interact with buildings. It is the composition of a multitude of the eddies of varying sizes and rotational characteristics carried in a general stream of air moving relative to earth's surface (Mendis et al 2007). Eddies are created by gustiness and the turbulent nature of the wind. The wind speed increases with the increase in height, while gustiness decreases. The wind vector at any point is the sum of mean wind component and the dynamic or turbulent component as expressed in equation1.

$$V(z,t) = \tilde{V}(z) + v(z,t) \qquad \text{---------- (1)}$$

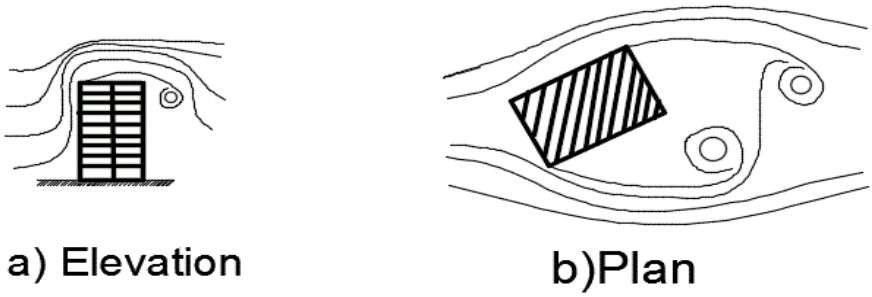

Figure 1: Generation of eddies around typical buildings

Wind-induced loadings on buildings depend dominantly on the structure of eddies as shown in Figure 1 (Mendis et al 2007), among other factors. Tall buildings under the action of wind are considered bluff bodies. Unlike a streamlined body, the bluff bodies have large regions of separated flow, large drag forces and the potential of the formation of vortex shedding. Figure 2 shows a schematic plan view of the flow around a bluff body with a rectangular section (Kim 2013).

As one can see from the Figure 2 the separated flow has an inner and outer region in which inner region has viscous effects. We have a thin free shear layer which has complex flow characteristics with high shear vorticity that separates the inner and outer regions (Holmes 2007). As seen in the Figure 2, we have a reattachment point and second separation point that could occur when the bluff body is long enough. This has an advantage as it reduces the intensity of wake formed at the lee of the body. We can also see the formation of the separation bubble between the shear layer and the body from initial point of separation and the reattachment point (Djilali 1992; Taylor et al. 2011). The wake region in the downstream has low velocity with turbulent flow

(Holmes 2007). Due to this separation and reattachment of airflow around bluff body create highly fluctuating loads called as buffeting and vortex shedding.

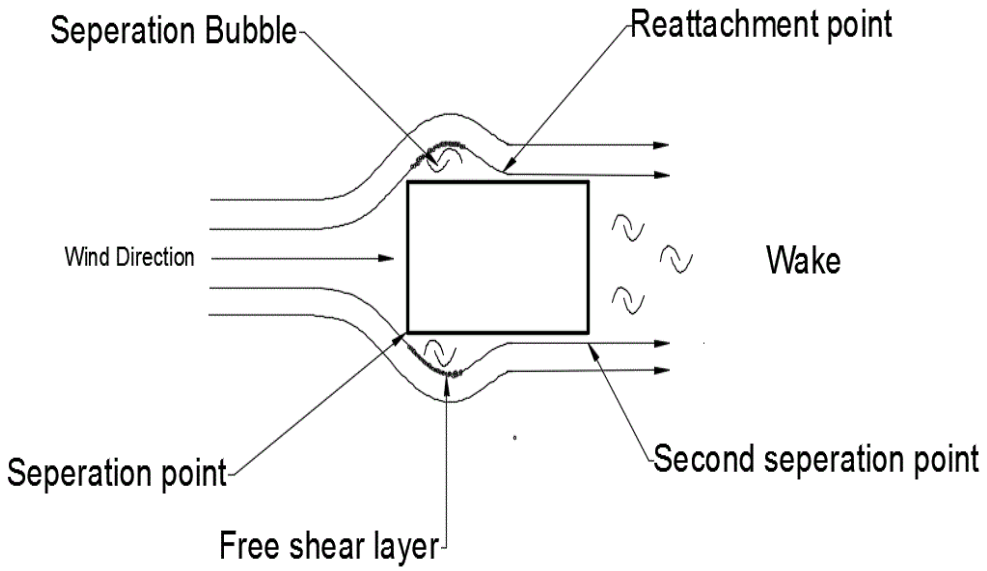

Figure 2: Schematic diagram of airflow around a bluff body

Here is a brief definition of common terminology related to the loading mechanisms on bluff bodies under wind.

Buffeting:

The gustiness or natural turbulence of the approaching flow or the atmospheric boundary layer is termed buffeting.

Vortex shedding:

The unstable flows that are generated due to separation and reattachment of flow is called vortex shedding. The response of a tall building under wind load has three components in along-wind, cross-wind and torsional directions, as shown in Figure 3 (Mendis et al 2007).

Along-wind load:

The along-wind load is generated from the net pressure fluctuations acting in the direction parallel to the main wind flow. The along-wind load is calculated by applying the quasi-static approach (Richards and Hoxey 2004), which considers fluctuating pressure on the windward face on the structure varies directly with the fluctuation of the longitudinal wind velocity upstream. Therefore, the along-wind load is considered as the sum of forces acting on the windward and leeward sides of the structure (Kim 2013). The load on the leeward face of the structure is caused by the pressure fluctuations in the wake circular region.

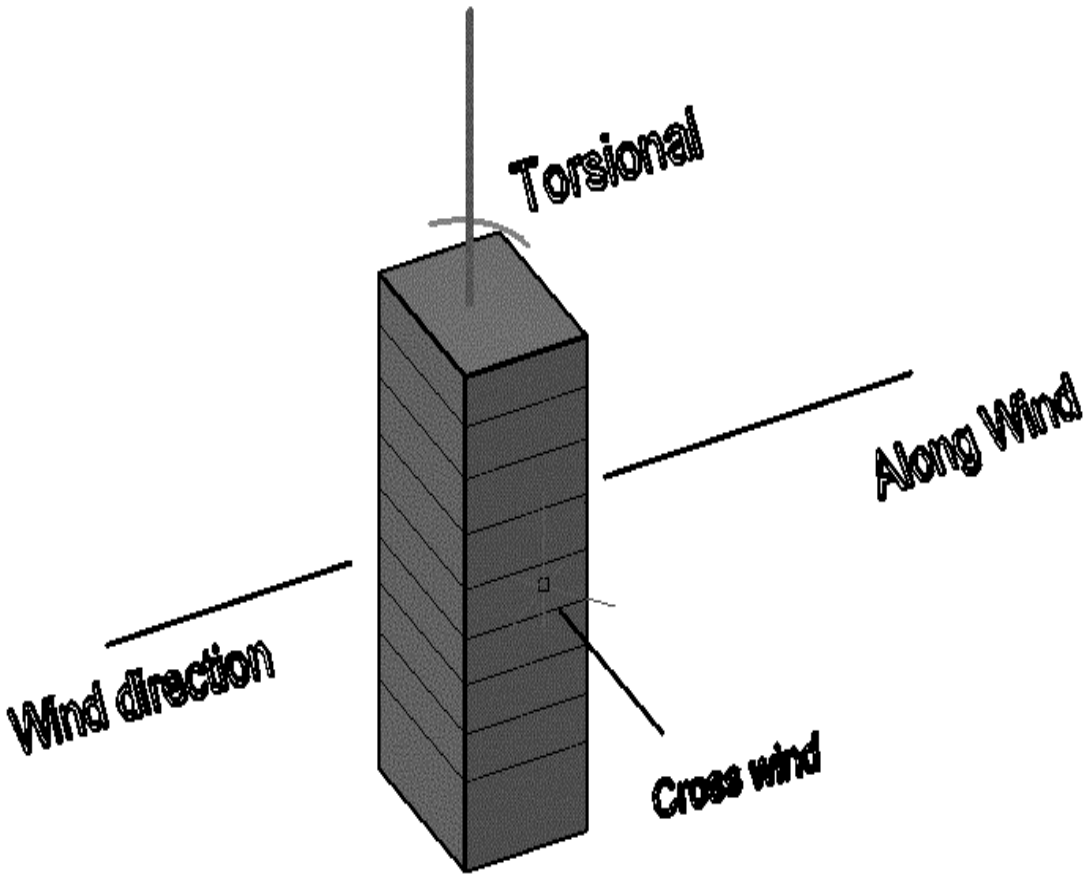

Figure 3: Components of wind loads

Cross-wind load:

The vortex shedding, which we discussed earlier is the main reason for the generation of the cross-wind load on tall structures. The frequency of these alternating forces, i.e. due to vortex shedding, can be expressed as a non-dimensional value called Strouhal number (S_t). The Stroual number can be defined by equation 2 (Simiu 1996; Holmes 2007).

$$s_t = \frac{n_s\, d}{V} \qquad \text{---------- (2)}$$

where n_s is the Strouhal frequency, or the frequency of vortex shedding, and 'd' is the characteristic length of cross-wind (plan dimension perpendicular to the direction of wind flow); '*V*' is the mean velocity of approaching flow. The forces generated by the shedding of vortices on a tall building depend dominantly on its natural frequency, shape, and turbulence in the upstream flow, among other factors (Davenport 1966). The cross-wind load can be larger than the along-wind load if the bluff body and the generated vortices are in resonance, with a potential to bring more damage to the building. In addition, aerodynamic damping could be significant, which can impact the cross-wind response (Gu et al. 2014). Consequently, cross-wind loads may be considered dominant design loads than the along-wind loads in tall buildings.

Torsional Load:

This is another component of wind forces on tall buildings which causes the twisting motion in the bluff body. This arises due to non-uniform pressure distribution around the wall faces of bluff bodies.

Wind loading prediction

A vital part of the design of modern tall buildings is the prediction of wind-induced motion and the assessment of its effects on occupant comfort. One of the primary purposes of wind engineering research is to predict wind-induced forces on structures. Wind-induced forces are dependent on the shape of the building (Gu et.al. 2013; Dragomirescu and Tun, 2014), its location, and the characteristics of the wind flow, such as, the wind speed and the wind direction angle. Traditionally, wind loading on buildings can be evaluated analytically using some codes and formulas (ASCE 7-2010 2010; Eurocode 1 2004; Kareem 1992, 1998; Zhou et al. 2003). However, these standards provide little guidance for the critical cross-wind and torsional loading. This is partially attributed to the fact that the cross-wind and torsional responses, unlike the along-wind, result mainly from the aerodynamic pressure fluctuations in the separated shear layers and the wake flow fields, which have prevented, to date, any acceptable direct analytical relation to the oncoming velocity fluctuations (NatHaz 2015). Also, these methods have limitations, especially when other tall structures exist in the vicinity of the building under consideration. Moreover, the evaluation process depends on many assumptions. To alleviate these problems, wind tunnel testing can provide a more reliable solution.

Despite recent advancements in computational fluid dynamics, wind tunnel simulation of a scaled model is still the most common tool used to predict wind loading. Wind loads may be derived through multiple point synchronous scanning of pressures or by measuring forces on the model mounted on a high frequency force balance (HFFB). High frequency force balance (HFFB) technique has been widely recognized for conveniently quantifying generalized wind forces on tall buildings (Kareem and Cermak 1979; Boggs and Peterka 1989). The generalized forces are then utilized for estimating building response with given structural characteristics. The HFFB technique

generally requires mode shape corrections which are either based on empirical corrections, or analytical formulations derived on the basis of assumed wind loading models.

The integrated pressure modal load or IPML technique has the potential of addressing all of the limitations of the conventional high-frequency force-balance technique while still maintaining the same advantages that the technique has over the aeroelastic modeling (Rosa et al 2012; Aly 2013a). Surface pressure measurement is favorable over force balance measurement as it gives the load distribution over the building surface and it cancels out the inertial effects (Zasso et. al.2008). The pressure integration technique can also be used to examine higher modes with no monotonic mode shapes. The advantage of this technique is also that a single model used in a single testing session can produce both overall structural loads and cladding loads.

Comfort criteria:

Wind-induced motions in high-rise buildings arise comfort issues. A building designer must be able to meet these comfort issues so that occupants do not have any fatigue problems. A number of studies were conducted in developing a standard criteria for comfort in tall buildings' design. The criteria concerned tall buildings that vibrate in a low frequency range of 0-1 Hz. This criteria include occupant's expectancy and orientation, visual and acoustic cues, amplitude, frequency and accelerations that the occupants are subjected. Table 1 lists some guidance with acceptable acceleration limits in tall buildings (Mendis et al 2007).

Earthquake loadings

Unlike wind, earthquake is a different phenomenon which generates a ground motion. The intensity or acceleration of the earthquake depends upon the magnitude and location of its epicenter. The seismic waves caused by the earthquake cause inertial forces in the building. The inertial forces are created when an outside force tries to move a body in rest, which happens in this

Table 1: Acceleration limits for buildings under earthquakes

Level	Acceleration limit (m/s^2)	Effect on occupants
1	<0.05	Occupants cannot feel the movement
2	0.05-0.1	a. people who are sensitive can feel the building motion b. Hanging objects may move slightly
3	0.1-0.25	a. Majority of occupants can feel the building motion b. It may affect the desk work. c. Long term exposure results in motion sickness
4	0.25-0.4	a. Desk works become difficult or almost impossible b. Ambulation still possible
5	0.4-0.5	a. Occupants perceive strong motion b. It gets difficult to walk and people may lose balance
6	0.5-0.6	Most people cannot tolerate motion and are unable to walk naturally
7	0.6-0.7	People cannot walk and tolerate motion
8	>0.85	Things begin to fall and people may get injured.

case as seismic waves tries the move the building in rest. When a building is subjected to inertial forces it should obey the Newton's second law of motion as follows,

$$F = M.a \qquad \text{---------- (3)}$$

where ‘F’ is inertial force and ‘M’ denotes mass of the building and ‘a’ is the acceleration with which the building is moved due to seismic activity.

Duration, velocity and displacement:

From the newton’s second law, it is evident that acceleration is a key factor in determining the forces on a building. But there is one more criteria that we have to look into is the duration of the earthquake. Earthquake that has moderate acceleration, sustained over time, can cause much more damage to buildings than a single much larger peak. It weakens the building structure and reduces its durability. The strong-motion duration is often termed as “bracketed duration” (Arnold 2013). This is the shaking duration above a certain threshold acceleration value, which is 0.05g, and is defined as the time between the first and last peaks of motion that exceeds this threshold value (Arnold 2013). The strong motion in Northridge and Loma Prieta earthquake lasted for about 10 seconds and in San Francisco earthquake, it lasted about 45 s (Arnold 2013).

In addition to the duration two other measures of wave motion (velocity, displacement) are related to the acceleration and can be measured mathematically. Velocity refers to the rate of motion of the seismic waves as they travel through the earth. There are two kinds of waves caused by seismic activity called S-waves and P-waves in the earth which travel very fast. The P-waves travels at a velocity of 3000m/s to 8000m/s and S wave which is slow compered to P-waves travels at a velocity of 2000m/s to 5000m/s (Arnold 2013). The velocity of motion on the ground is very less compared to the velocity of waves inside the earth. The velocity varies from 0.02 m/s to 0.6 m/s (Arnold 2013). Another measure of wave motion is displacement, defined as the distance that points on the ground are moved from their initial locations by the waves. The displacement varies

with the distance of the points from the epicenter. Let us consider in the case of Northridge earthquake where a parking structure 29 km from the epicenter recorded a displacement of 0.04 at the roof at an acceleration of 4.6 m/s^2 and Olive View Hospital, 12 km from the epicenter recorded a roof displacement of 0.34 m at an acceleration of 14.7 m/s^2 (Arnold 2013). We can see that with the increase in distance from the epicenter the effect of earthquake decreases.

In earthquakes, the values of ground acceleration, velocity and displacement vary with the frequency of the wave motion. In high frequency waves (>10 Hz) the acceleration amplitudes are high and displacement amplitudes are small and vice versa for low-frequency waves.

Natural frequency:

It is the important characteristic of earthquake waves which is used for determining seismic forces. It is defined as no of cycles of seismic wave that will occur in a second and is measured in Hz. All the objects have natural frequency and when the natural frequency of seismic waves matches with that of the natural frequency of building, resonance occurs and causes maximum damage to the building. The Period of ground motion ranges from 0.5 s (rock) to 2.5 s (soft soil) depending upon the soil conditions. In the same way buildings also possess a fundamental dynamic response frequency which is usually considered as 0.1 s time's number of stories. This implies that a 76 story building has a fundamental period of vibration of 7.6 s and for buildings of medium story say 20 have 2.5 fundamental period. As we already know that damage is caused when building and ground vibrates in resonance. Therefore, as we said earlier, if ground shakes between fundamental periods of 0.5 s to 2.5 s, buildings ranging from 5-25 story range has greater damage and tall buildings falls out of this range or effected only little when compared to the wind loads.

Even though the effect of earthquake seems to be low on tall buildings they vibrate under inertia loads under ground motion which cause excessive stresses in weak walls, columns, beams and joints which damaged the building to a greater extent. Also taller buildings tend to shake longer than short buildings. As they are built to withstand the wind loads and precautions are taken to increase the damping which may make them deform less under earthquakes (Ammon 2015). Compared to windstorm disasters, the mortality in earthquakes is relatively high owed to the difficulty in predicting the event over a time sufficient for evacuation (Geller et al., 1997; Kanamori et al, 1997). The California quakes of 1971, San Fernando, the1989 Loma Prieta, and the 1994, Northridge are the 6th, 9th, and 10th most deadly events (Vranesand and Pielke, 2009). According to Vranes and Pielke (2009), the 1906 San Francisco earthquake and fire adjusts to $39–$328 billion is likely the most costly natural disaster in U.S. history in normalized 2005 values.

Earthquake loading prediction

Designing structures to withstand earthquakes is expensive. The choice of building design is a compromise between appearances, function, structure, strength and cost. Standards are established through building codes, which regulate the design and construction of buildings (ex. Eurocode 8 2003: ASCE 7-2010). The building codes are designed to protect the occupants first, and then the building integrity.

They are usually drafted to meet the demands of the expected shaking in a given region that are summarized by seismologists and earthquake engineers in hazard maps. These maps are constructed by examining

- The earthquake history of the region to estimate the probability of an earthquake.
- The expected shaking intensity (Peak acceleration) produced by the earthquake.

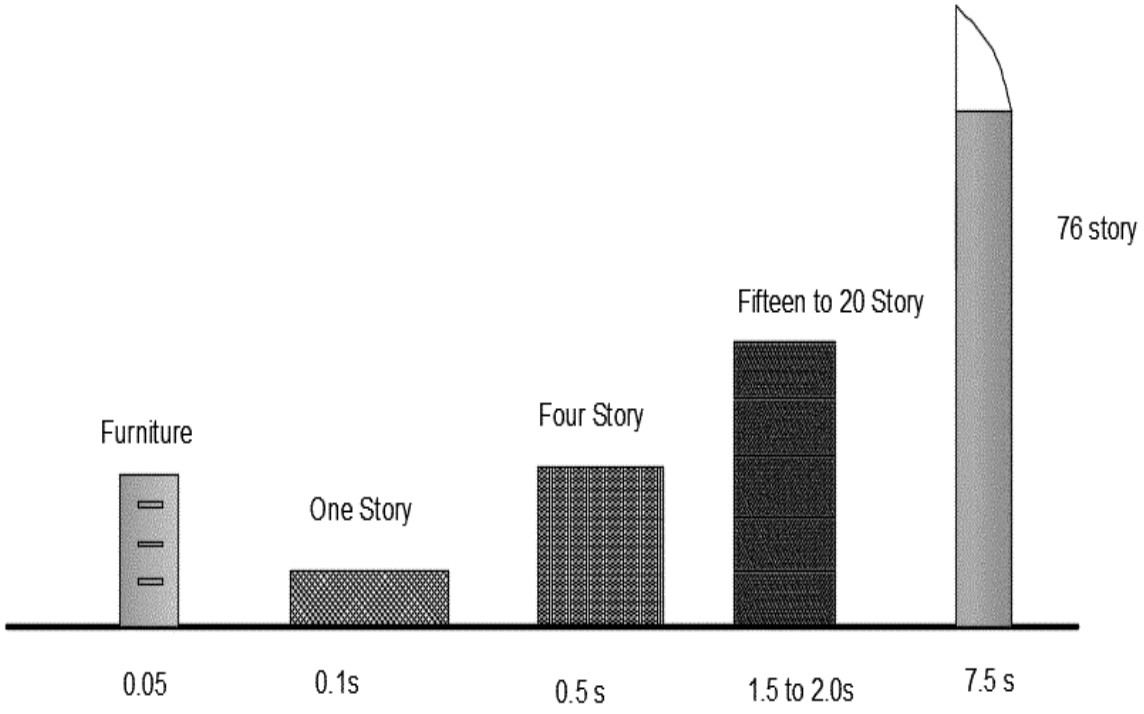

Figure 4: Approximate fundamental periods of buildings with height (Arnold 2013)

- The frequency of the shaking, the distance from the fault as discussed earlier.
- The regional geology and site conditions.

Earthquakes occurrence can be predicted through electromagnetic emissions before few days to a few hours. According to Koulouras et al. (2009), laboratory studies show that electromagnetic emissions in a wide frequency spectrum from kilohertz (kHz) to very high megahertz (MHz) frequencies are produced by the opening of micro cracks, with the MHz radiation appearing earlier than the kHz radiation. As earthquakes occur due to large-scale fractures in the earth crust, the radiated kHz-MHz electromagnetic emissions can be detectable at the geological scale. A technique using this phenomena in Greece is discussed by Koulouras et al. (2009).

Chapter 2
Dampers

With the technology, comes the problems which need solutions. The increase in construction of high-rise Buildings has led to many researches, on how to mitigate the vibration caused by dynamic loads (wind or seismic) on them. The research has resulted in many dynamic vibration absorbers (DVA) typically called as dampers which can be used to counter the dynamic vibration and keep the structure stable.

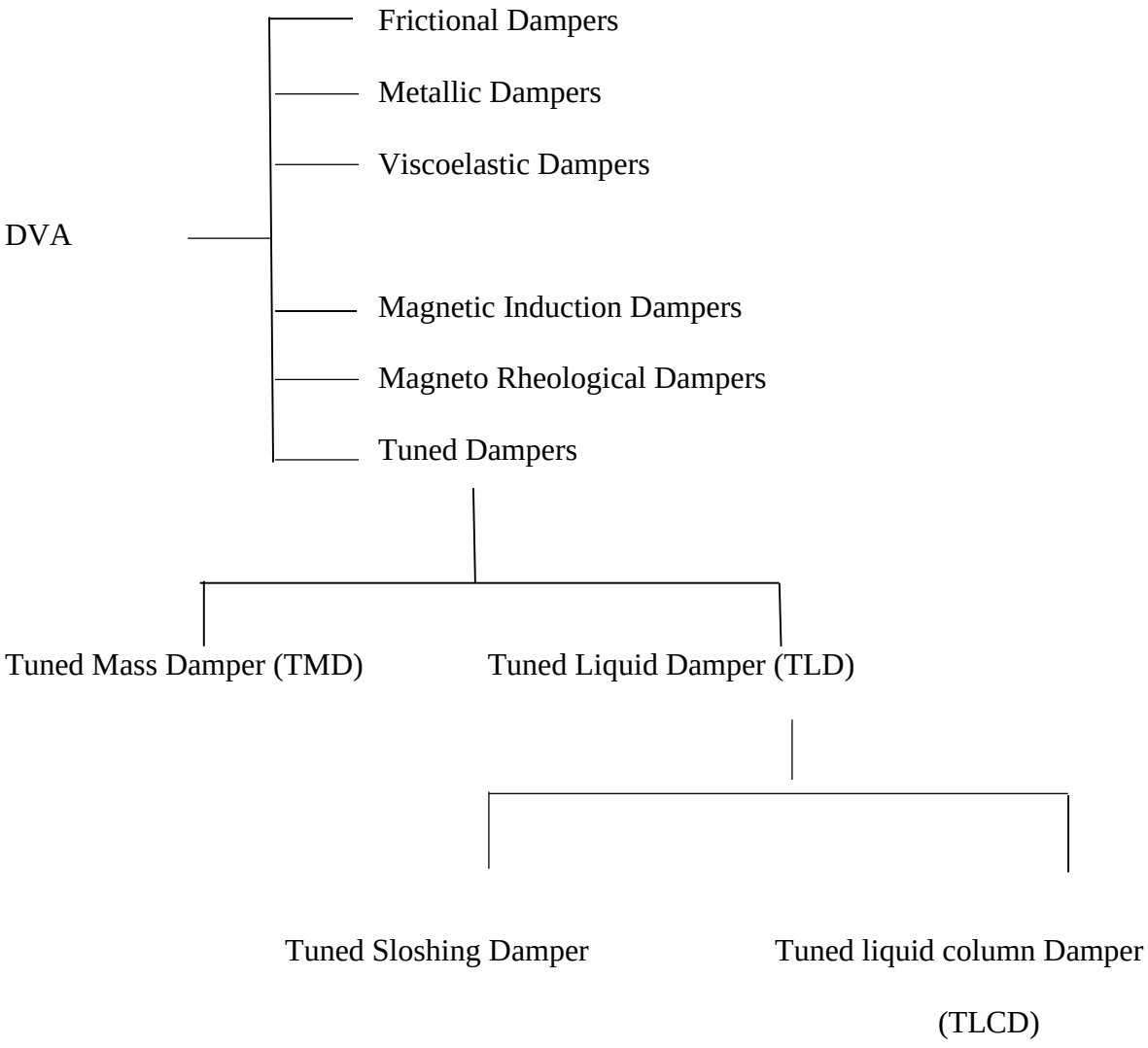

Of all the dampers tuned mass dampers (TMD) are most effective and are most used dampers. Using the same principle as of TMD tuned liquid dampers (TLD) are developed which

uses liquid (i.e. water….) instead of a mass in TMD. In this chapter we talk about the working principle of the TMD and the factors affecting its performance.

Tuned mass damper (TMD)

It is a passive device which utilizes a secondary mass attached to a main structure through spring and dashpot. The secondary mass system has a natural frequency of the primary structure which depends on the mass and stiffness (Yao 1972; Aly 2014a, 2014b; Rezaee and Aly 2015).

Concept:

When the structure is excited the excess energy developed in the structure is transferred to the secondary mass and is dissipated by the TMD. By knowing the mass ratio of the secondary mass to the structure mass, the frequency ratio between two masses the optimum damping ratio of secondary mass can be obtained.

The equation of motion of the TMD system is expressed as follows,

$$m_2\ddot{x}_2 + c_2(\dot{x}_2 - \dot{x}_1) + k_2(x_2 - x_1) = 0 \qquad \text{---------- (4)}$$

$$m_1\ddot{x}_1 + c_1(\dot{x}_1) + c_2(\dot{x}_1 - \dot{x}_2) + k_1(x_1) + k_2(x_1 - x_2) = f \qquad \text{---------- (5)}$$

In equation 5 the attached TMD increases the damping and stiffness of the combined system and reduces the vibration.

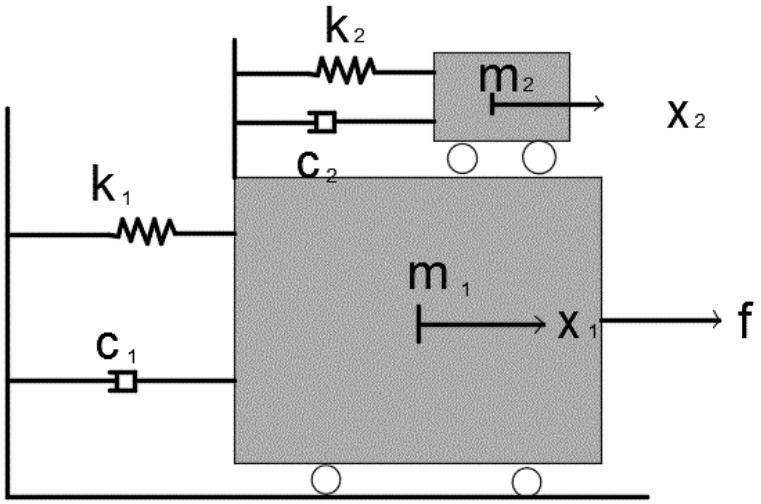

Figure 5: Schematic diagram of TMD

Factors affecting the performance of a TMD

For performing any analysis or for calculating the effectiveness of damping by TMD we should first model it. The parameters of the TMD that affect the structural response and damping are:

Mass ratio

$$\mu = \frac{m_A}{M^*} \quad \text{---------- (6)}$$

Where $\mathbf{m_A}$= absorber mass; $\mathbf{M}^*$ =generalized mass of the primary structure corresponding to the vibration mode being suppressed. The mass ratio is a key parameter that does affect significantly the performance of the TMD. Figure 6 shows the effect of increasing the mass ratio from 0.25% to 5% on the normalized displacement and acceleration responses of the primary structure, under

wind and earthquake excisions, for different optimization objectives. The normalized response is defined as follows:

$$\text{Normalized response} = \frac{\text{response with TMD}}{\text{response without TMD}}$$

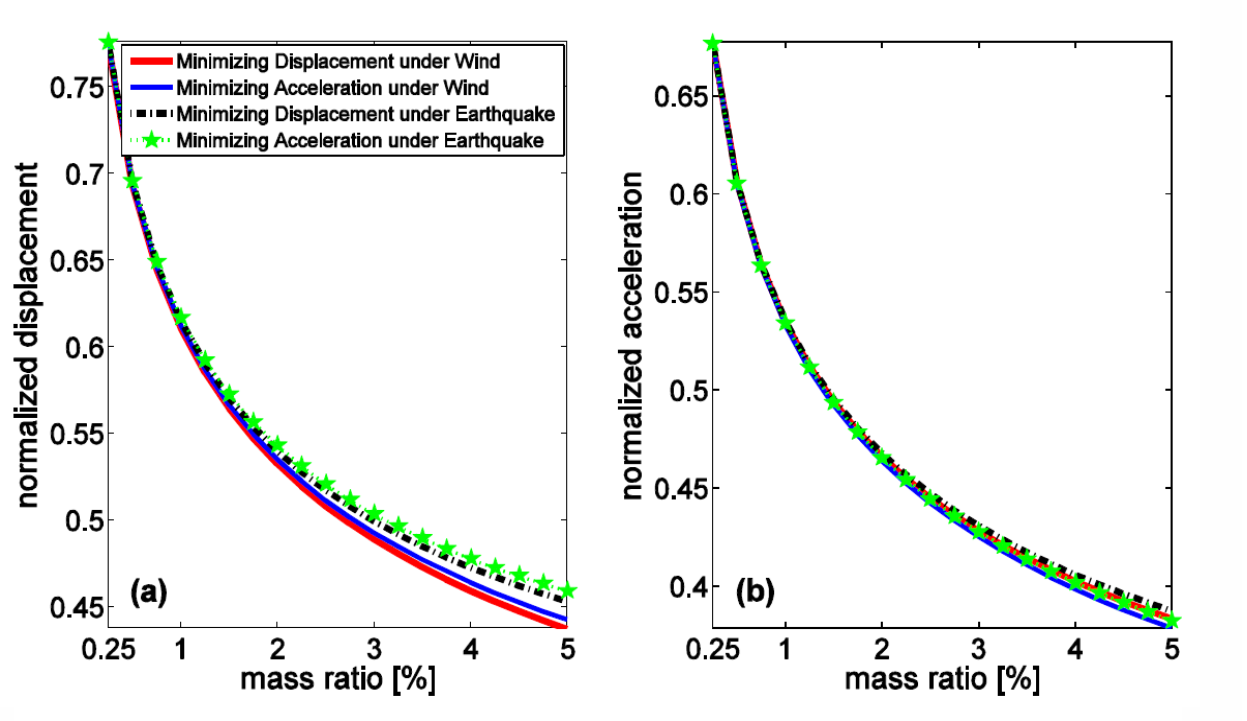

Figure 6: Building and TMD normalized displacement and acceleration as a function of the TMD‟s mass ratio: (a) building displacement, (b) building acceleration (Aly 2014a, 2014b)

Figure 6 presents the results when the optimization was carried out based on minimization of displacement and acceleration under wind and earthquake input excitations. The main difference between the wind and the earthquake input excitations is that the latter causes inertial loads on both the primary structure and the TMD (base excitation) while the wind load is considered external white-noise acting on the primary structure (force excitation). For a certain primary structure under earthquake or wind excitation, one can obtain the uncontrolled displacement and acceleration response (without the TMD), then from Figure 6 according to the required reduction

in the displacement and/or the acceleration response, the required mass ratio of the TMD can be estimated (Aly, 2014).

Tuning frequency ratio

The ratio of frequency of secondary mass to structural natural frequency is called the tuning ratio.

$$\Omega = \frac{f_{tmd}}{f_s} \quad \text{---------- (7)}$$

Where f_{tmd} = natural frequency of TMD and f_s = natural frequency of the generalized primary structure in the mode that the dynamic motions are to be suppressed (Tait et al 2008).

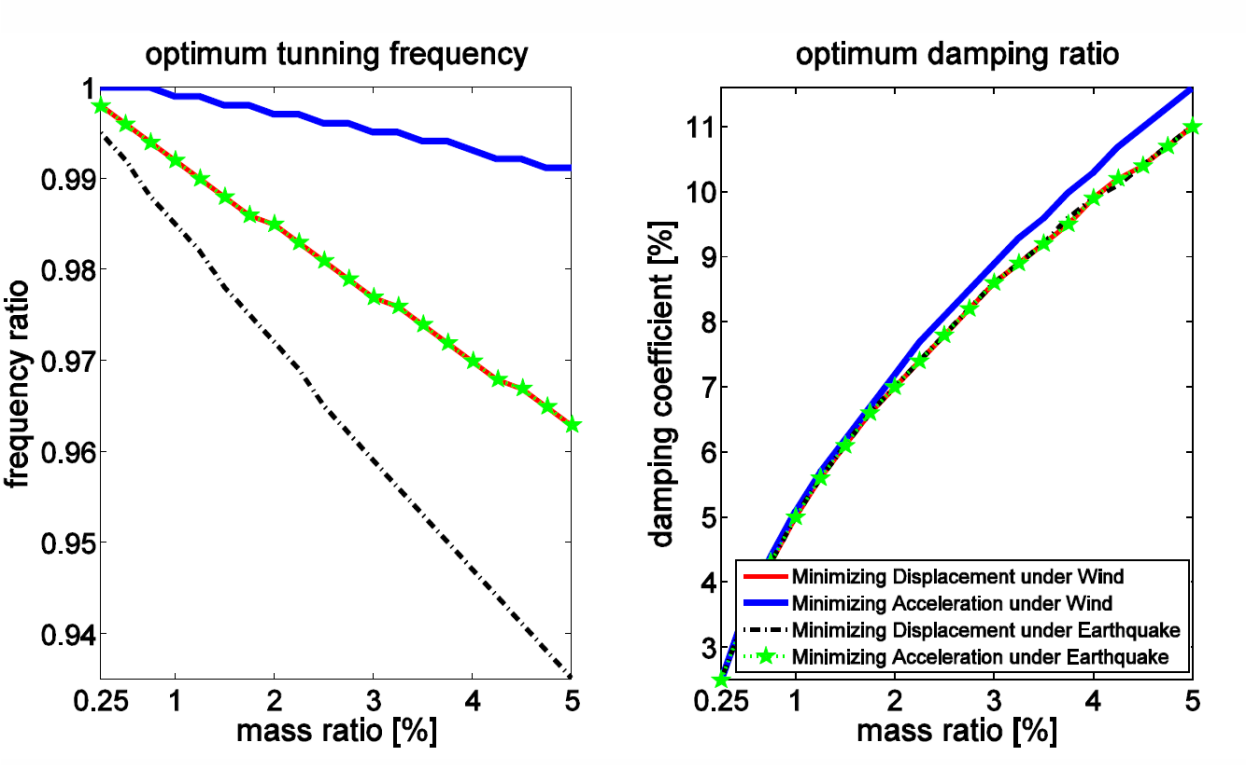

Figure 7: Optimal frequency ratio and damping coefficient of the TMD as functions of the mass ratio (Aly, 2014a, 2014b).

Figure 7 can be used to obtain the optimal tuning frequency and the damping ratio of the TMD for a certain mass ratio (Aly 2014a, 2014b).

Damping ratio

Performance of TMD in vibration mitigation is quite sensitive to the damping ratio of the TMD. TMD splits the natural frequency of primary structure into a lower and higher frequency. If the damping is too low, then resonance occurs at the two undamped resonant frequencies of the combined system (Saidi et al. 2011). If the damping is too large, the mass block may be locked and the TMD may lose the ability to absorb energy. The damping ratio is given by

$$\xi = \frac{c}{2m\omega_n} \quad \text{---------- (8)}$$

and optimal damping ratio is given by

$$\xi_{opt} = \sqrt{\frac{3\mu}{8(1+\mu)}} \quad \text{---------- (9)}$$

Where μ is the mass ratio as described earlier.

During the last several decades, many other types of dampers have also been introduced to replace the viscous dampers, such as friction dampers (Farshi and Assadi 2011; Lin et al. 2012) and MR dampers (Weber and Maslanka 2012; Zemp et al. 2011). Some dampers even demand continual maintenance (Collette 1998), which may be unrealistic because of the transmission tower's remoteness. Another drawback of the TMD is its ineffectiveness during strong earthquakes. Because of the limitation in the installation space in real engineering structures, the TMD may get into a nonlinear phase or collide with the boundary under over intensive loads. Yan et al. (2010) extensively investigated this phenomenon and found out that the TMD is not effective if its impact parameters are not reasonably designed.

Pounding TMD

In recent years Pounding TMD has gained popularity over conventional TMD in reducing the accelerations produced by seismic activity. Most of the studies using Pounding TMD are done for reducing earthquake effects in power transmission towers. One such study is done by Zhang et al. (2013). By taking these results into consideration, it is adapted to high-rise buildings in this study to check its efficiency under multi-hazard.

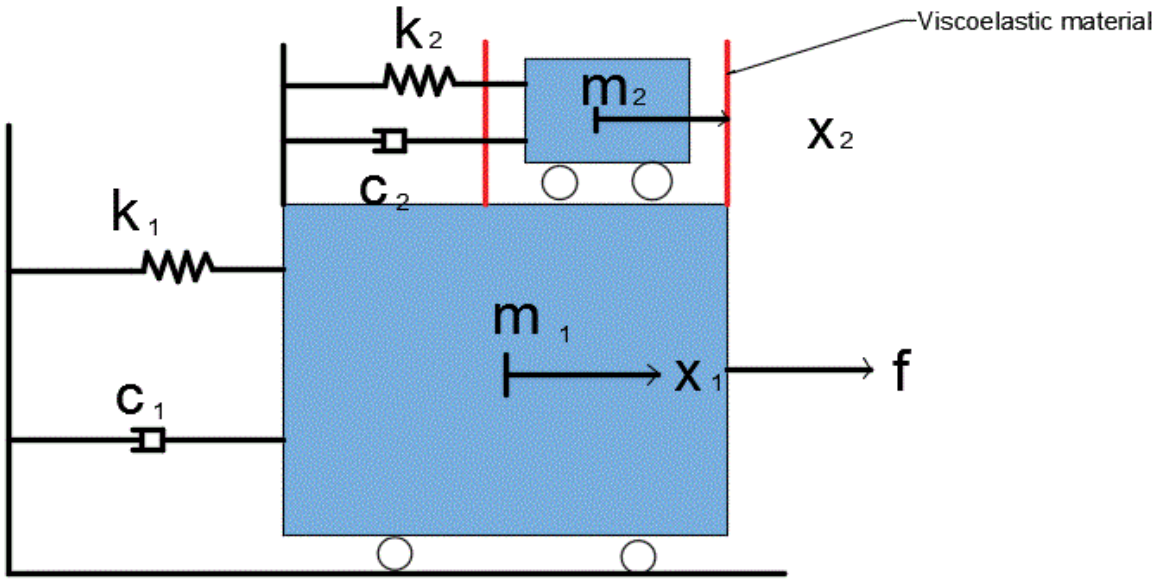

Figure 8: Schematic diagram of PTM

A PTMD is similar to a traditional TMD, but the movement is constrained by using viscoelastic damping material. The major difference between a PTMD and TMD is the additional motion limitation collar lined with viscoelastic (VE) material on the inner rim as shown in Figure 10 (Zhang et al 2013). The working principle of a PTMD is, that the vibration amplitude of the structure is reduced by transferring momentum between structure and added mass of the PTMD. Then the absorbed mechanical energy is dissipated as heat energy when impact occurs between

the constrained mass and the viscoelastic damping material (Zhang et al 2013). The dynamic characteristics of the TMD, such as stroke, the amount of added mass and damping properties of viscoelastic material determines the effectiveness of PTMD.

The determination of the pounding force of the PTMD is of major concern. In recent years, many studies were conducted and many models were used to determine the pounding force. The linear spring model (Maison and Kasai 1990, 1992; Kasai et al 1990) was used to find the pounding force during impact.

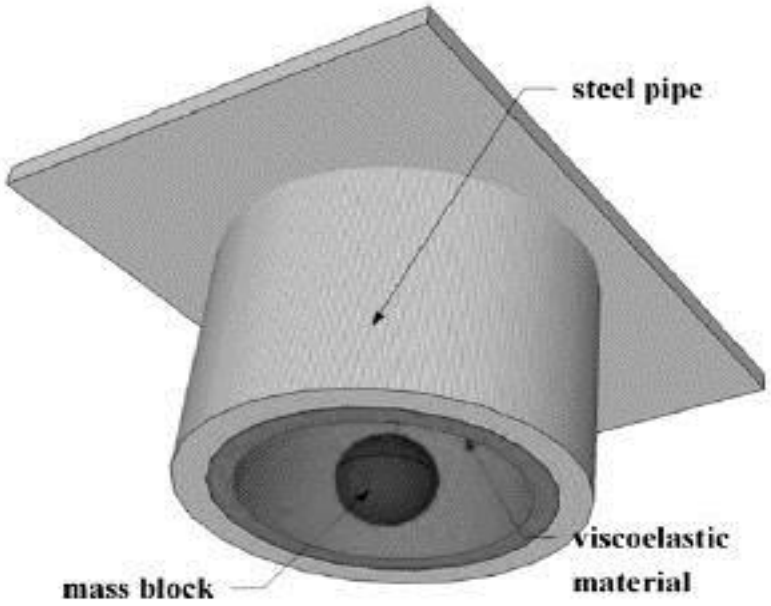

Figure 9 : 3d view of PTMD

Another model called Kelvin model combined linear spring with a damper (Wolf and Skrikerud 1980). The main drawback of these models was they cannot describe pounding as a highly nonlinear phenomenon. Recently a nonlinear spring model based on Hertz contact law has addressed the issues that other models can't. The Hertz contact law is a representative of elastic impact, but excludes the energy dissipation during impact (Zhang et al 2013). This Hertz law was

used by Zhang et al. (2013) for finding the pounding force of PTMD in his studies for transmission tower. The pounding force, according to Hertz law is given by equation 10.

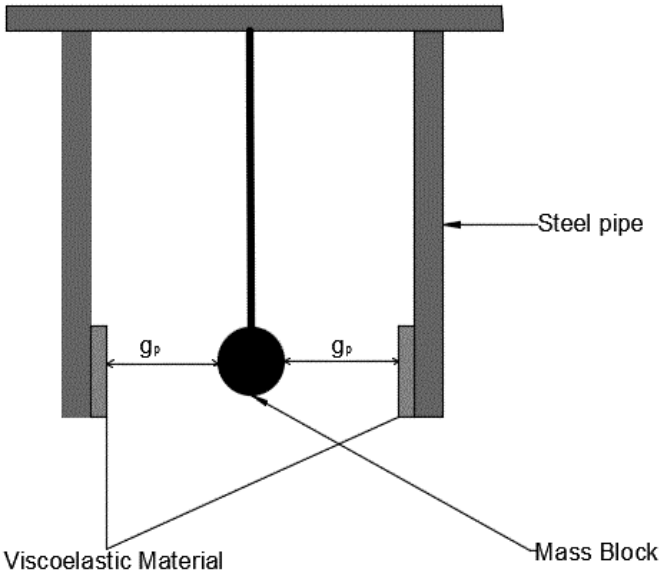

Figure 10: Cross section of PTMD

$$F=\begin{cases}\beta(x_1-x_2-g_p)^{3/2}+c(\dot{x}_1-\dot{x}_2) & x_1-x_2-g_p>0 \ \ and \quad \dot{x}_1-\dot{x}_2>0\\ \beta(x_1-x_2-g_p)^{3/2} & x_1-x_2-g_p>0 \ \ and \quad \dot{x}_1-\dot{x}_2<0\\ 0 & x_1-x_2-g_p<0\end{cases} \quad \text{----- (10)}$$

Where $x_1 \ and \ x_2$ = the displacements of the pounding motion limiting collar and the mass block and g_p is the gap between them. There fore $x_1-x_2-g_p$ represents the relative pounding deformation; $\dot{x}_1-\dot{x}_2$ denotes the relative velocity and β the pounding stiffness coefficient, which mainly depends on material properties and geometry of colliding bodies. The impact damping 'c' is not constant as the VE material is highly nonlinear and it depends on the pounding stiffness and the deformation of the VE layer (Zhang et al 2013). As proposed by Zhang et al. (2013) at any instant of time damping 'c' is given by equation 11.

$$c=2\xi\sqrt{\beta\sqrt{x_1-x_2-g_p}}\,\frac{m_1m_2}{m_1+m_2} \quad \text{---------- (11)}$$

Where $m_1, m_2$the masses of the two colliding bodies and ξ is the impact damping ratio and is given by equation 7.

$$\xi = \frac{9\sqrt{5}}{2}\frac{1-e^2}{e[e(9\pi-16)+16]} \quad \text{---------- (12)}$$

It is correlated with the coefficient of restitution *e.* It is defined as a relationship between the post impact relative velocity $\dot{x}_1{}^f - \dot{x}_2{}^f$, and the prior-impact relative velocity $\dot{x}_1{}^0 - \dot{x}_2{}^0$, of two colliding bodies (Zhang et al 2013).

$$e = \frac{\dot{x}_1{}^f - \dot{x}_2{}^f}{\dot{x}_1{}^0 - \dot{x}_2{}^0} \quad \text{---------- (13)}$$

The 'e' value can also be determined experimentally by dropping a sphere on a massive plane plate and noting the rebound height (Zhang et al 2013). It is calculated from equation 14.

$$\text{e} = \sqrt{\frac{h^f}{h^0}} \quad \text{----------} \quad (14)$$

Where h^f and h^0 are the rebound and the initial height of the ball being dropped. When *e*=1 denotes a fully elastic collision and *e=0* implies for a perfectly plastic impact. The pounding stiffness **β** is determined using the least mean square method in a small-scale experiment (Zhang et al 2013). The simulated and experimental results of the pounding force resulted nearly same. Equation of motion of the PTMD and High-rise building can be expressed similarly to the PTMD-tower system in (Zhang et al 2013).

$$M\ddot{x}(t) + C\dot{x}(t) + Kx(t) = -M\Lambda\ddot{x}_g(t) + H\Gamma F(t) \quad \text{---------- (15)}$$

Where $\ddot{x}(t)$, $\dot{x}(t)$ and $x(t)$ are acceleration, velocity and displacement of the High-rise buildings of the PTMD and $\ddot{x}_g(t)$ is the ground acceleration. F (t) is the pounding force calculated and M, C

and K are the mass, damping and stiffness matrices. In equation 15 Λ is a column vector of ones Γ denotes the location of pounding force and H is defined to determine the direction of pounding force (Zhang et al 2013).

Factors effecting the performance of PTMD

The key factors that govern in obtaining an efficient PTMD are pounding stiffness (**β**), the gap between the mass block and the VE material (g_p), and the mass ratio.

Pounding stiffness:

It is the key parameter for determining the pounding force and it mainly depends on the material properties and geometry of the colliding bodies. (Zhang et al 2013).

Gap:

The main function of PTMD is to absorb the kinetic energy of the building and dissipate this during impact. The gap between the mass block and the VE material will influence the PTMD's performance both in absorbing and dissipating (Zhang et al 2013). When the ground acceleration is very high the TMD and the building oscillate more and increases.

Mass ratio:

Increasing the mass ratio can improve the reduction performance, but there is an economic mass ratio, beyond which adding more mass can only slightly improve performance (Zhang et al 2013). In the TMD design, 1–2 % (Saidi et al. 2011) is recommended as the mass ratio. This value can also be used for the PTMD.

Chapter 3
An Application Example of High-Rise Building

A 76-story benchmark building is adopted in this study to test the performance of TMD under multi-hazard. The building is an office tower proposed for the city of Melbourne, Australia which has a height of 306m. The plan of the building is square with two cut corners and has a height-to-width ratio of 7.3 (Kim and Adeli 2005) as shown in Figure 11. The building is a reinforced concrete structure having a concrete core and an exterior concrete frame. The ground floor is 10m high and stories 38-40 and 74-76 have a height of 4.5m (Kim and Adeli 2005). All the other stories have a typical height of 3.5m. The total mass of the building is 153000t including the heavy machinery.

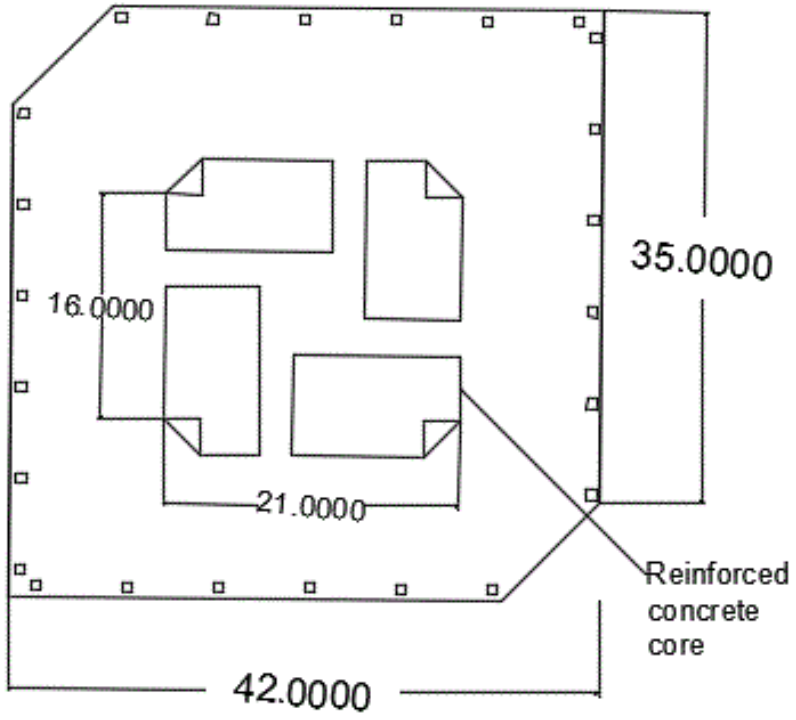

Figure 11: Plan view of the 76-story building

Wind loading

The structural analysis is performed in two dimensions based on the symmetric nature of the building and the first three natural frequencies of the structure based on these analyses are 0.16, 0.77 and 1.99HZ. The corresponding mode shapes for the first three natural frequencies are shown in Figure 12.

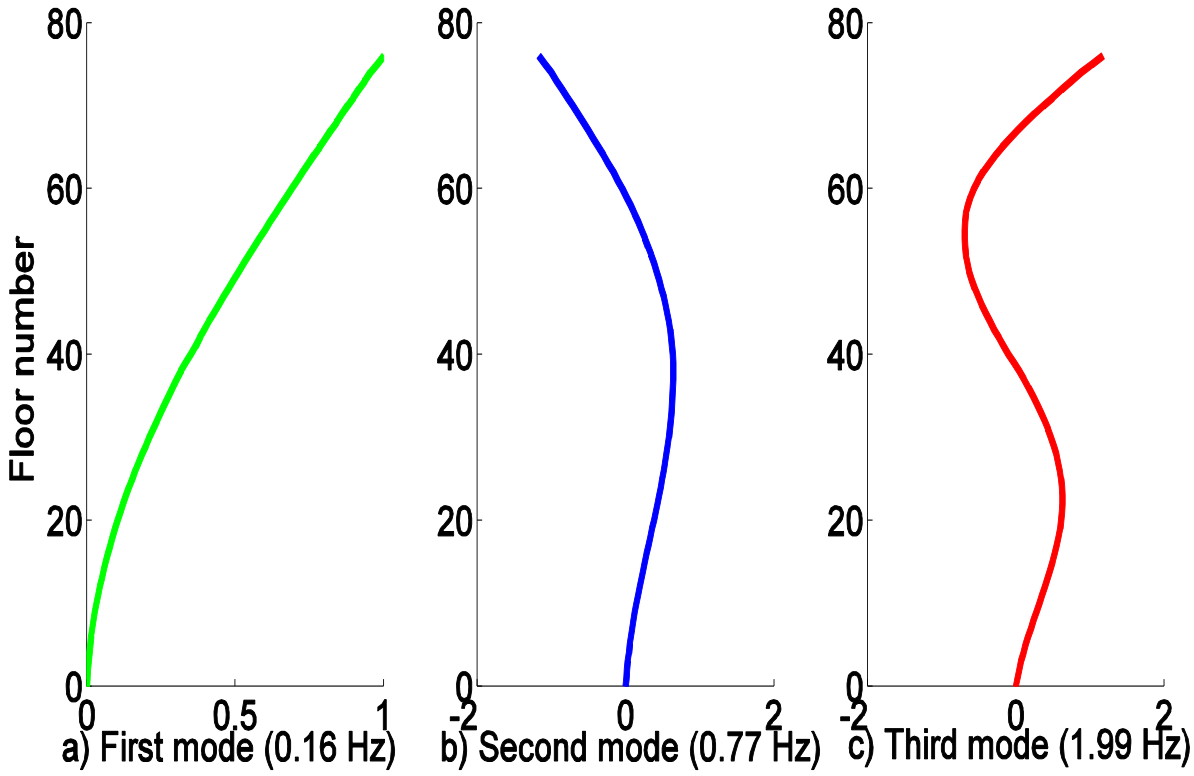

Figure 12: Mode shapes of 76-story building

The wind data is obtained from the wind tunnel tests to evaluate the effectiveness of various control systems against the wind. The obtained wind tunnel tests data is from a building model scale of 1:400 and a velocity scale of 1:39 (Yang et al 2004). A total of 3600s of wind data obtained 900s (15min) of this data is used in research. Figure 13shows the time histories of wind loads for full 3600s.

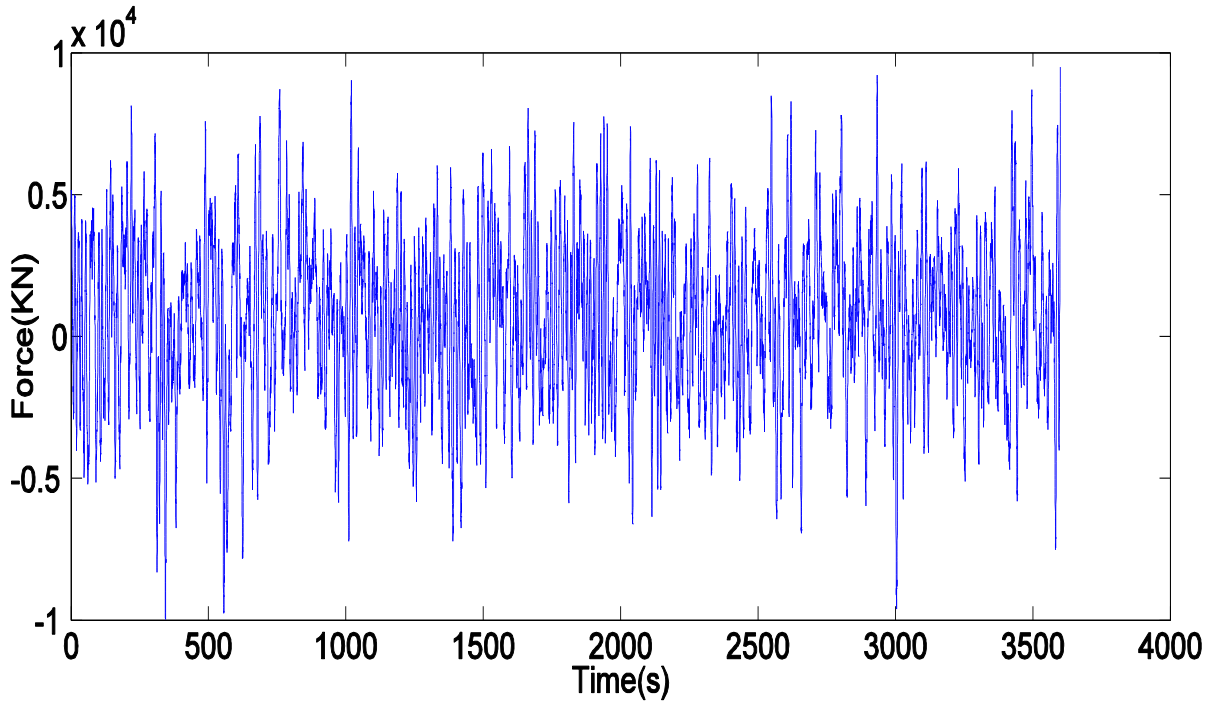

Figure 13: Time history of wind load

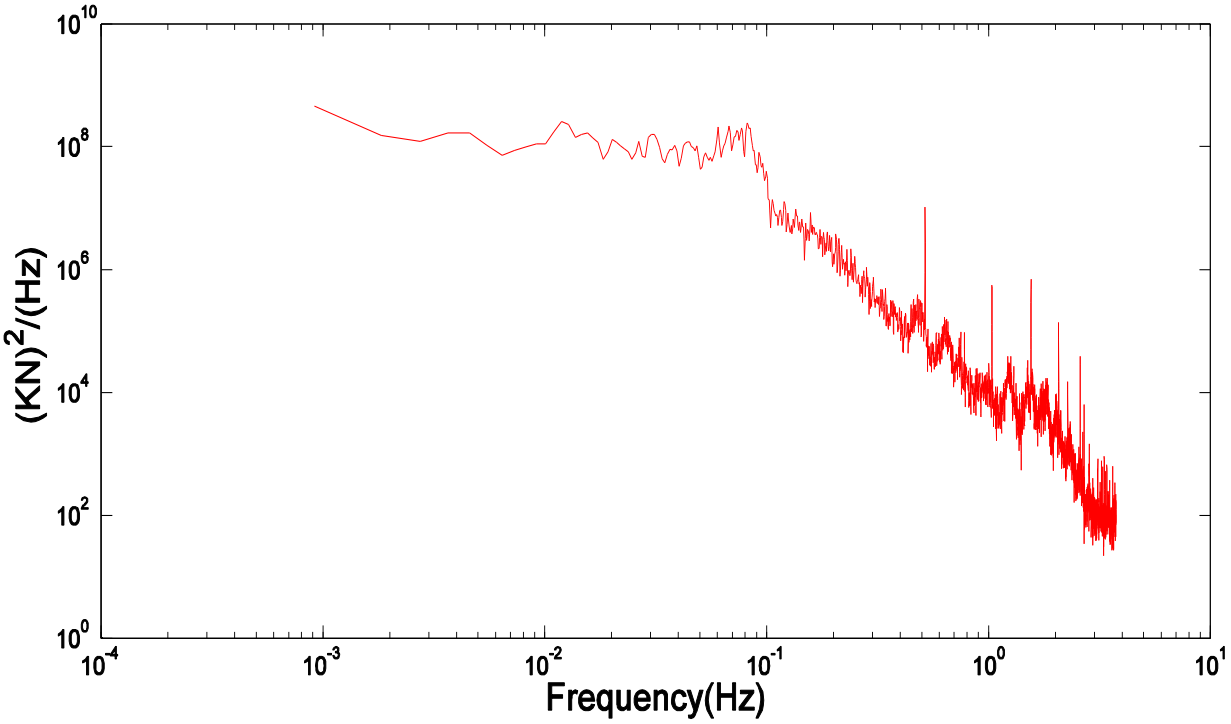

Figure 14: Spectrum of wind load

Earthquake loading

El Centro earthquake occurred in 1940 in the Imperial Valley in southern California, which has a moment (Richter) magnitude of 6.9 when measured by the Mercalli intensity scale. It resulted in the death of 9 people and damaged almost 80% of the buildings to some degree. It was the first major earthquake recorded by a strong-motion seismograph located next to fault rupture. The data of this earthquake is taken for this study. Figure 15 shows the time history and spectrum of the earthquake data obtained.

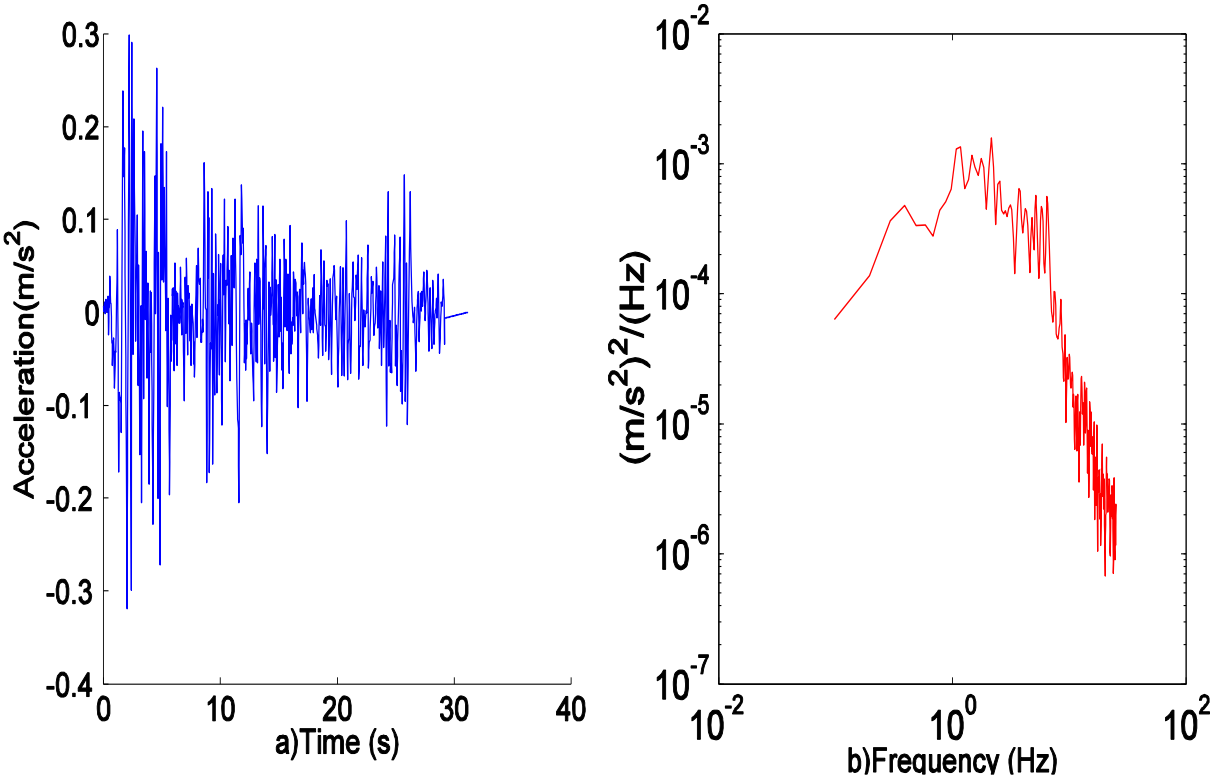

Figure 15: a) Time history and b) spectrum of earthquake acceleration

Chapter 4
Responses of High-Rise Building under Multi-Hazard

As mentioned in Chapter 2, of all the damping devices, TMD is most efficient device. So in this research the performance of TMD against wind and earthquake loads is studied. The mass (m) of the TMD is taken as 500tons and damping ratio (n) is as 0.20. Assuming the building and TMD, in resonance tuning frequency is taken as 1.0. The following equations are used for calculating the stiffness and damping of the TMD.

$$\omega\,(frequency\,) = Tuning\ frequecy * (2\pi f) \text{ --------- (16)}$$

$$k = m\omega^2 \text{ (Stiffness of the TMD) ---------- (17)}$$

$$c = 2m\omega n \text{ (Damping of the TMD) ---------- (18)}$$

The TMD is placed on the top of the building as shown in
Figure 16. The mass, stiffness and damping matrices are adapted accordingly with equations 19, 20 and 21 due to the addition of TMD

$$M77 = \begin{bmatrix} M76 & 0 \\ 0 & m \end{bmatrix} \text{ (`}m\text{' Mass of TMD) -------- (19)}$$

Stiffness matrix

$$K77 = \begin{bmatrix} K76 & -k \\ -k & k \end{bmatrix} \text{ (`}k\text{' Stiffness of TMD) -------- (20)}$$

Damping matrix

$$C77 = \begin{bmatrix} C76 & -c \\ -c & c \end{bmatrix} \text{ (`}c\text{' Damping of TMD) --------- (21)}$$

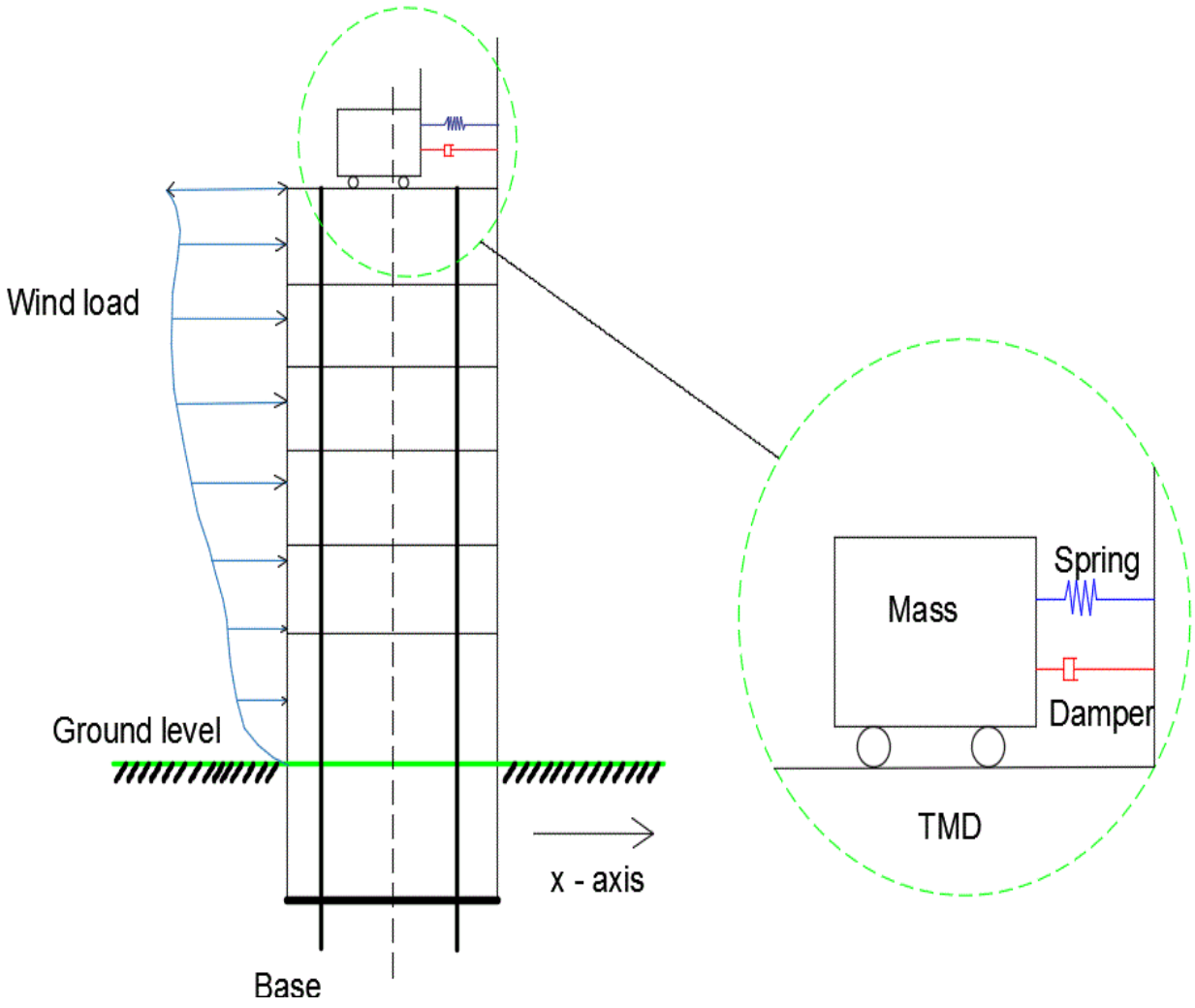

Figure 16: Building with TMD on Top floor

Where M76, K76, C76 are respectively the mass, stiffness and damping matrices of the 76- story building. After assembling the matrices a Simulink model is developed using the state space equations.

Modeling in state space

The engineering systems in recent year's trend to greater complexity, due to complex tasks and requirements of good accuracy. Today the complex systems have multiple inputs and multiple

outputs and sometimes may be time varying like our system. As to meet these requirements and with the availability of large scale computers, modern control theory, which is a new approach to the analysis and design of complex control systems was developed. It is based on the concept of the state which has been in existence in the field of classical dynamics (Ogata 2010).

The difference between the modern control theory with that of the conventional control theory is the former is applicable to multiple-input, multiple-output systems (Ogata 2010). They may be linear, non-linear and can be time varying or not. But the conventional control systems are applicable to only linear time-invariant single-input and output systems (Ogata 2010). Modern control theory is both time-domain and frequency-domain approach. Before we proceed further we need to know the following:

State:

In a dynamic system a state is the smallest set of variables (called as state variables) such that knowledge of these variables at t=t_0, together with knowledge of the input for t $\geq t_0$, completely determines the behavior of the system for any time t $\geq t_0$ (Ogata 2010). This concept of state can be applied to physical, biological, social, economic and other systems.

State variables:

The smallest set of variables that determine the state of dynamic system are termed as state variables (Ogata 2010). For example, if n variables $x_1, \ldots \ldots x_n$ are needed to describe the behavior of a system then such variables are called state variables. These state variables should not be physically measurable or observable quantities. Variables that do not represent physical quantities and those that are neither measurable nor observable can also be chosen as state variables which is an advantage of the state-space methods (Ogata 2010).

State vector:

To describe the behavior of a system, if *n* state variables are needed, then these *n* state variables can be considered the *n* components of vector **x** which is called state vector. Therefore state vector is the one which determines uniquely the system state x (t) for ant time t $\geq t_0$, once the state at t $= t_0$ and the input u (t) for t $\geq t_0$ is specified (Ogata 2010).

State space:

It is an n-dimensional space which consist of x_1 axis, x_2 axis, x_n axis as coordinate axes where x_1,x_2, x_n are state variables (Ogata 2010). Any state can be represented by a point in the state space.

State-space equations:

In state-space analysis input, output and state variables are required in the modeling of dynamic systems. The state-space representation for a given system is not unique, except that the number of state variables is the same for any of the different state-space representation of the same system (Ogata 2010).The following model of state space representation is used for modelling of our dynamic systems in this study.

The dynamic system should contain elements that memorize the values of input for t $\geq t_1$. In a continuous –time control systems integrators serve as memory devices, therefore the output of these integrators can be considered as the variables that define the internal state of the dynamic system (building with TMD) (Ogata 2010). Thus the outputs of integrator's serve as state variables. The number of state variables required to completely define the dynamics of the system is equal to the number of integrators present in the system.

Consider a system with multiple inputs and outputs containing *n* integrators. If this system has *r* inputs $u_1(t), u_2(t), \ldots\ldots, u_r(t)$ and *m* outputs $y_1(t), y_2(t), \ldots\ldots, y_m(t)$, then define *n* outputs of

the integrators as state variables $x_1(t), x_2(t), \ldots\ldots, y_n(t)$. Therefore the dynamic system can be described as follows (Ogata 2010):

$$\begin{aligned}
\dot{x}_1(t) &= f_1(x_1, x_2, \ldots\ldots\ldots, x_n; u_1, u_2, \ldots\ldots, u_r; t) \\
\dot{x}_2(t) &= f_2(x_1, x_2, \ldots\ldots\ldots, x_n; u_1, u_2, \ldots\ldots, u_r; t) \\
&\vdots \\
\dot{x}_n(t) &= f_n(x_1, x_2, \ldots\ldots\ldots, x_n; u_1, u_2, \ldots\ldots, u_r; t)
\end{aligned} \tag{22}$$

The outputs $y_1(t), y_2(t), \ldots\ldots, y_m(t)$ of the system may be given by (Ogata 2010)

$$\begin{aligned}
y_1(t) &= g_1(x_1, x_2, \ldots\ldots\ldots, x_n; u_1, u_2, \ldots\ldots, u_r; t) \\
y_2(t) &= g(x_1, x_2, \ldots\ldots\ldots, x_n; u_1, u_2, \ldots\ldots, u_r; t) \\
&\vdots \\
y_m(t) &= g_m(x_1, x_2, \ldots\ldots\ldots, x_n; u_1, u_2, \ldots\ldots, u_r; t)
\end{aligned} \tag{23}$$

If we define them in matrix form (Ogata 2010)

$$x(t) = \begin{bmatrix} x_1(t) \\ x_2(t) \\ . \\ . \\ . \\ x_n(t) \end{bmatrix}, \quad \text{f(x,u,t)=} \begin{bmatrix} f_1(x_1, x_2, \ldots\ldots\ldots\ldots, x_n;\ u_1, u_2, \ldots\ldots, u_r; \text{t}) \\ f_2(x_1, x_2, \ldots\ldots\ldots\ldots, x_n;\ u_1, u_2, \ldots\ldots, u_r; \text{t}) \\ . \\ . \\ . \\ f_n(x_1, x_2, \ldots\ldots\ldots\ldots, x_n;\ u_1, u_2, \ldots\ldots, u_r; \text{t}) \end{bmatrix}$$

$$y(t) = \begin{bmatrix} y_1(t) \\ y_2(t) \\ . \\ . \\ . \\ y_m(t) \end{bmatrix}, \quad \text{f(x,u,t)=} \begin{bmatrix} g_1(x_1, x_2, \ldots\ldots\ldots\ldots, x_n;\ u_1, u_2, \ldots\ldots, u_r; \text{t}) \\ g_2(x_1, x_2, \ldots\ldots\ldots\ldots, x_n;\ u_1, u_2, \ldots\ldots, u_r; \text{t}) \\ . \\ . \\ . \\ g_n(x_1, x_2, \ldots\ldots\ldots\ldots, x_n;\ u_1, u_2, \ldots\ldots, u_r; \text{t}) \end{bmatrix}$$

$$u(t) = \begin{bmatrix} u_1(t) \\ u_2(t) \\ . \\ . \\ . \\ u_r(t) \end{bmatrix}$$

Then the equations 22 and 23 can be written as (Ogata 2010)

$\dot{x}_1(t) = f(x,u,t)$ …… (24)

$y(t) = g(x,u,t)$ …… (25)

Equation 24 is the state equation and equation 25 is the output equation. If vector functions **f** or **g** involve time t, then it is called time-varying system. If equations 24 and 25 are linearized about the operating state, then the linearized state and output equation are given by equation 26 and 27 (Ogata 2010).

$$\dot{x}(t) = A(t)X(t) + B(t)U(t) \quad \text{---------- (25)}$$

$$y(t) = C(t)X(t) + D(t)U(t) \quad \text{---------- (26)}$$

where A (t) is called the state matrix, B (t) the input matrix, C (t) the output matrix and D (t) the direct transmission matrix. Figure 17 represents equations 25 and 26.

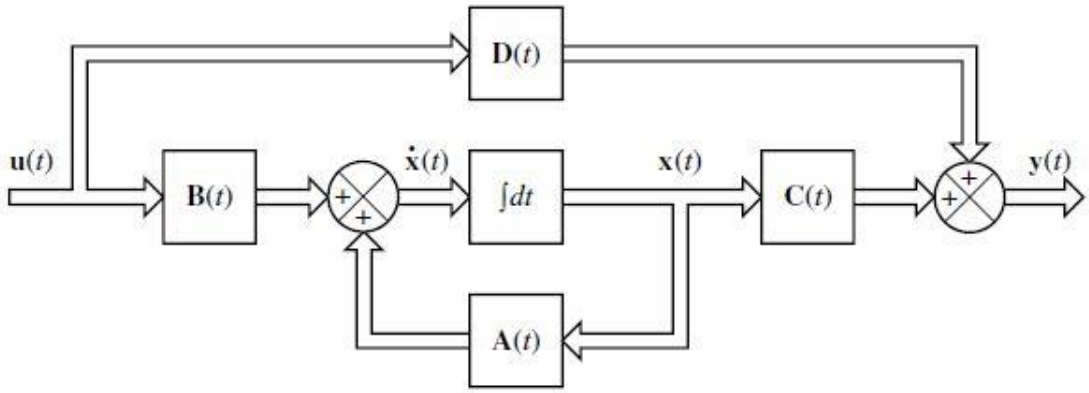

Figure 17: Block diagram of linear, continuous-time control system represented in state space (Ogata 2010)

If vector functions **f** and **g** do not involve time explicitly, then the system is called a time-invariant system as in our case, then they are represented by following equations (Ogata 2010)

$$\dot{x}(t) = AX(t) + BU(t) \quad \text{…….. (26)}$$

$$y(t) = CX(t) + DU(t) \quad \text{…….. (27)}$$

Then we change the mass, damping and stiffness matrix described above into the required form such that they can use the state space model in MATLAB (Attaway, 2009) as shown in Figure 19 to perform the analysis.

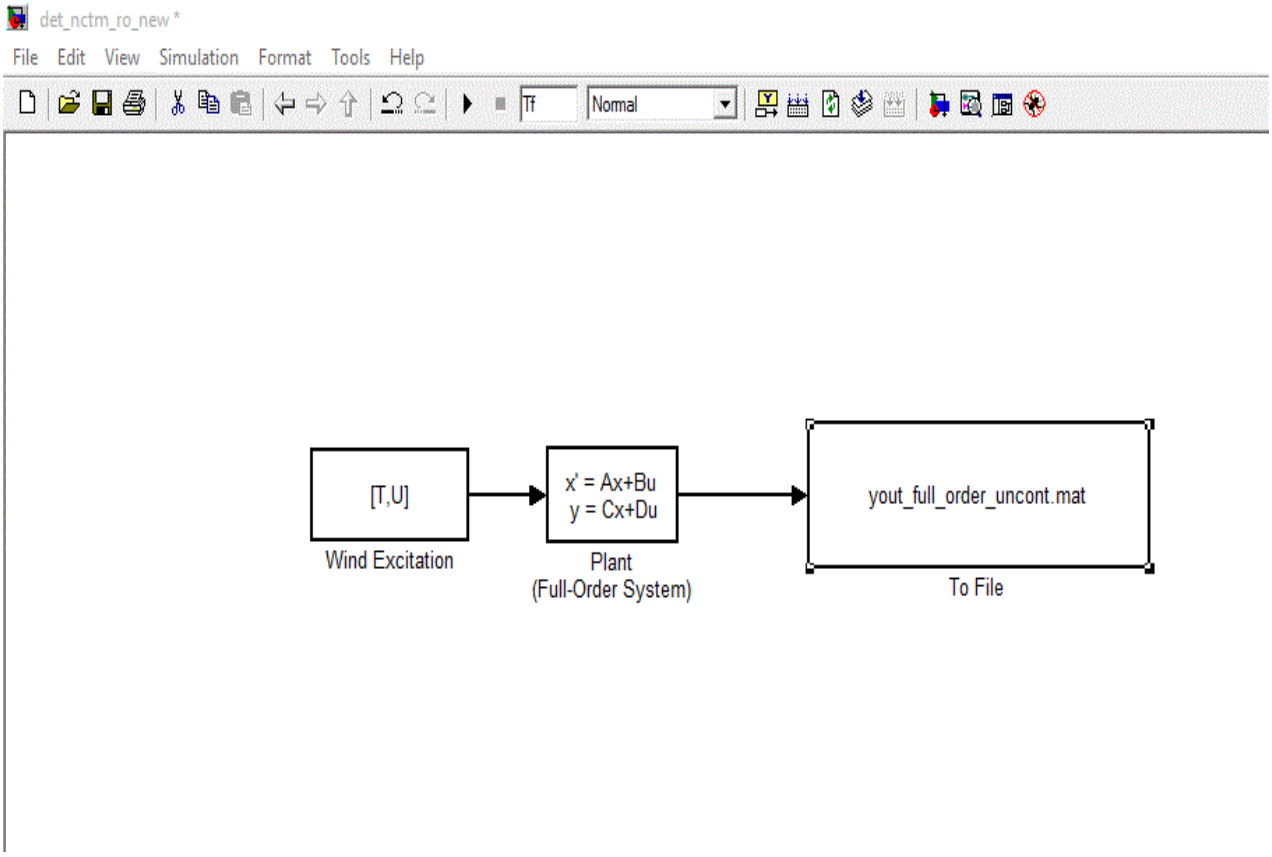

Figure 18: Simulink model for uncontrolled high-rise building under wind load

After the code is written a Simulink model was created that uses state-space model to perform analysis of our dynamic systems (building with and without TMD) and gives the state of this dynamic system as an output. It is shown in Figure 18. It takes the wind excitation as input and feeds into the state-space model and it is done for the given time interval. The state of the dynamic system (building with and without TMD) is stored for each and every time step. The number of integrators in this model is 228 for building without TMD and 231 for building with TMD.

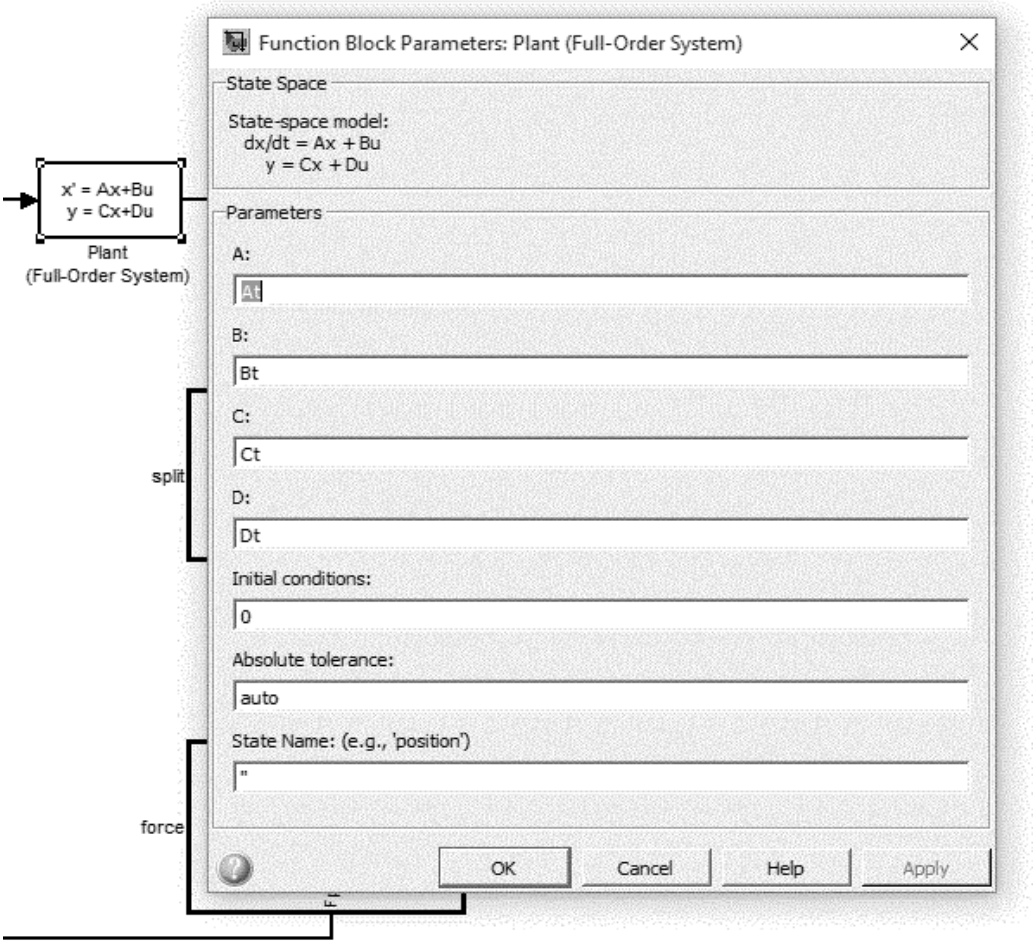

Figure 19: State-space model in MATLAB

The Simulation is performed for full order (FO) and reduced order (RO) of the building with and without TMD under Wind loading. The displacement, velocity, and acceleration of all floors are obtained in full order analysis. In reduced order the outputs are obtained only for requested floors. For uncontrolled building the output floors are 9 [1, 30, 50, 55, 60, 65, 70, 75, 76] and for building with TMD, the output floors are 10 [1, 30, 50, 55, 60, 65, 70, 75, 76, 77].

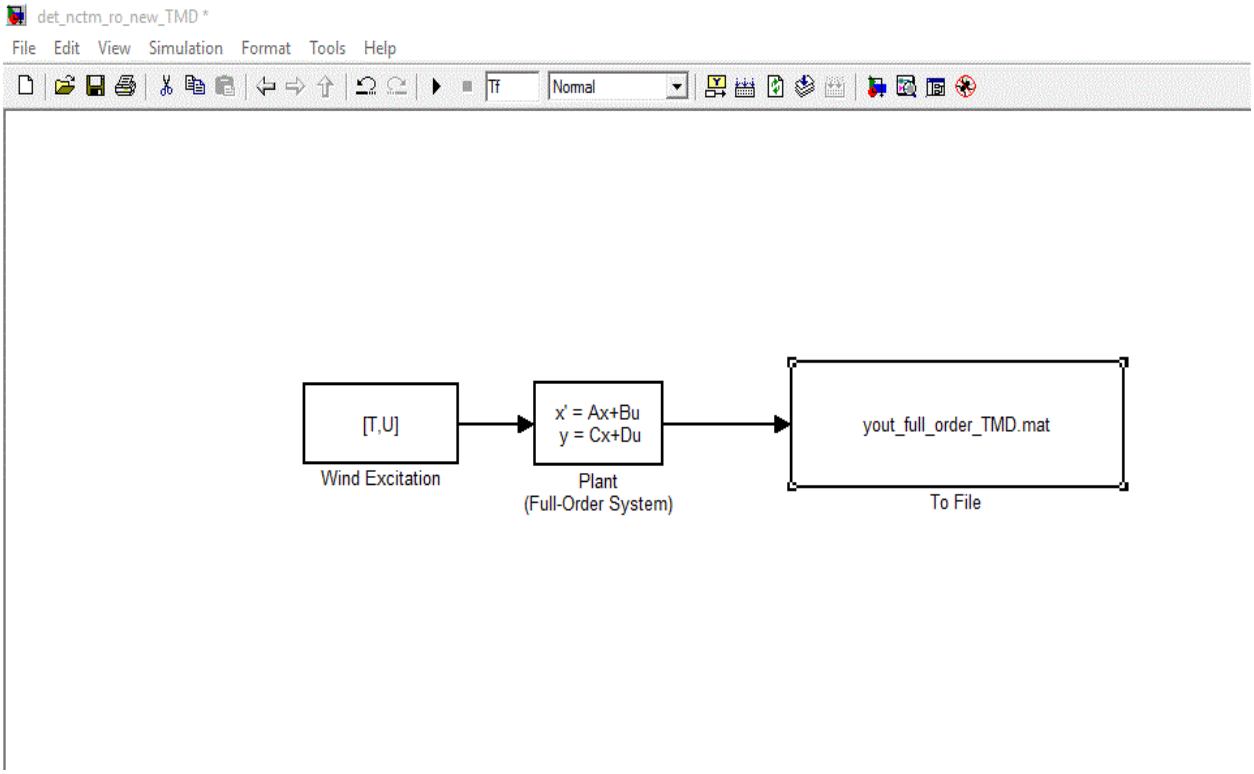

Figure 20: Simulink model of high-rise building with TMD under wind loading

Responses of the building with and without TMD under wind loads

For wind analysis the integration time step is taken as 0.0001 s and sampling time step as 0.001 s. Even though 3600 s of wind load data is available 900 s are sufficient for benchmark comparisons. The TMD is tuned to the first mode, at a frequency of 0.16Hz. The simulations are run for both full order and reduced order of the uncontrolled building and building with TMD. The reason for performing the reduced order simulations is to save time if full order takes a lot of time. It helps when calculating the robustness or optimal TMD parameters. After performing simulations for building with and without TMD under the wind loading, maximum and standard deviation of displacement, velocity and acceleration are plotted for building for both full order and reduced order.

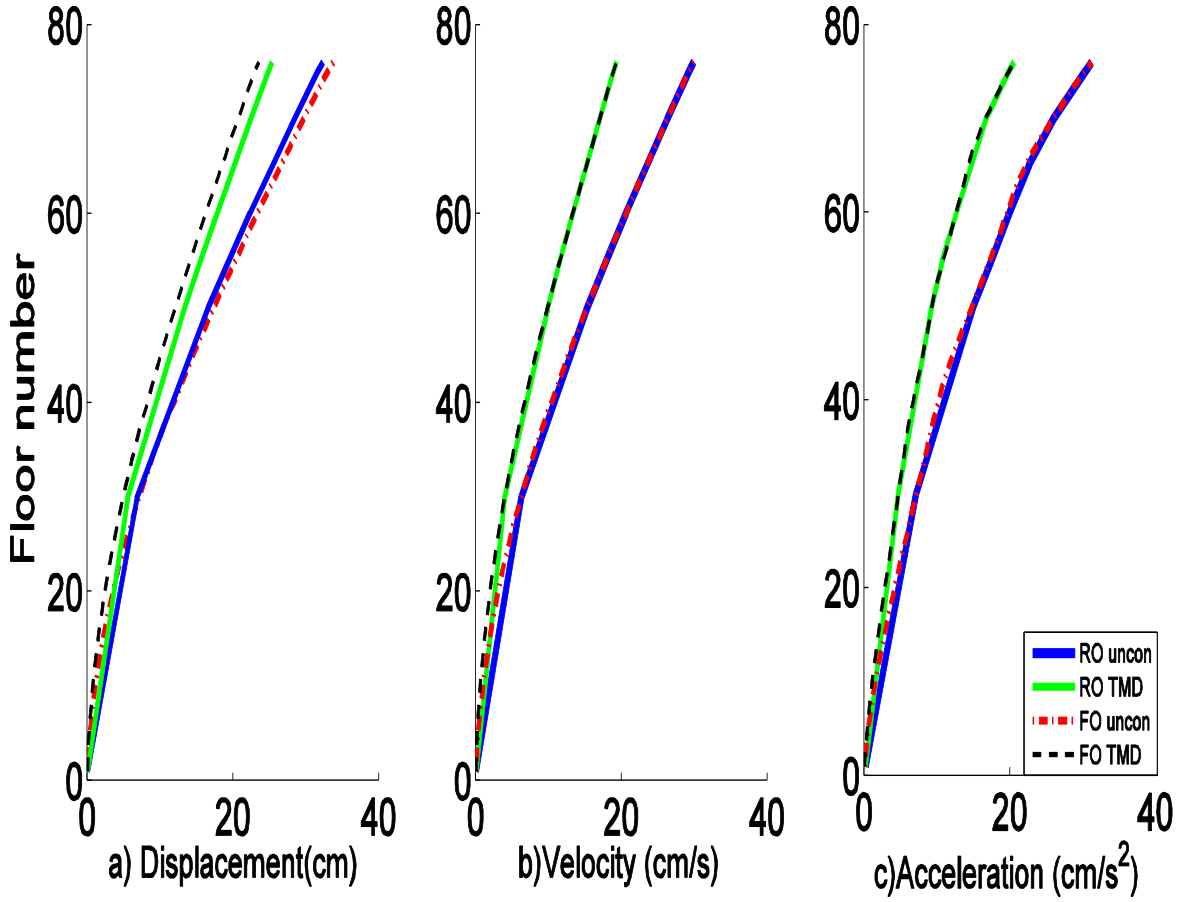

Figure 21: Max displacement, velocity and acceleration of (RO) and full order (FO) of building controlled with and without TMD under wind loading.

From the Figure 21 and Figure 22 it is clear that reduced order and full order produce similar results. In this study, we only use full order for our analysis. The max displacement of the building is nearly 35cm near the top floor and 0cm near ground for uncontrolled building under wind. When TMD is added to the building the maximum displacement of the top floor is reduced to 25cm. There is a decrease of 10cm in maximum displacement of the top floor which is good. Similarly velocity is reduced from 30cm/s to 19cm/s and acceleration is reduced from 32cm/s² to 22cm/s² approximately. As mentioned earlier, if the acceleration was in between 25cm/s² to 40cm/s² it is impossible to do desk work and causes ambulation. Due to reduction in acceleration

to 22cm/ s²people can feel the movement but will be able to do the desk work and no damage occur to the furniture inside.

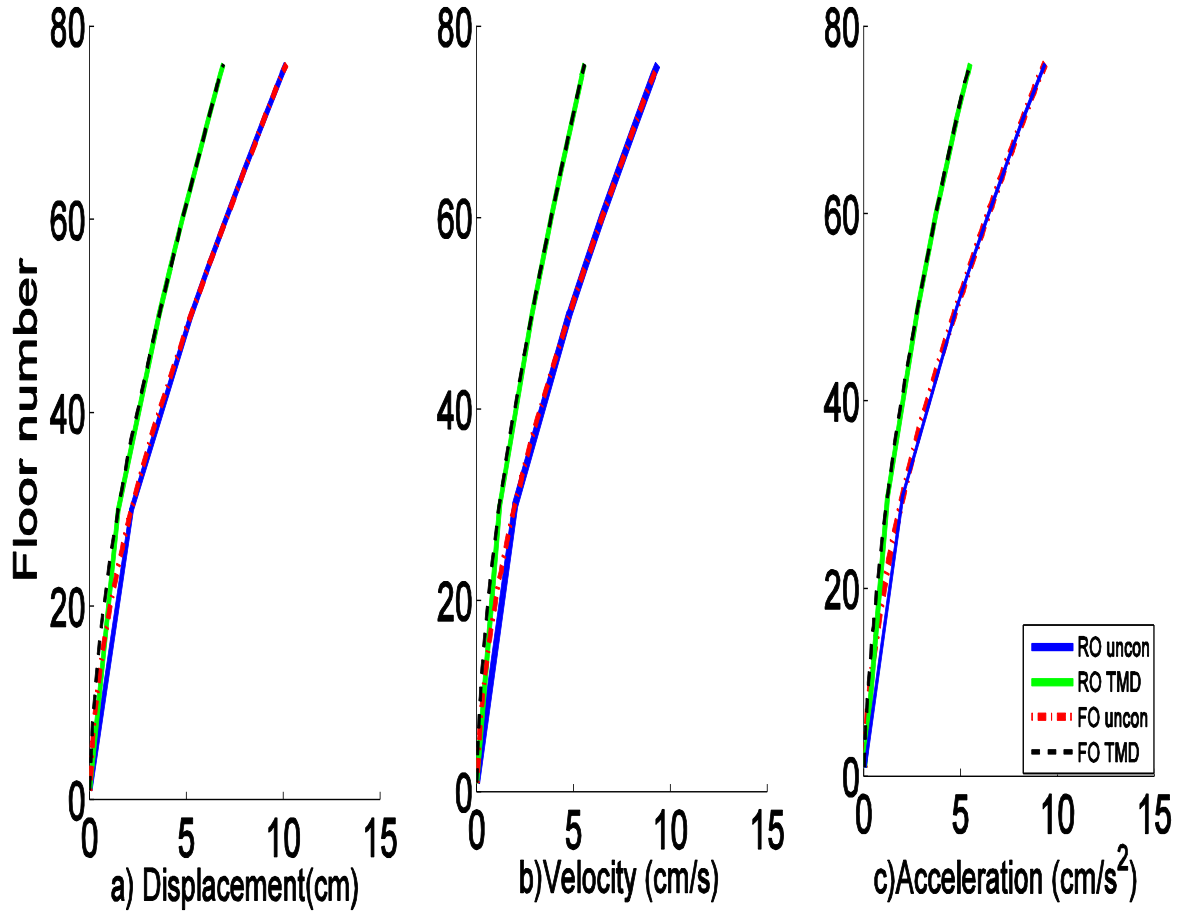

Figure 22 : Standard deviation of displacement, velocity and acceleration of reduced order (RO) and full order (FO) of building controlled with and without TMD under wind loading.

Similarly the standard deviation of displacement is reduced from 12cm to 7cm, velocity from 10cm/s to 5cm/s and acceleration value from 10cm/s² to 5cm/ s² for the top floor of the building which is significant. We can see below the acceleration and displacement of floor 76 vs time history in Figure 23and Figure 24.

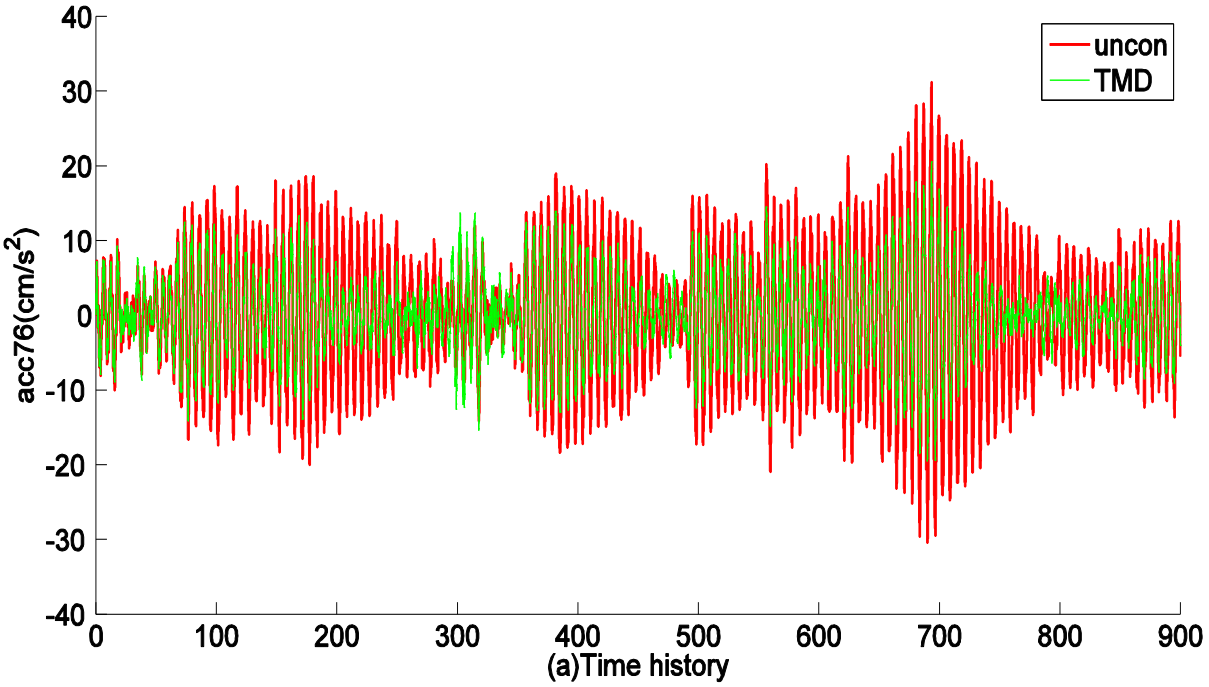

Figure 23: Acceleration of 76th floor of building with TMD under wind loading

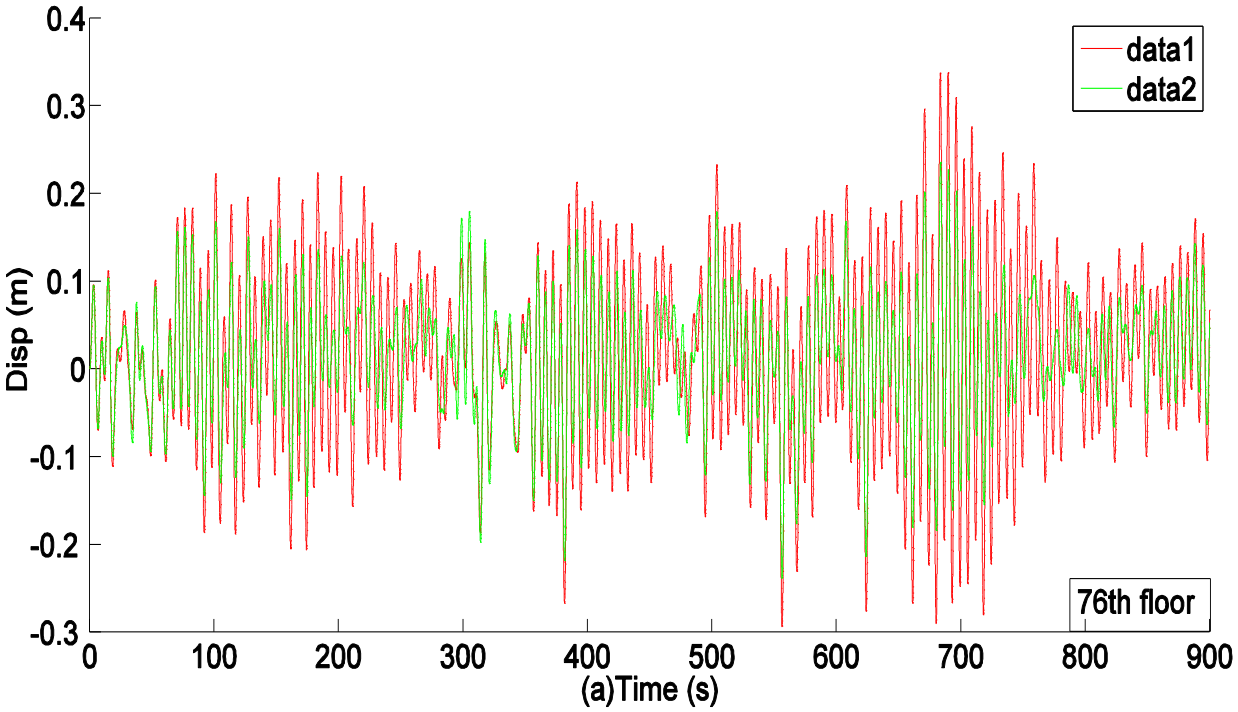

Figure 24: Displacement of 76th floor of building with TMD under wind loading

The maximum and standard deviation of shear force and bending moment is calculated for building with and without TMD and plotted as shown in Figure 25and Figure 26. As wind force is considered as maximum at the top of the building the shear force and moment increase as going downwards. Max shear force is reduced only by an amount of 0.6E5 N and standard deviation of shear force by 2.5E4 N with the addition of TMD at the ground floor. Reduction in bending moment is also similar to that of shear force whose maximum and standard deviation is reduced by 2.0E9N-cm and 5.0E8 N-cm at ground floor. The decrease in both shear force and bending moment decrease the stresses in the internal members thereby increasing the durability of the structure.

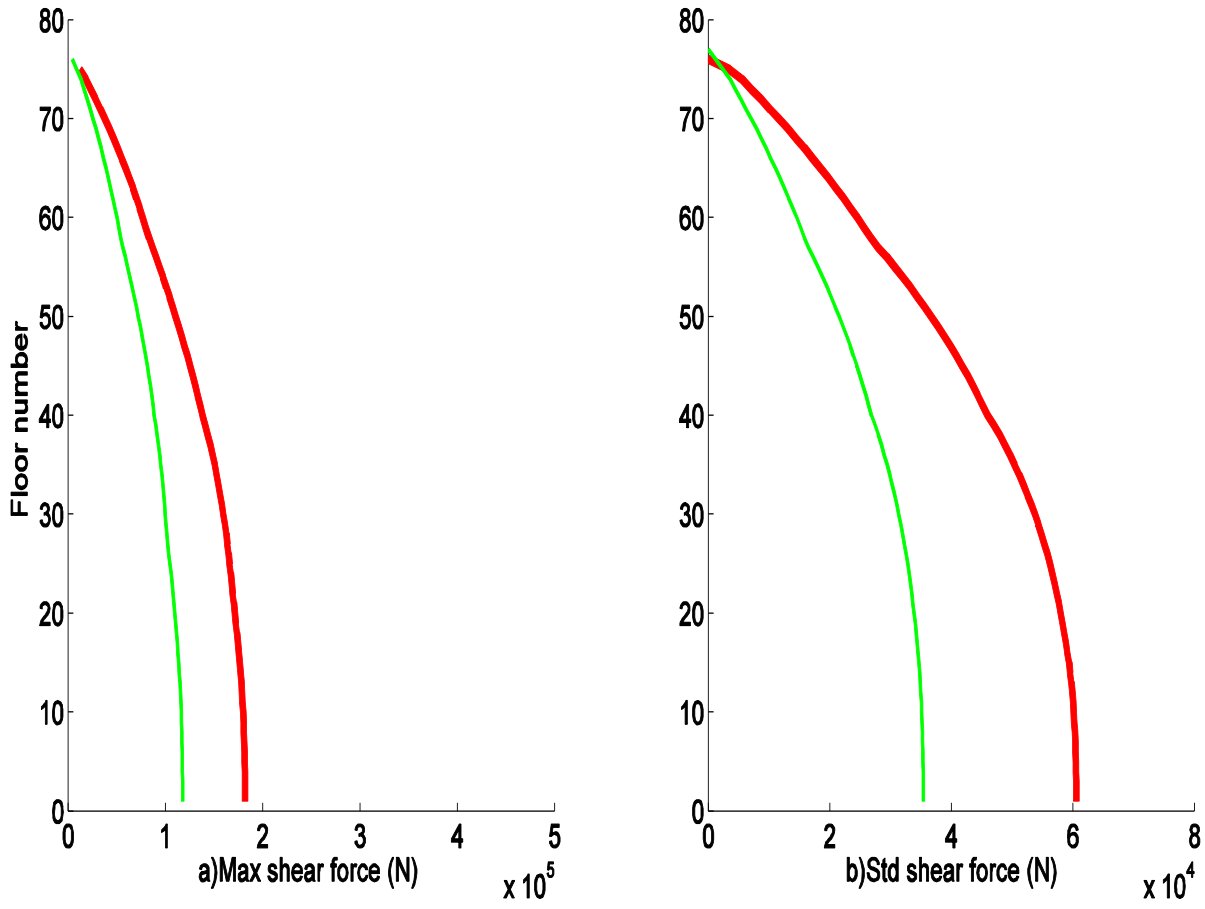

Figure 25: Shear force vs floor number with and without TMD under wind loading

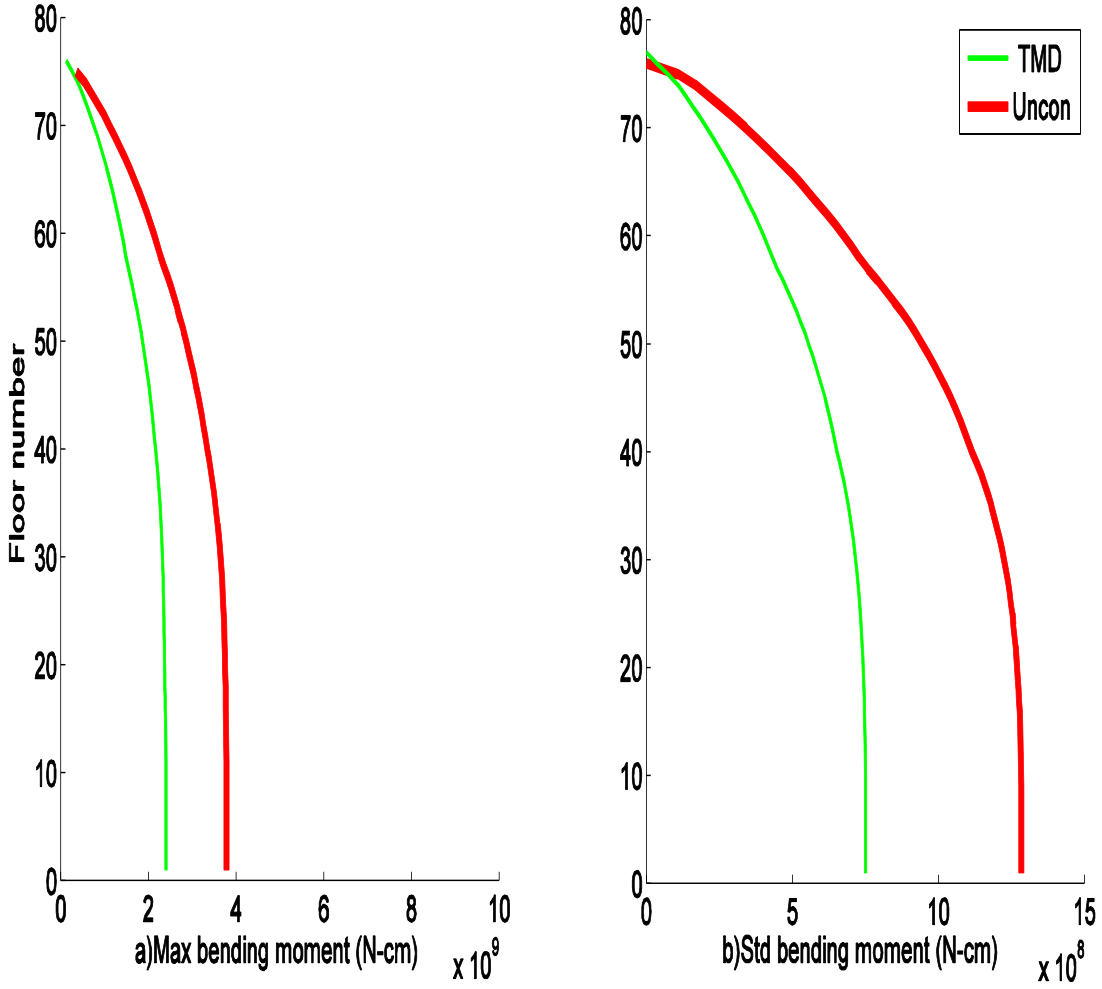

Figure 26: Bending moment vs floor number with and without TMD under wind loading

Responses of the building with and without TMD under earthquake

Earthquake loading is applied on the building with and without TMD. The parameters of the TMD are same as used for wind analysis. From Figure 27(a) the maximum displacement of the top floor of the building is nearly 1.0m (100cm) which is very high when compared to that of the wind.

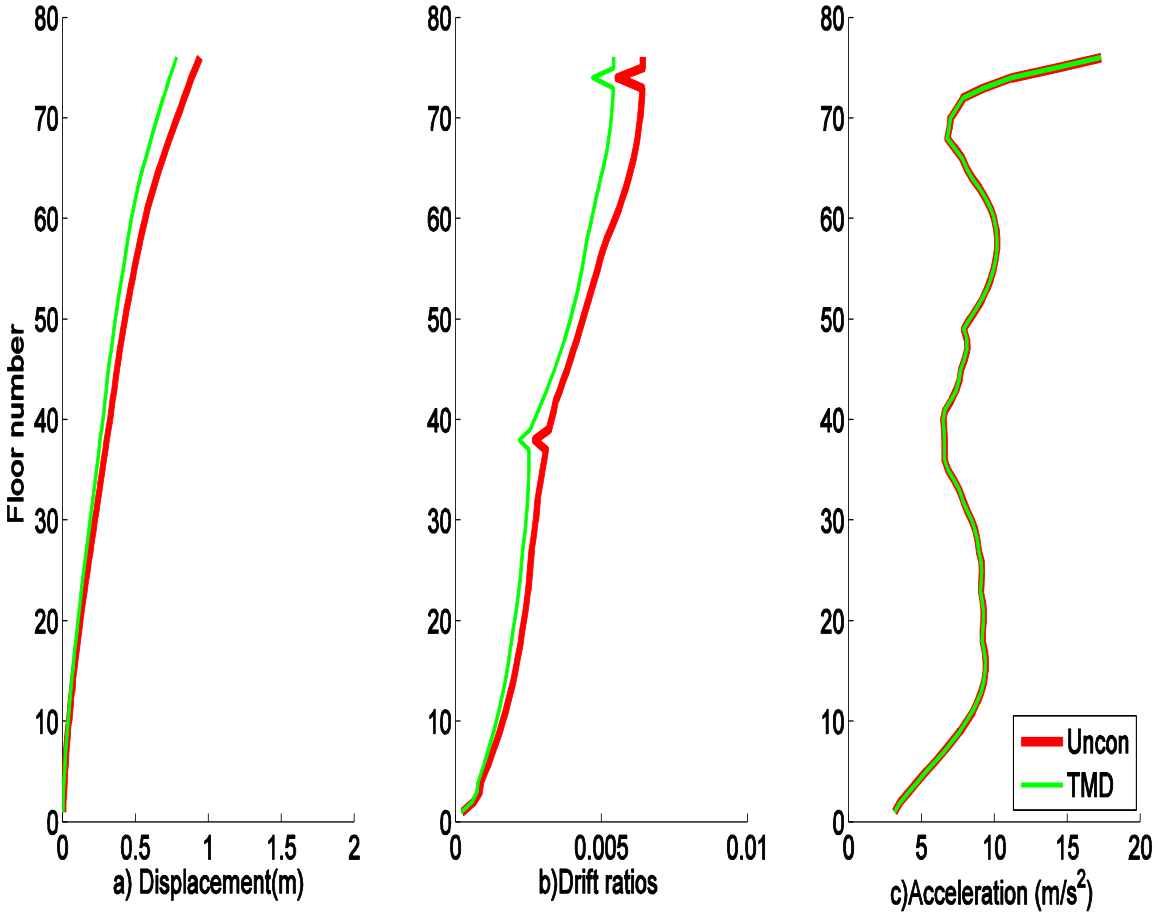

Figure 27: Max displacement, drift ratios and acceleration of full order (FO) of building controlled with and without TMD under earthquake.

The addition of TMD reduced the max displacement of top floor by 25cm. The drift ratio is also reduced by a significant amount by the addition of TMD. But TMD is ineffective in reducing both the maximum acceleration and standard deviation values of absolute acceleration throughout the building as seen in Figure 27(c) and Figure 28 (c). It has no effect on the acceleration. Similarly the bending moment and shear force values are also unchanged as shown in Figure 34 and Figure 33.

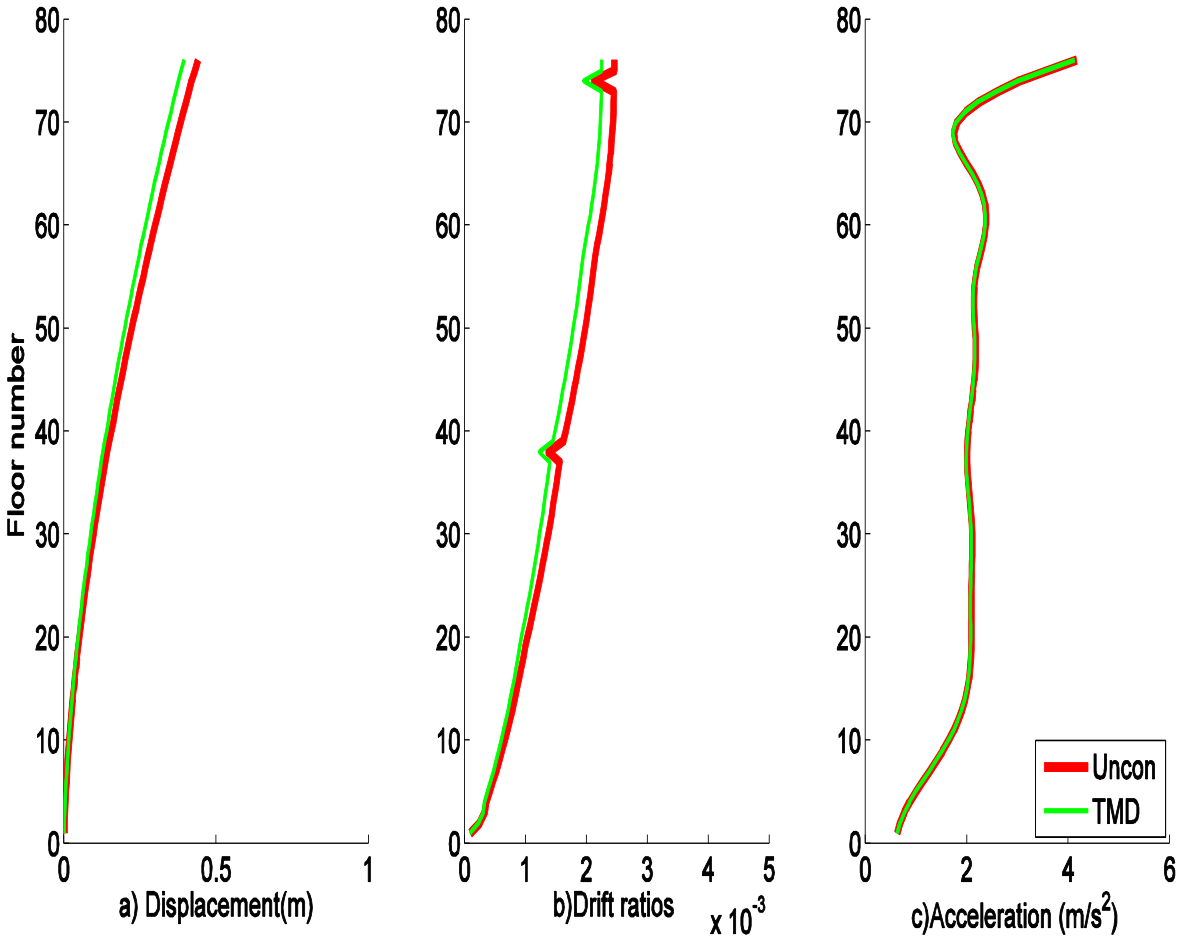

Figure 28: Standard deviation of displacement, drift ratios and acceleration of full order (FO) of building controlled with and without TMD under earthquake.

As we can see from the Figure 29and Figure 30there is no reduction in acceleration due to the addition of TMD. Unlike acceleration there is a slight reduction in displacement of floor, 70th and 76th as shown in Figure 32 and Figure 31. The peak acceleration is decreased by 0.15m in 76th floor between 15 s and 25 s of excitation. Similarly at the same time interval there is a reduction of 0.1m displacement in the 70th floor due to the addition of TMD under earthquake loading.

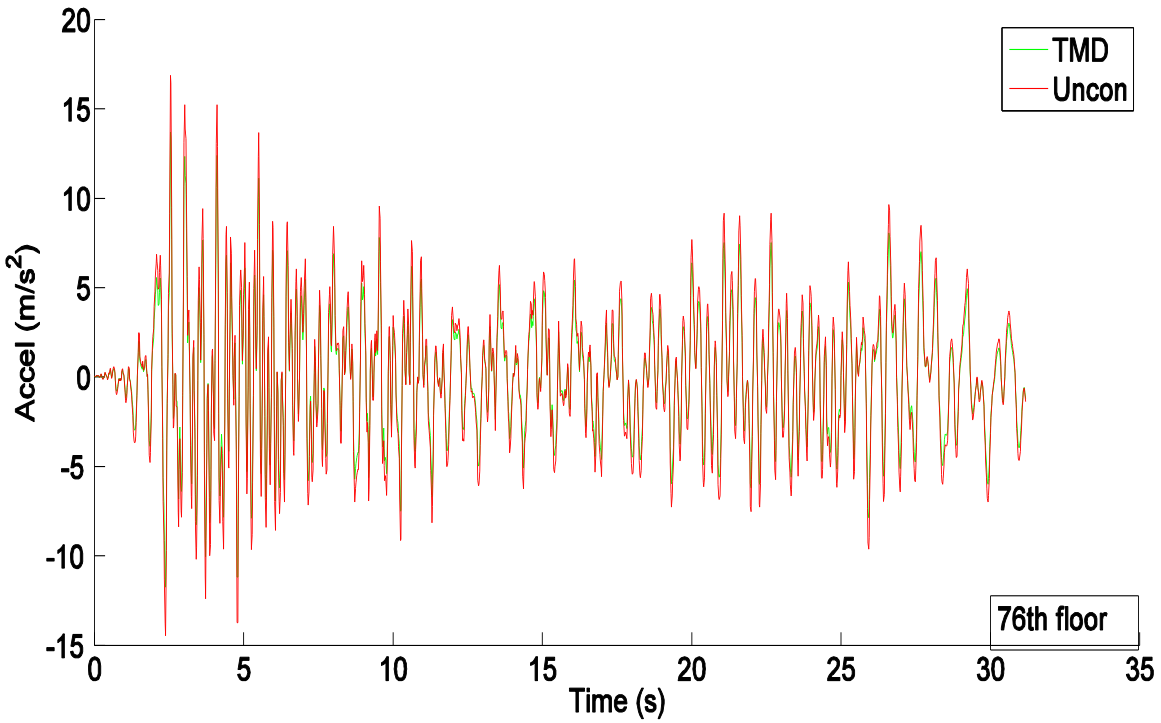

Figure 29: Acceleration of floor 76 of building under earthquake loading

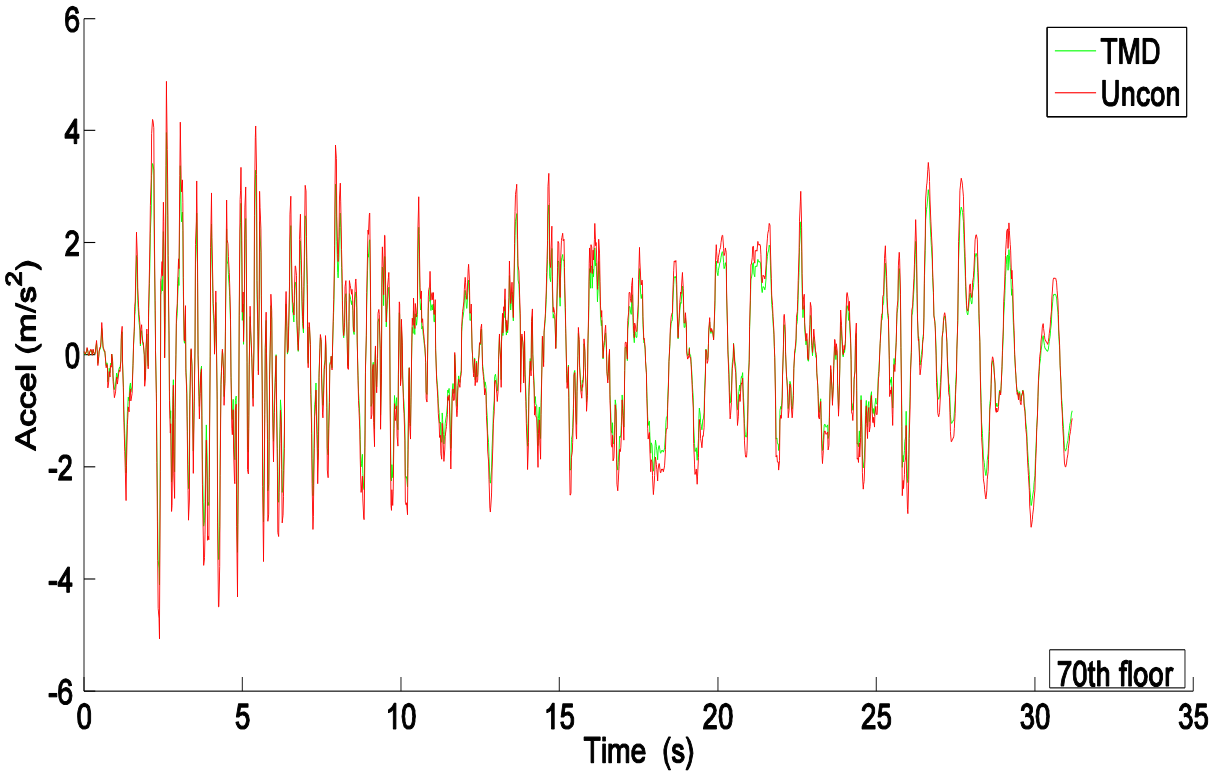

Figure 30: Acceleration of floor 70 of building under earthquake loading

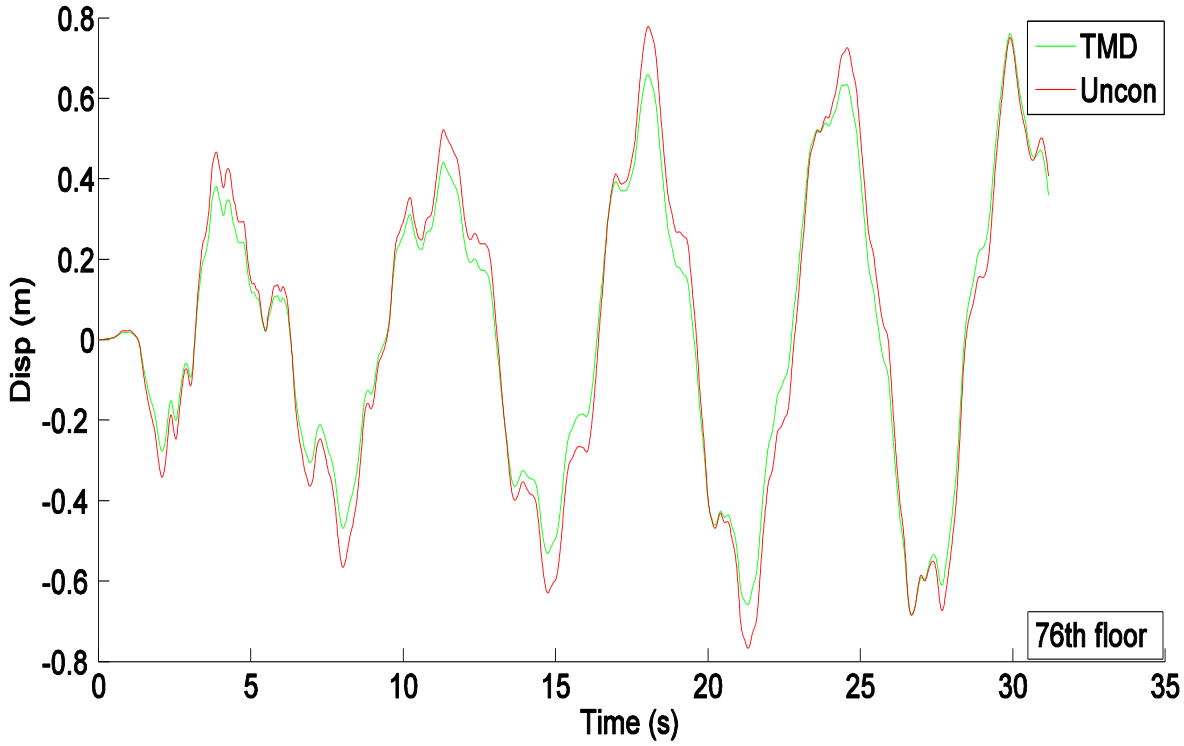

Figure 31: Displacement of floor 76 of building under earthquake loading

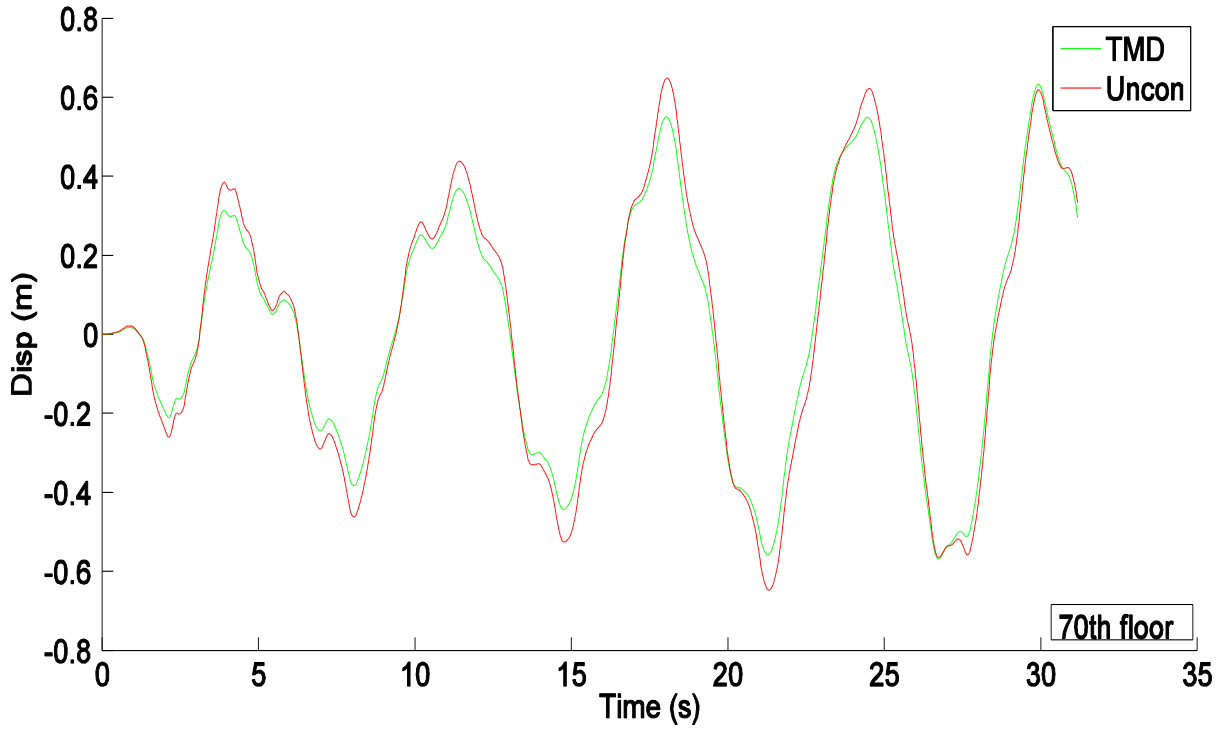

Figure 32: Displacement of floor 70 of building under earthquake loading

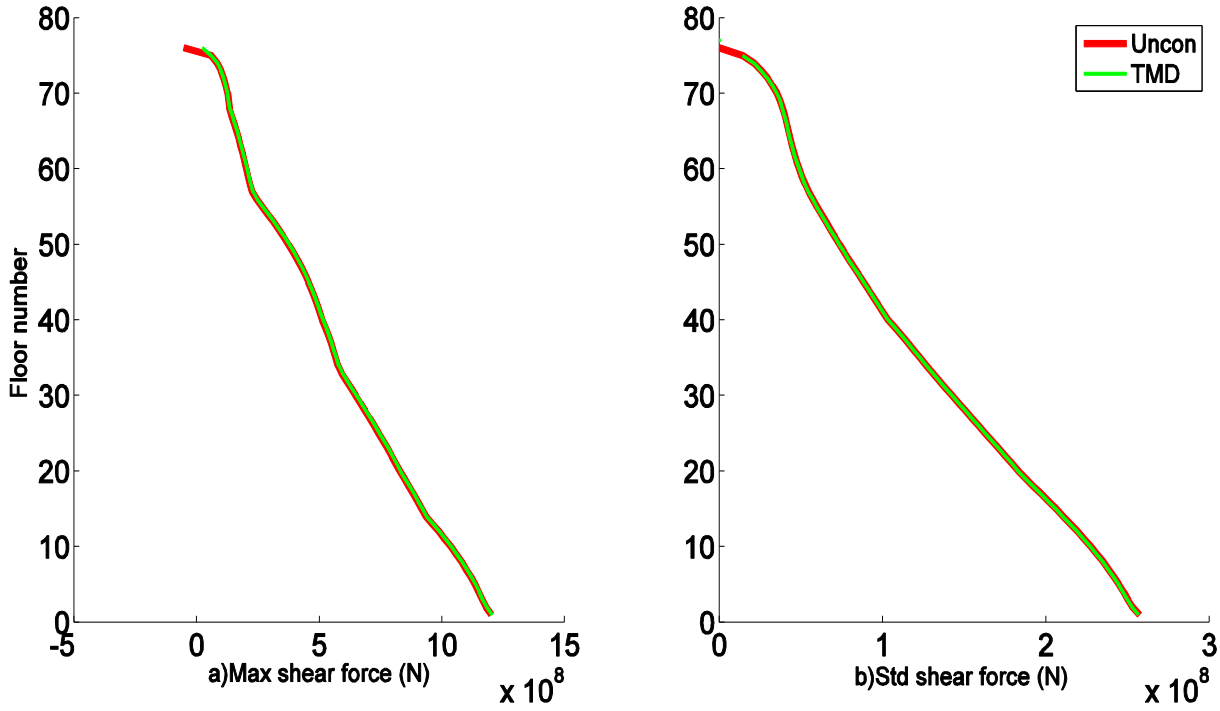

Figure 33: Shear force vs story's under earthquake

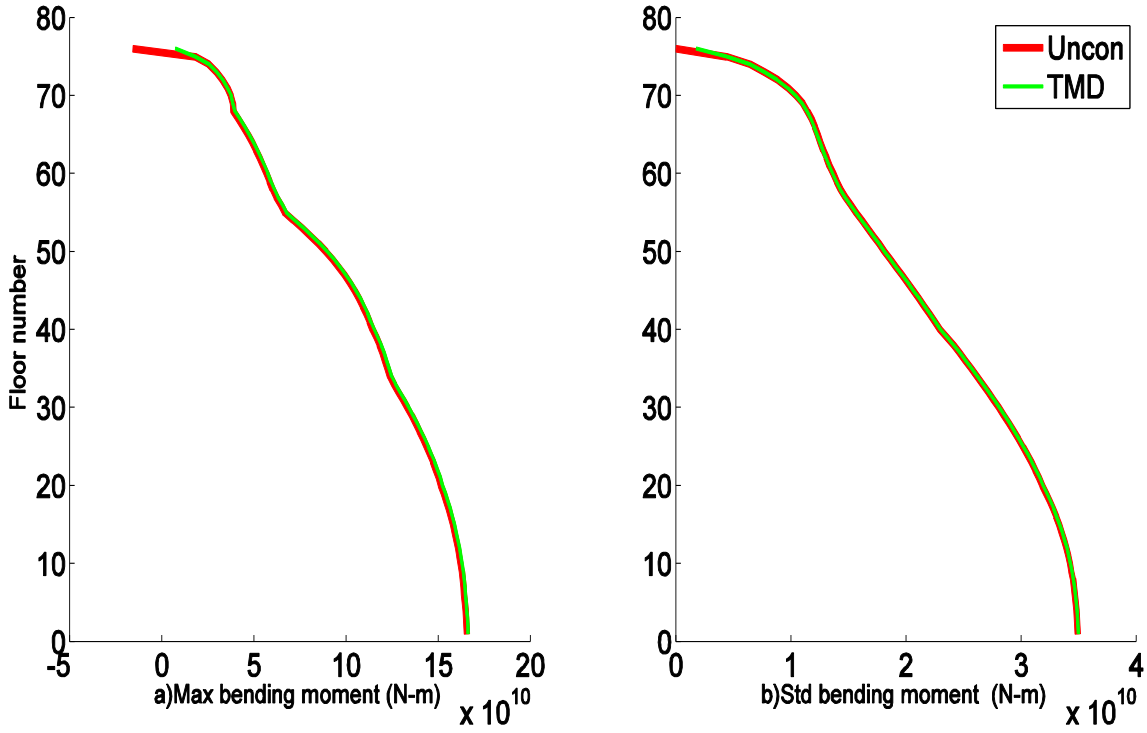

Figure 34: Bending moment vs story's under earthquake

Simulink model for the high-rise building with PTMD

It is similar to the Simulink model for the building with TMD, but there are some additional blocks for the calculation of pounding force, relative pounding deformation, relative velocity and damping of PTMD. Figure 35 **shows** the overview of all the blocks in the Simulink. Earth excitation block loads the earthquake loading data and sends it to the split1 block. From the split block wind loading is fed to the state-space equation block where the simulations are run according to the code written. In addition to the outputs mentioned in TMD model we have pounding force, stiffness component of pounding force, and damping component of pounding force, relative pounding deformation and relative velocity as outputs.

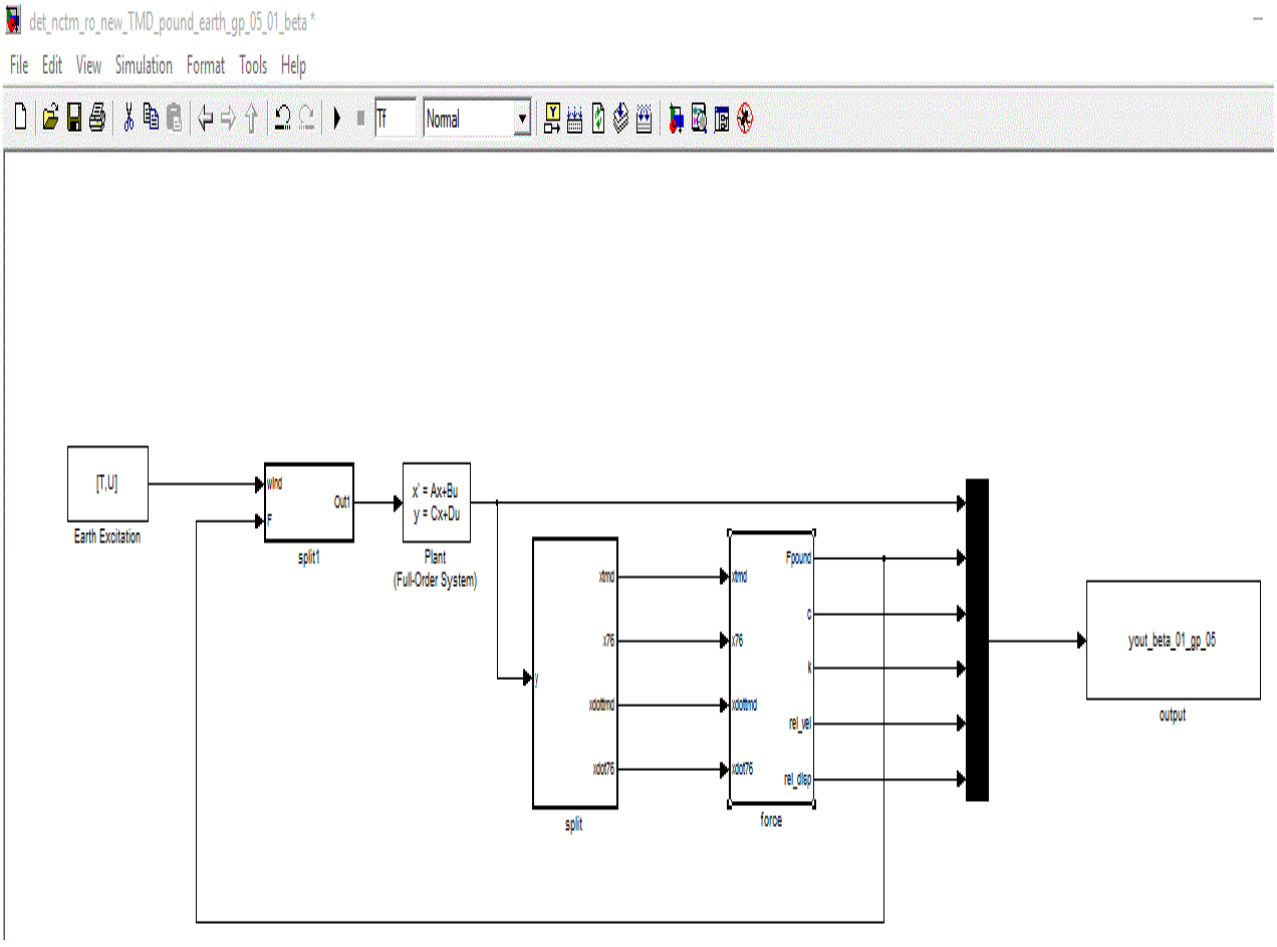

Figure 35: Simulink model for high-rise building under PTMD

In split1, the pounding force generated from the previous earthquake excitation of the building is added to the next earthquake excitation. A bus creator block is used as shown in Figure 36 to add pounding force to the oncoming earth excitation.

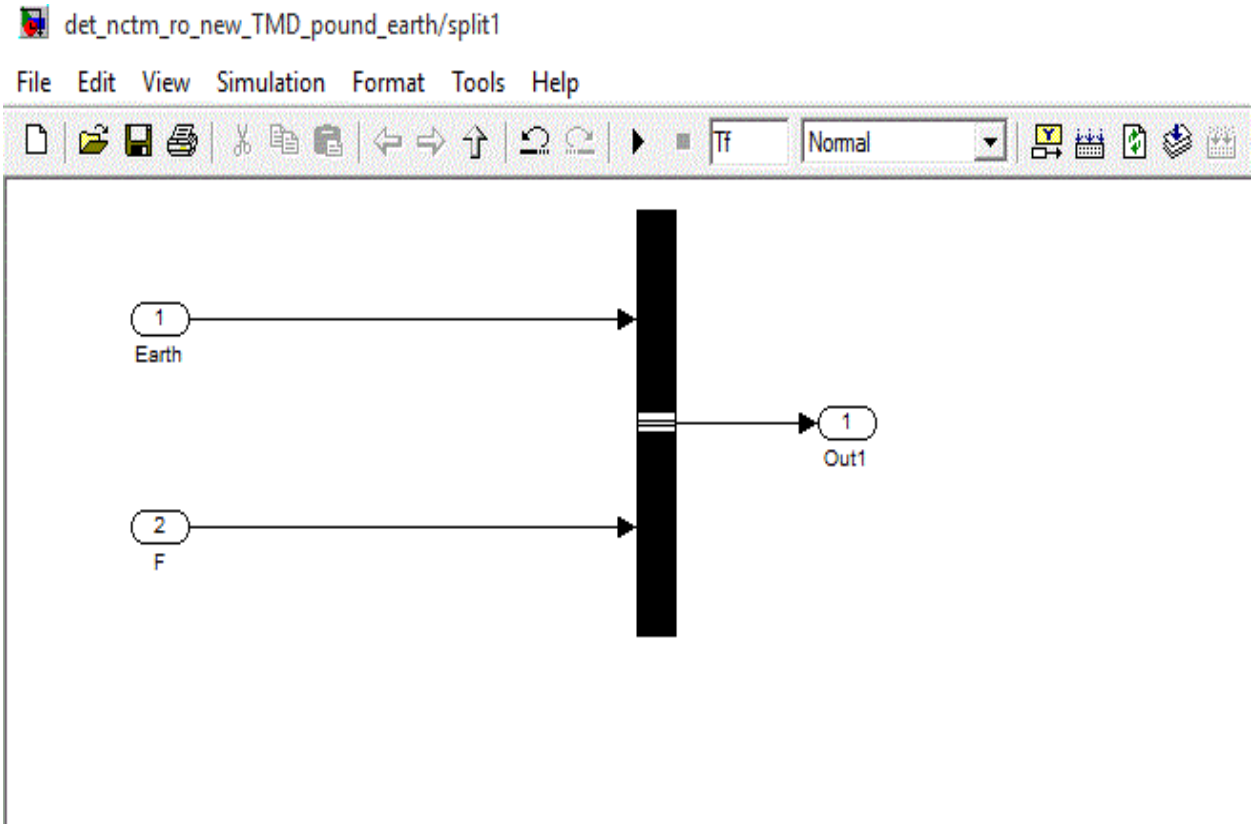

Figure 36: Block adding pounding force to the input earth excitation

Pounding force changes for every earth excitation depending on the contact of the pounding collar to the walls of VE material. So it has to be calculated using equation 10. After the first excitation of the building the outputs are taken and 4 outputs (displacement of PTMD and 76th floor and velocity of PTMD and 76th floor) are extracted by using the split block as shown in Figure 37, which are needed for calculating the pounding force. A bus creator and bus selector blocks are used to extract the required values. After the values are acquired they are fed into the force block for calculating the pounding force.

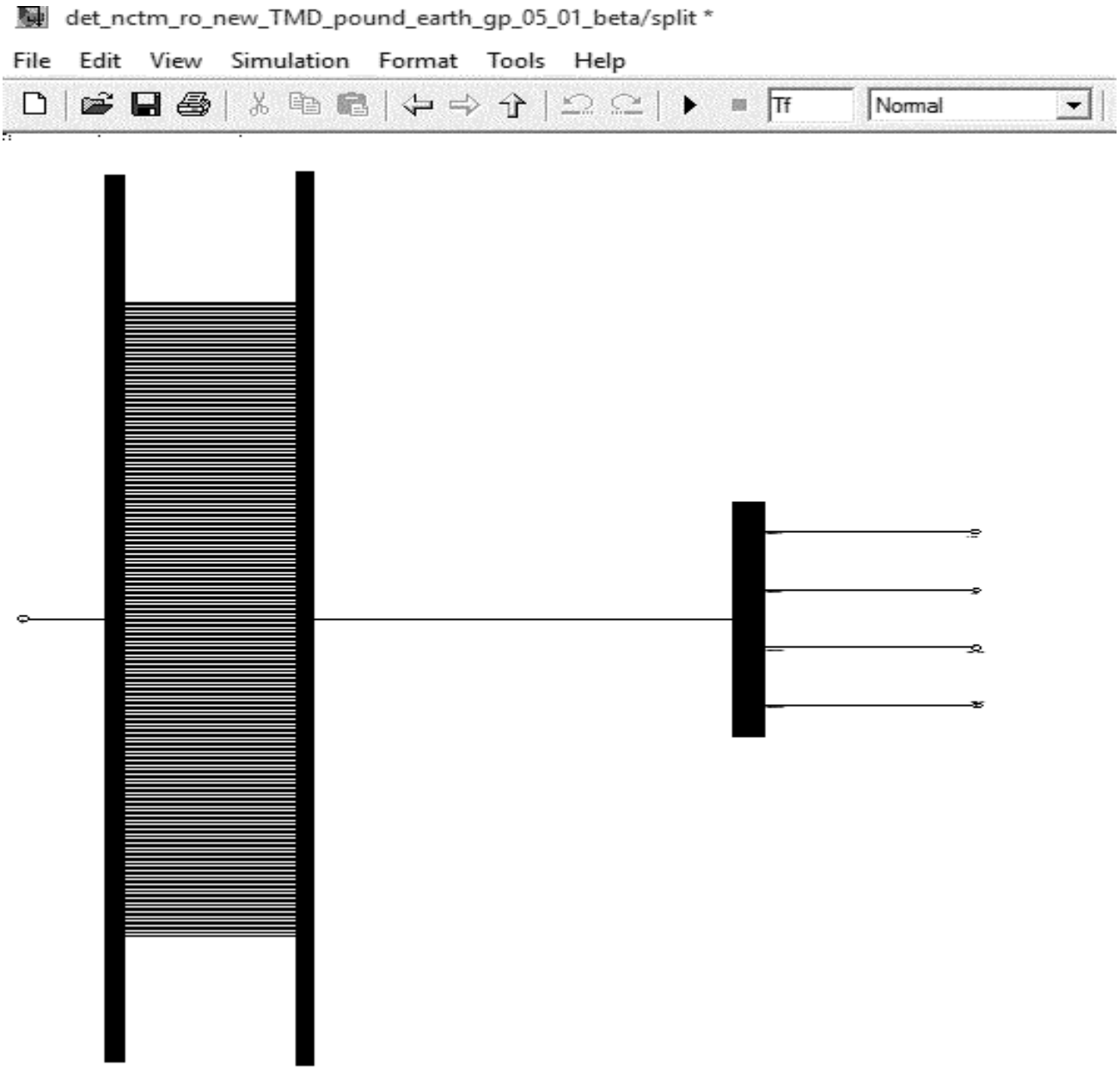

Figure 37: Block for selecting the required outputs

The pounding force as described in equation 10 is divided into three sub equations depending on the relative pounding deformation $(x_1 - x_2 - g_p)$ and relative velocity$(\dot{x}_1 - \dot{x}_2)$. The force block calculates the relative pounding deformation and relative velocity and pounding force accordingly.

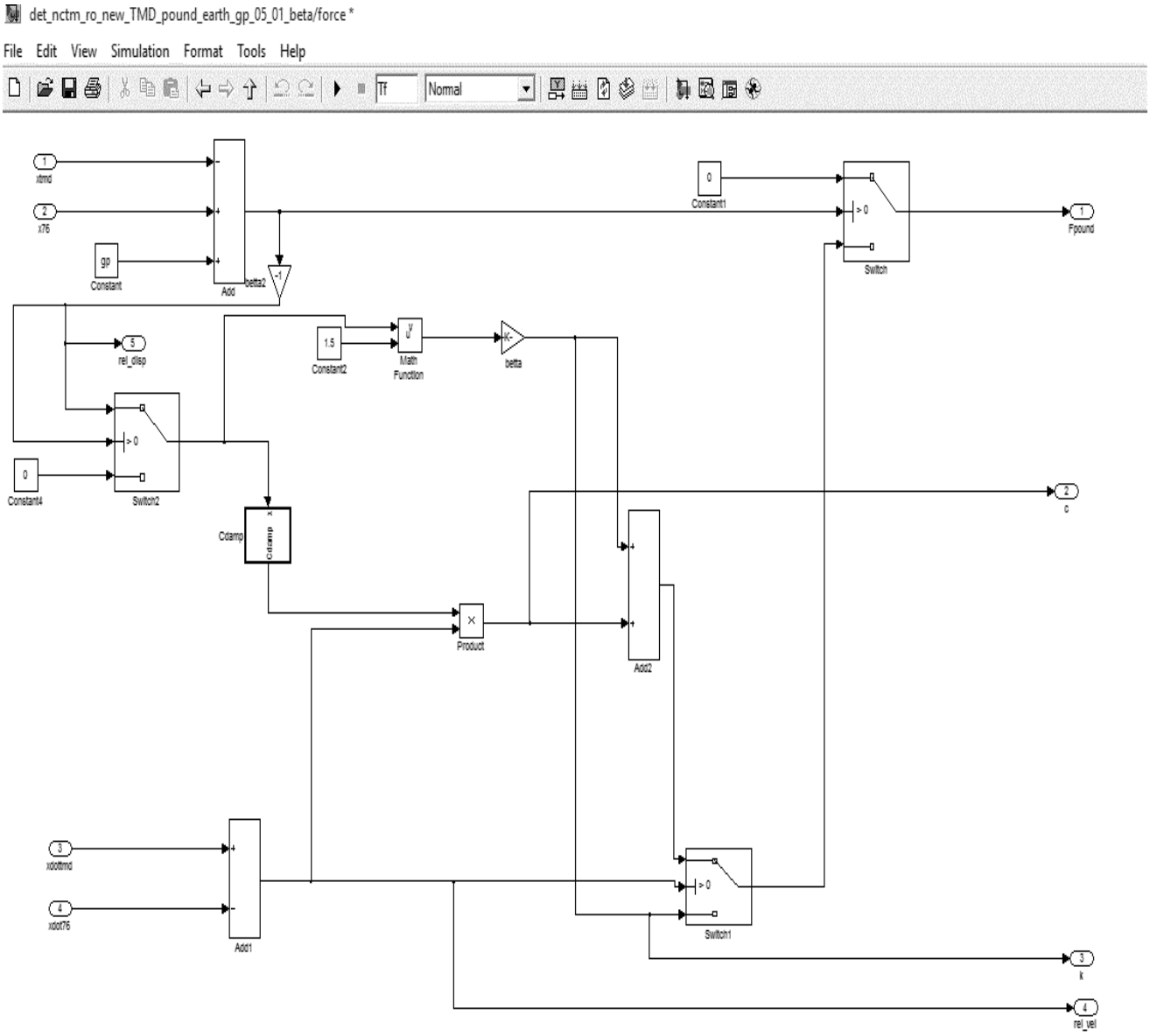

Figure 38: Block for calculating pounding force

As ‘c’ of PTMD is highly nonlinear and changes every time and depends on the relative pounding deformation. So it has to be calculated for every excitation. A Cdamp block is created to calculate ‘c’ of PTMD as described by equation 11 as shown in Figure 39.

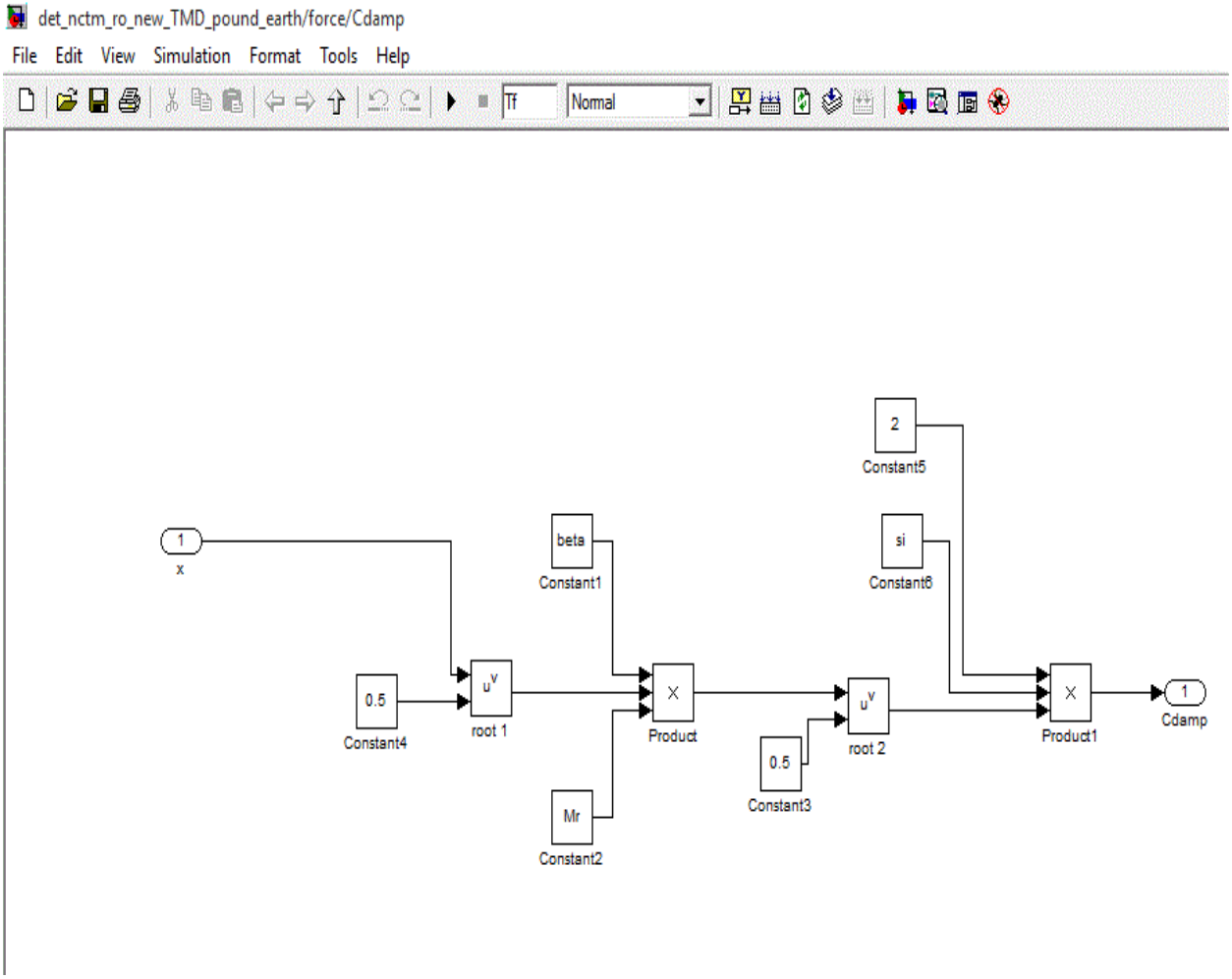

Figure 39: Block for calculating PTMD damping

After the Simulink model is developed the parameters of the PTMD are to be found out. Mass of the pounding collar is taken exactly as same as that of TMD i.e 500tons. Damping ratio is correlated with the coefficient of restitution given by equation 13. In this study, we are considering collision to be semi-elastic and thus the value of e=0.5.The gap length of the PTMD has major significance in the efficiency. In this study, we determine the optimal gap length of the PTMD by using the stroke length of the TMD under earthquake excitation as shown by Figure 40.

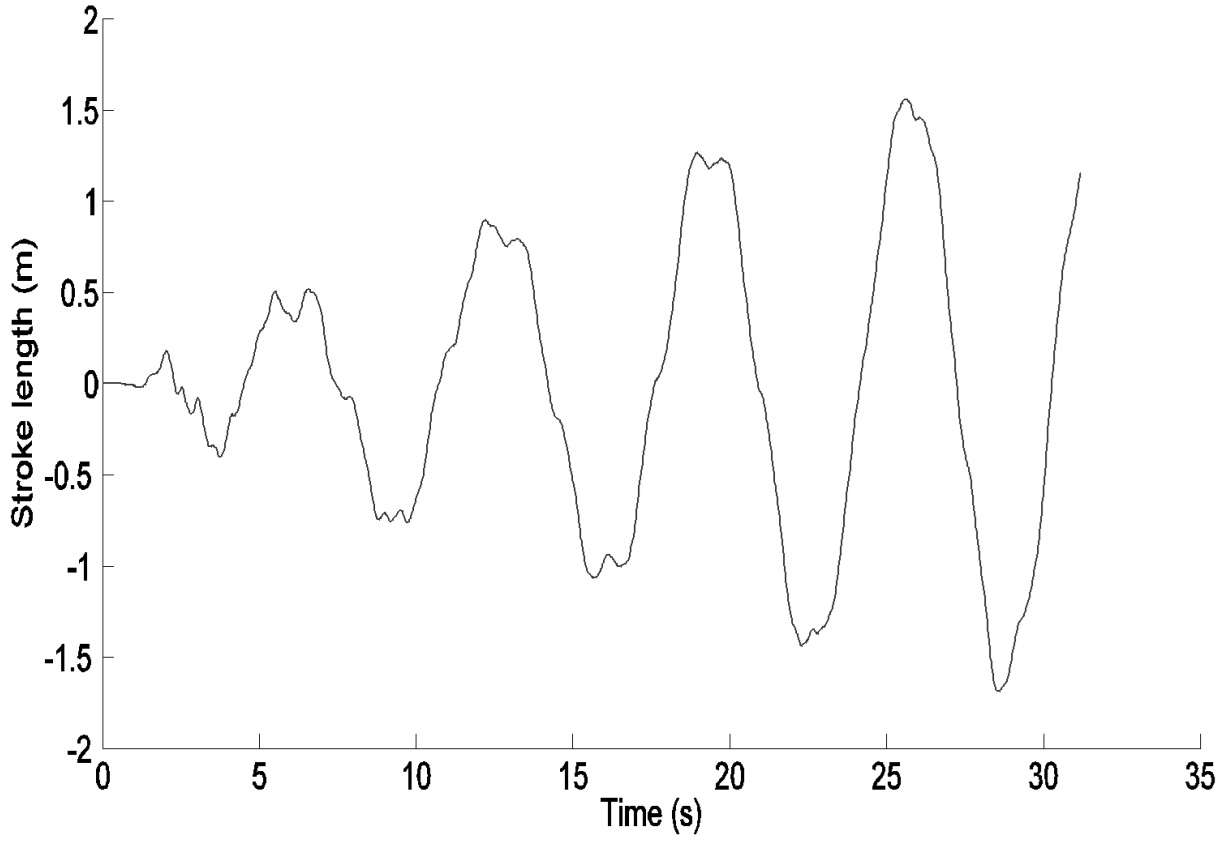

Figure 40: Stroke length of TMD under earthquake loading

As seen from Figure 40 the maximum value of the stroke length was 1.5m. In this study, we consider the gap length as 0.5m. The final parameter is pounding stiffness which depend on the properties of the viscoelastic material and the area of colliding bodies. In this study, we consider a range of values of pounding stiffness (i.e. 1.0E4 to 10.0E5) and find out the best value that increases the efficiency of PTMD.

Responses of the building with PTMD under wind loading

The stroke length of TMD under wind loading is very less when compared to that under earthquake loading. As we can see from Figure 41 the maximum value of stroke length is less than 45cm. As we considered the gap length of our PTMD as 50cm the pounding collar will not touch

the viscoelastic walls. It implies that the PTMD should act as a TMD under wind and the results should be same. It is also a good way to check whether the Simulink is modelled correctly for PTMD.

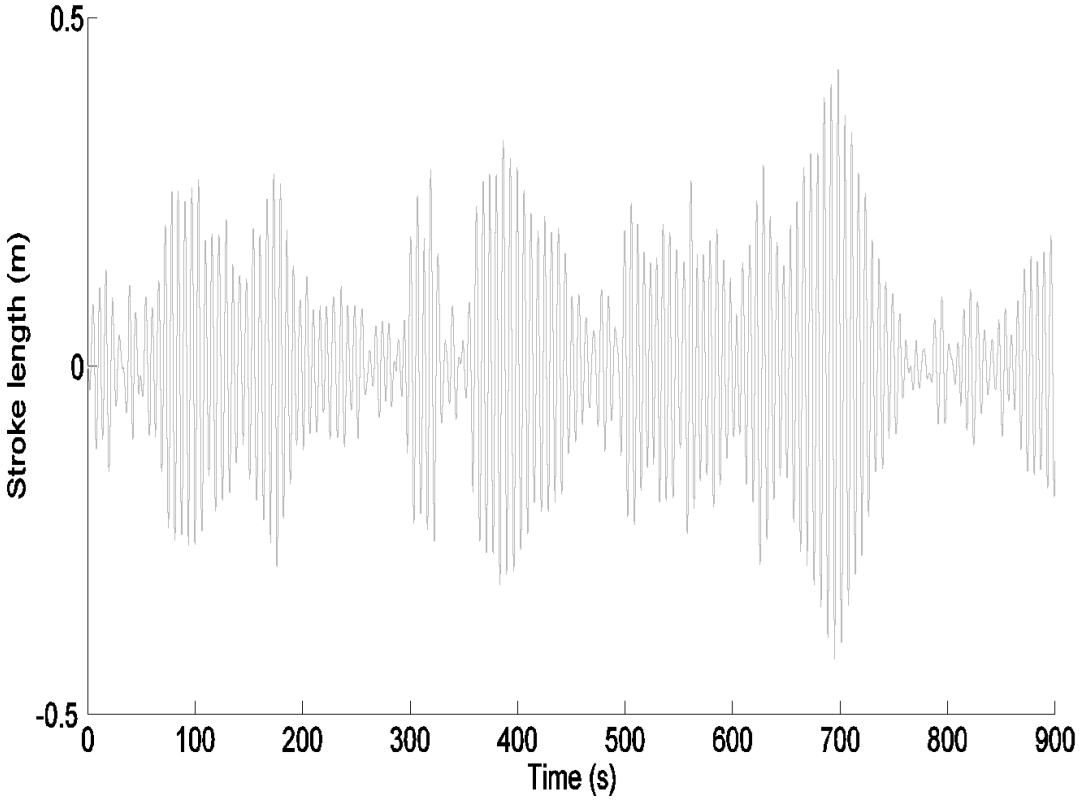

Figure 41: Stroke length of TMD under wind loading

By taking the parameters mentioned above and considering the pounding stiffness as 2.5E5 $N/3^{3/2}$ the analysis is performed on building with PTMD under wind load. As the pounding collar doesn't come into contact with the viscoelastic material any value of pounding stiffness has no effect on performance of PTMD. The results are plotted against the values of the TMD as shown in Figure 42 and Figure 43.

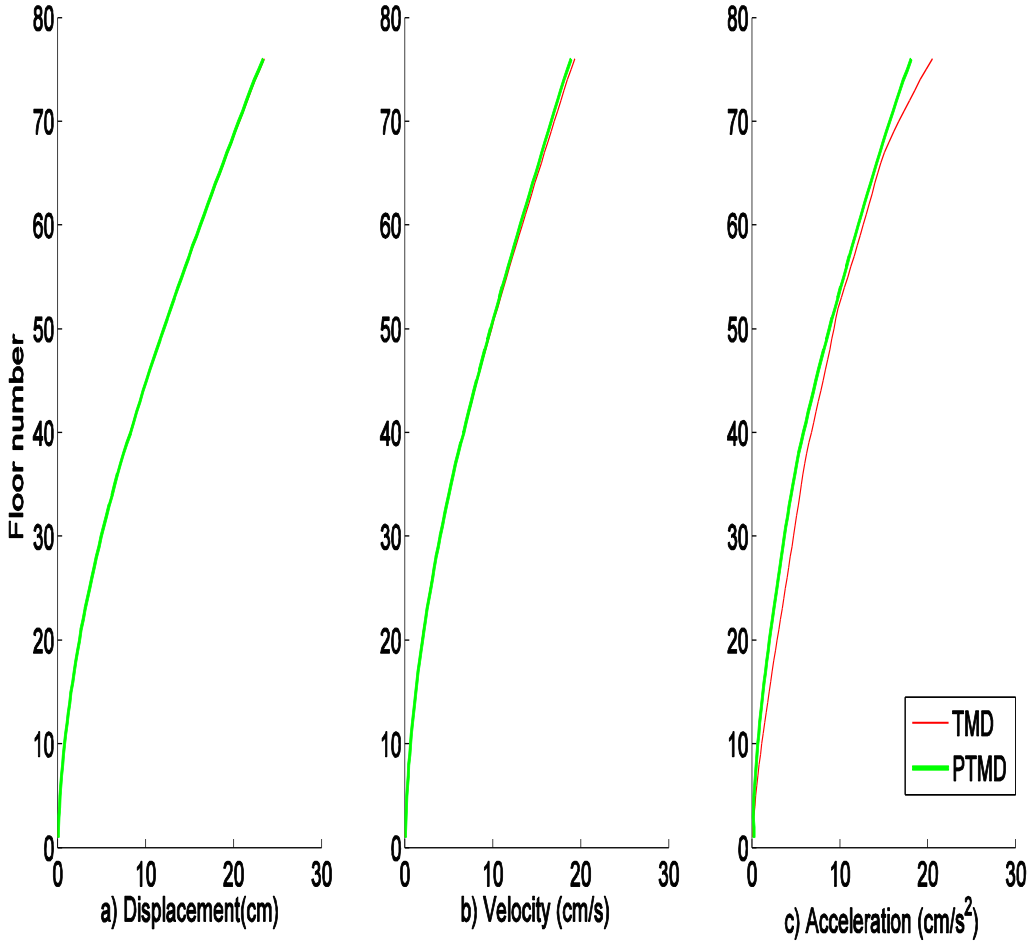

Figure 42: Max displacement, velocity and acceleration of controlled with TMD and PTMD under wind loading

As seen from Figure 42(a) and Figure 42(b) there was no change in the values of maximum displacement and max velocity for building with TMD and PTMD. In case of max acceleration as seen in Figure 42(c) there seems to be little amount of decrease in top floors which is negligible. In case of standard deviation of displacement, velocity and acceleration under wind loading there is no change as seen in Figure 43.

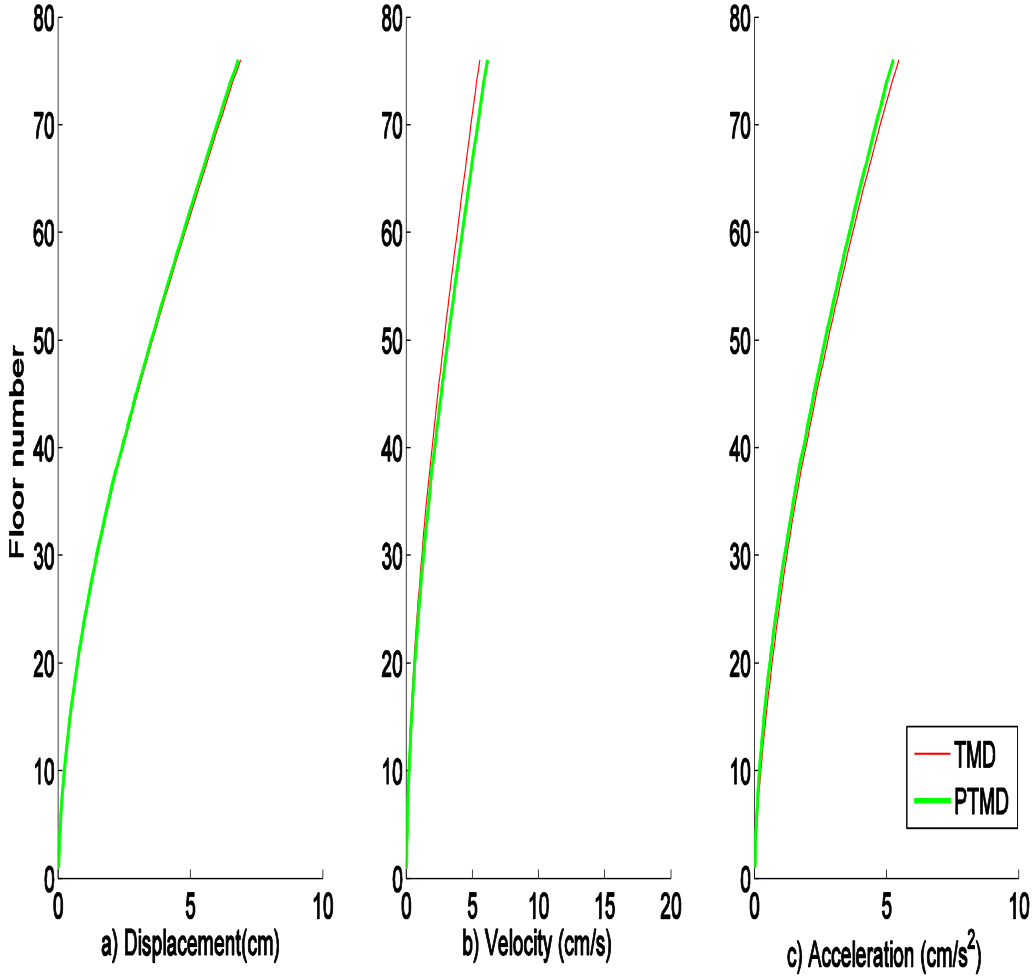

Figure 43: Standard deviation of displacement, velocity and acceleration of building controlled with TMD and PTMD under wind loading

Responses of the building with PTMD under earthquake loading

The simulations are run under the earthquake and the stroke length was plotted for different values of the pounding stiffness to find out the optimal value as shown in Figure 44. From the results we found out that for the same gap length, pounding stiffness has some impact on the reduction in stroke length which means the dissipation of energy. When we reduced the pounding stiffness by a significant amount (0.1E5 $N/m^{3/2}$) the VE material becomes too soft and allows the pouding collar penetrate through its surface without absorbing any energy. The stroke length for the remaining values of the pounding stiffness were the same until 10 s of excitation and shows

variation after that. It can be seen from Figure 44 that when pounding stiffness was 2.5E5 N/m$^{3/2}$ the stroke length is reduced after 10 s when compared to the other values. There we can form a primary conclusion for optimal pounding stiffness as 2.5E5 N/m$^{3/2}$.

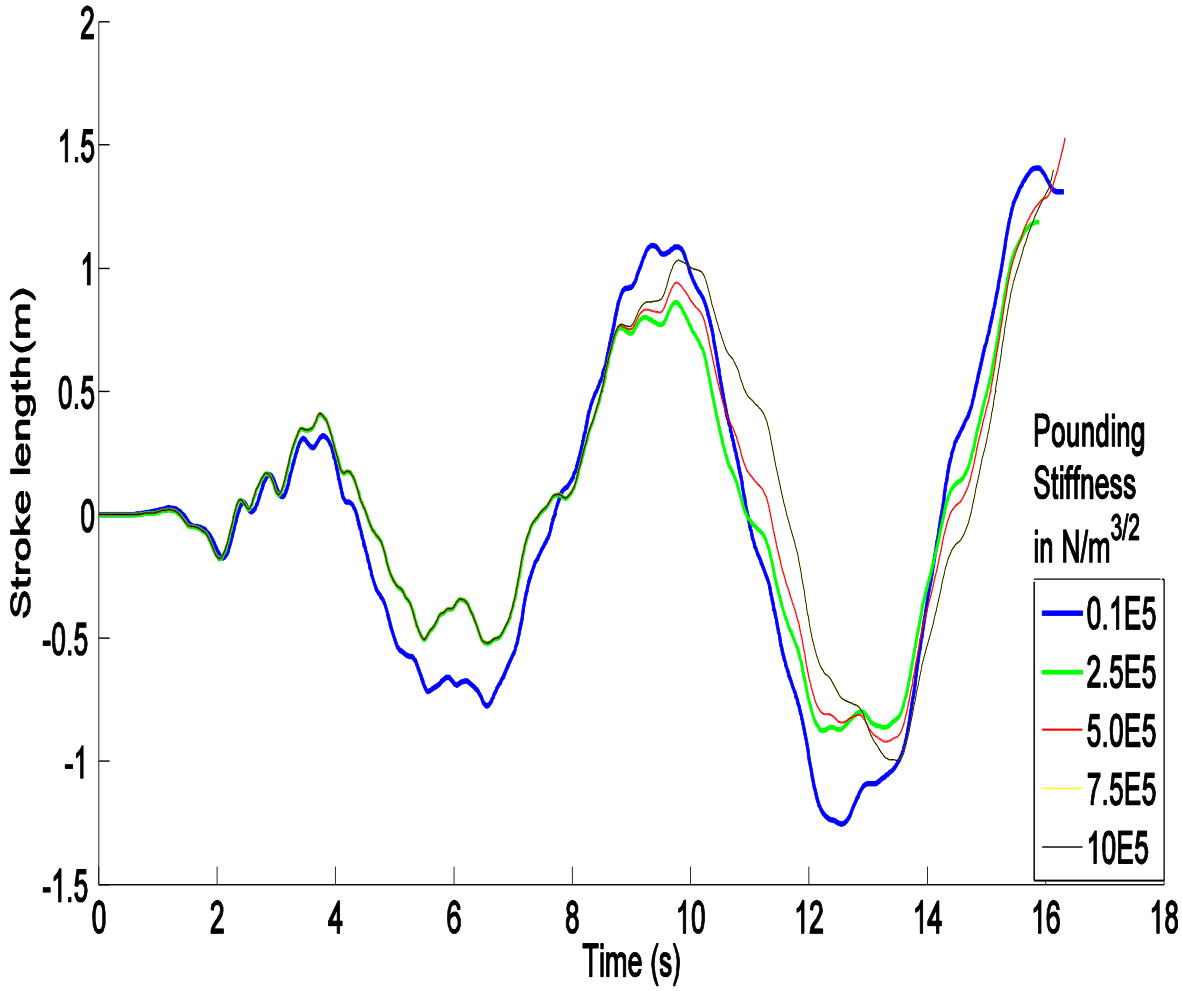

Figure 44: Stroke length for different values of pounding stiffness of PTMD

Even though we consider optimal pounding stiffness as 2.5E5 N/m$^{3/2}$, the stroke length of some of the other values of pounding stiffness were same until 10s and doesn't have a significant difference.

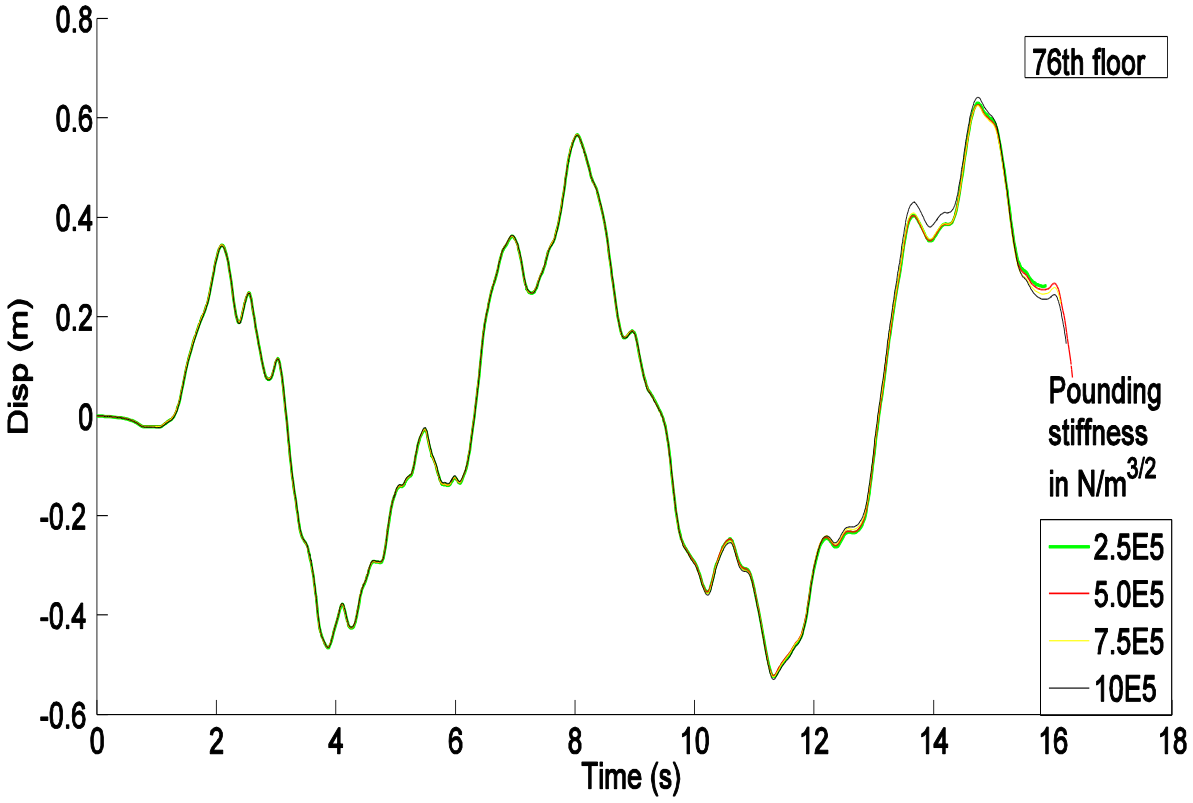

Figure 45: Displacements of the 76th floor for different values of pounding stiffness

Figure 45 shows the displacement of 76th floor of building with PTMD under earthquake. As from the observations from the figure there was no effect with the change in pounding stiffness until 13s. After 13s as we can see in Figure 45 there is a very less amount of reduction in displacement for values of 2.5, 5.0 and 7.5E5 pounding stiffness in 76th floor. Similarly from Figure 47 and Figure 48 shows the displacements of 70th floor where there is little reduction of 0.025 m after 13.5 s for some values of pounding stiffness. We cannot conclude from this the best value of pounding stiffness which increases the efficiency of PTMD. The accelerations plots should be observed further to find out the pounding stiffness value that gives the best results.

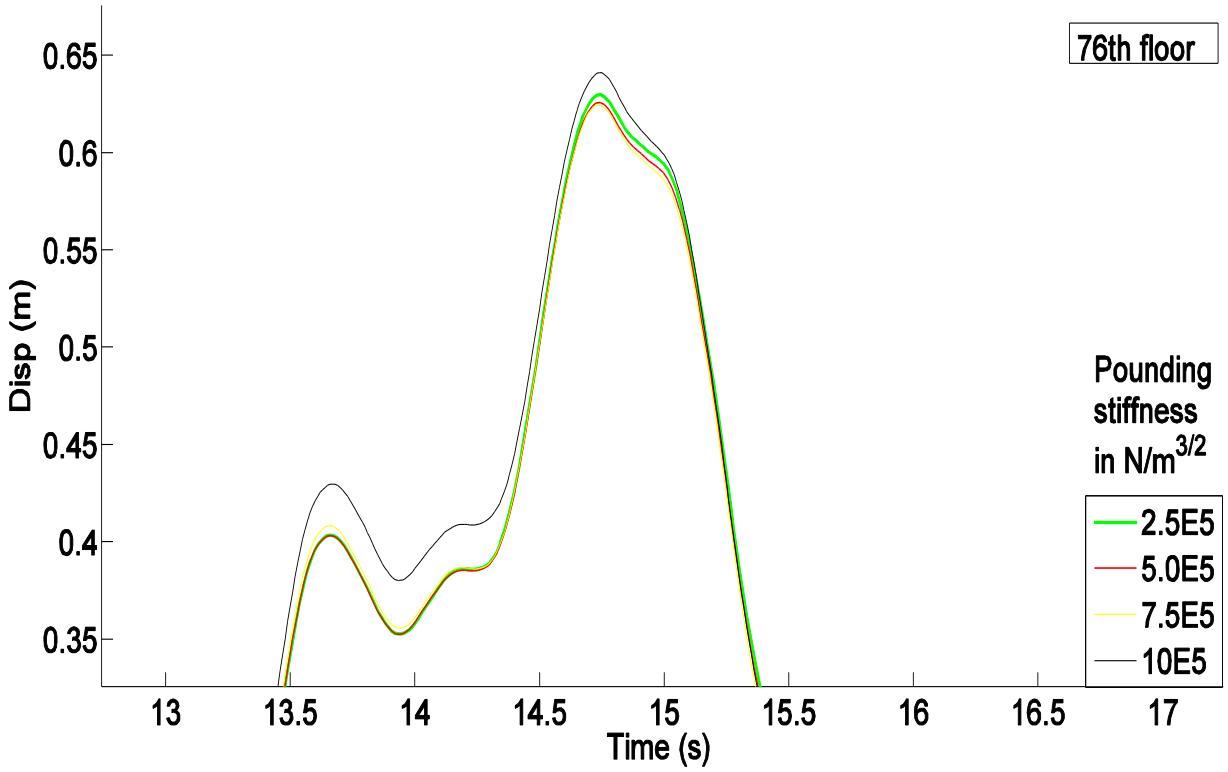

Figure 46: Displacements of the 76th floor in detail

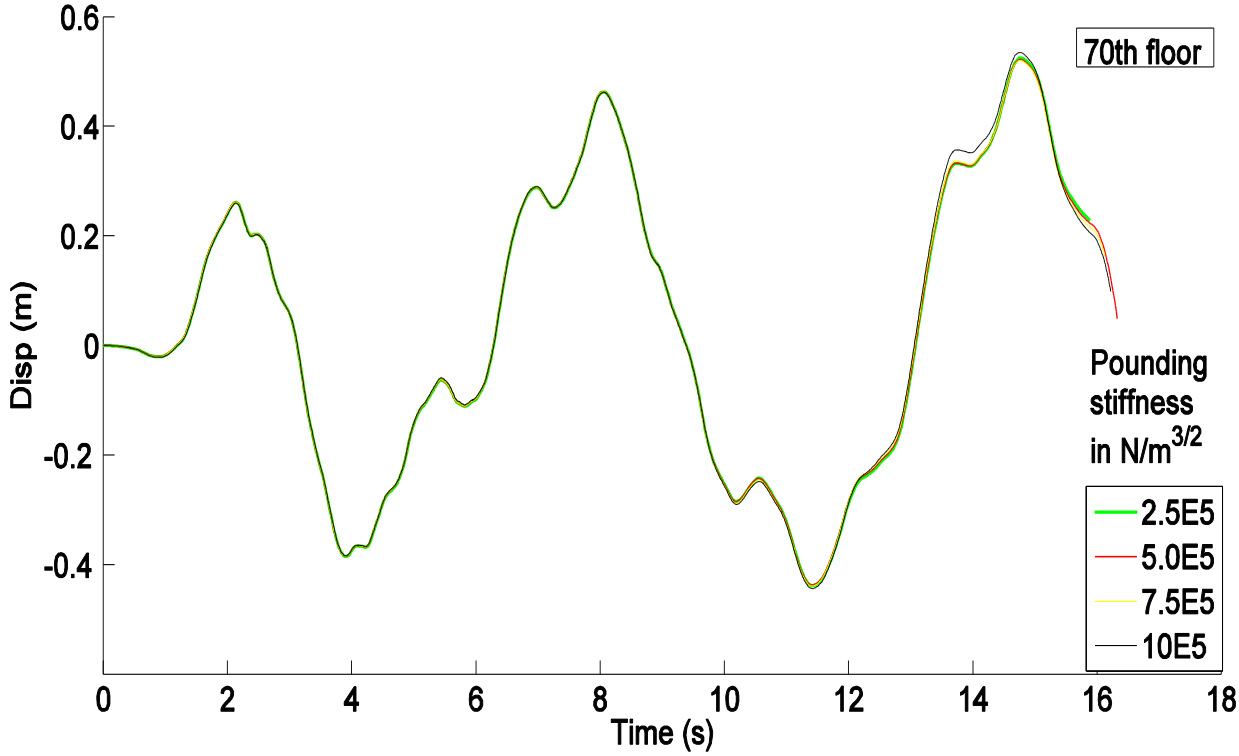

Figure 47: Displacements of the 70th floor for different values of pounding stiffness

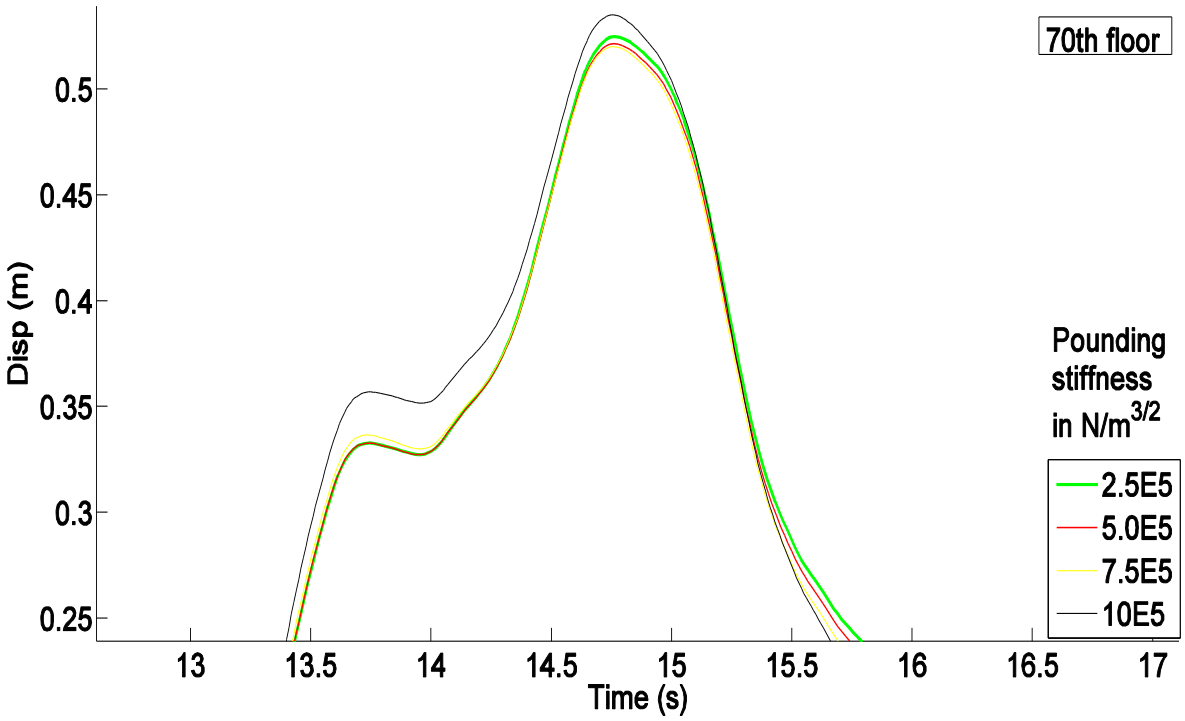

Figure 48: Displacements of the 70th floor in detail

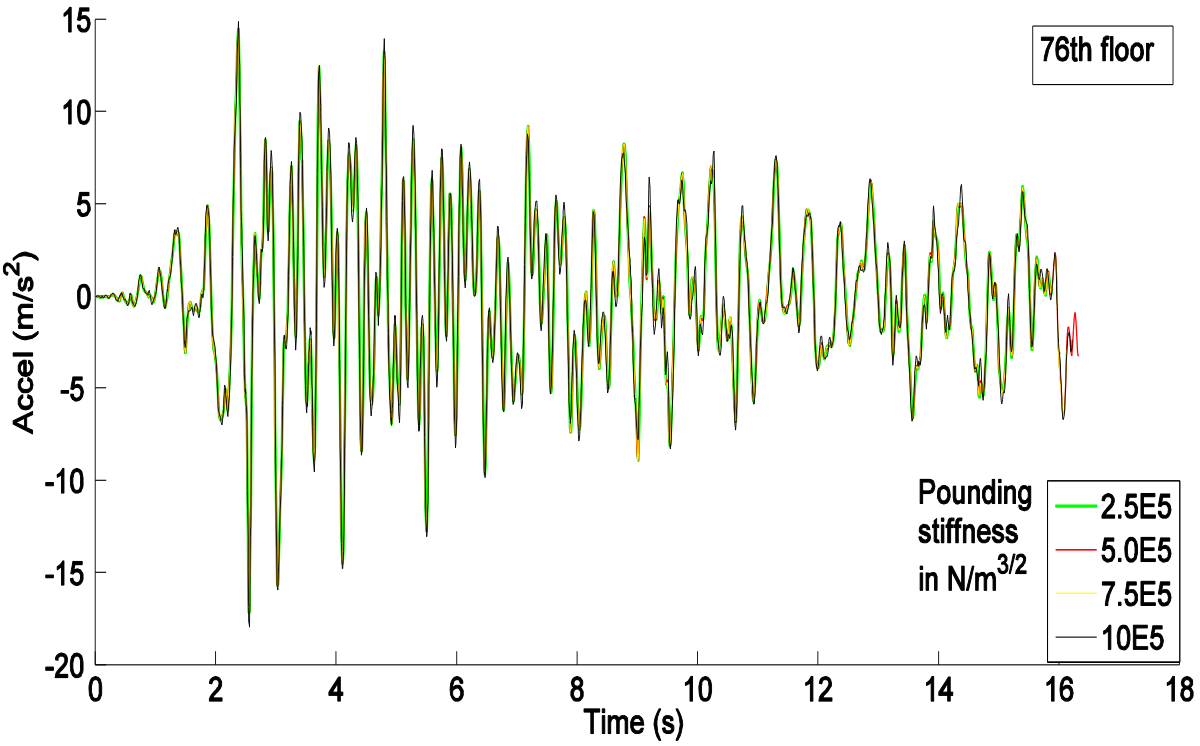

Figure 49: Acceleration of floor 76 for different values of pounding stiffness

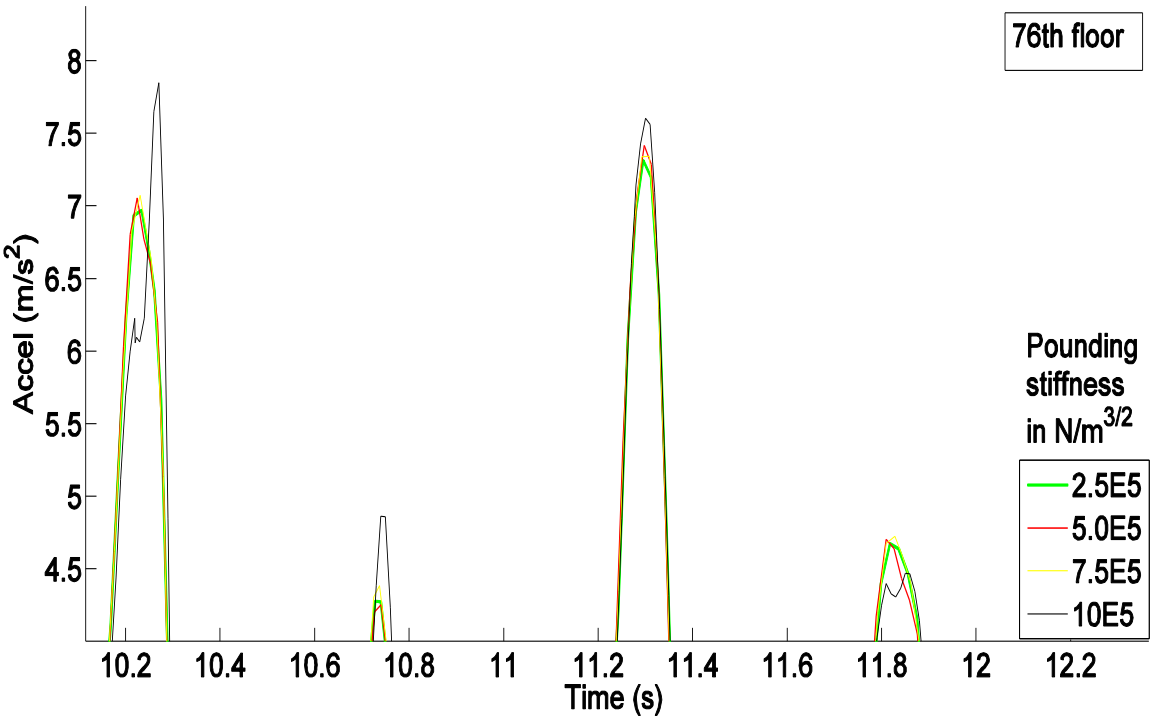

Figure 50 : Acceleration of floor 76 in detail

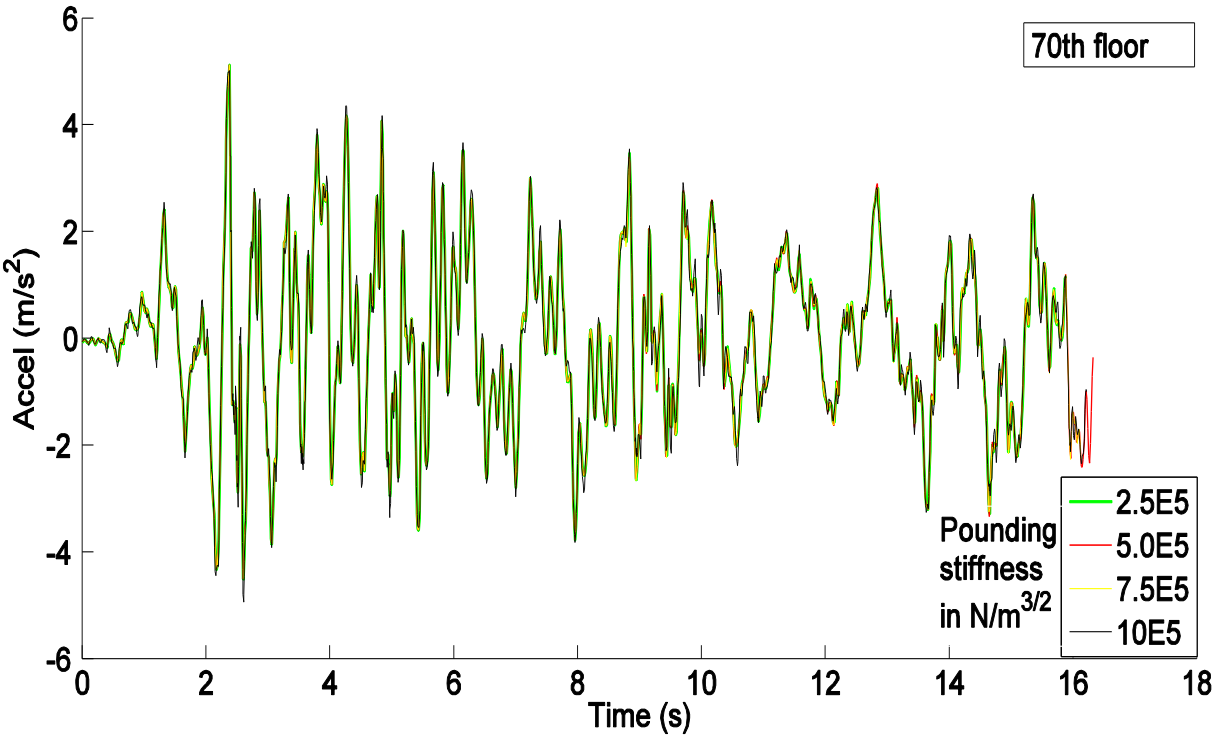

Figure 51 : Acceleration of floor 70 for different values of pounding stiffness

The accelerations of the top floor of the building is plotted for different values of pounding stiffness as shown in Figure 49. It looks alike for all the values of pounding stiffness, but when observed closely, there is a significant decrease of 1m/s² decrease in acceleration at 10.2 s and 0.5m/s² at 11.3 s of earth excitation for pounding stiffness value of 2.5E5 N/m³/². Similarly the acceleration of floor 70 is also plotted as shown in Figure 51and Figure 52.

We can see that there is a significant amount of reduction in acceleration at 9.7 s for pounding stiffness 2.5E5 N/m³/². But the acceleration at 10.1 is almost equal for all values of pounding stiffness. From this results, we can select the optimum value of pounding stiffness as 2.5E5 N/m³/².

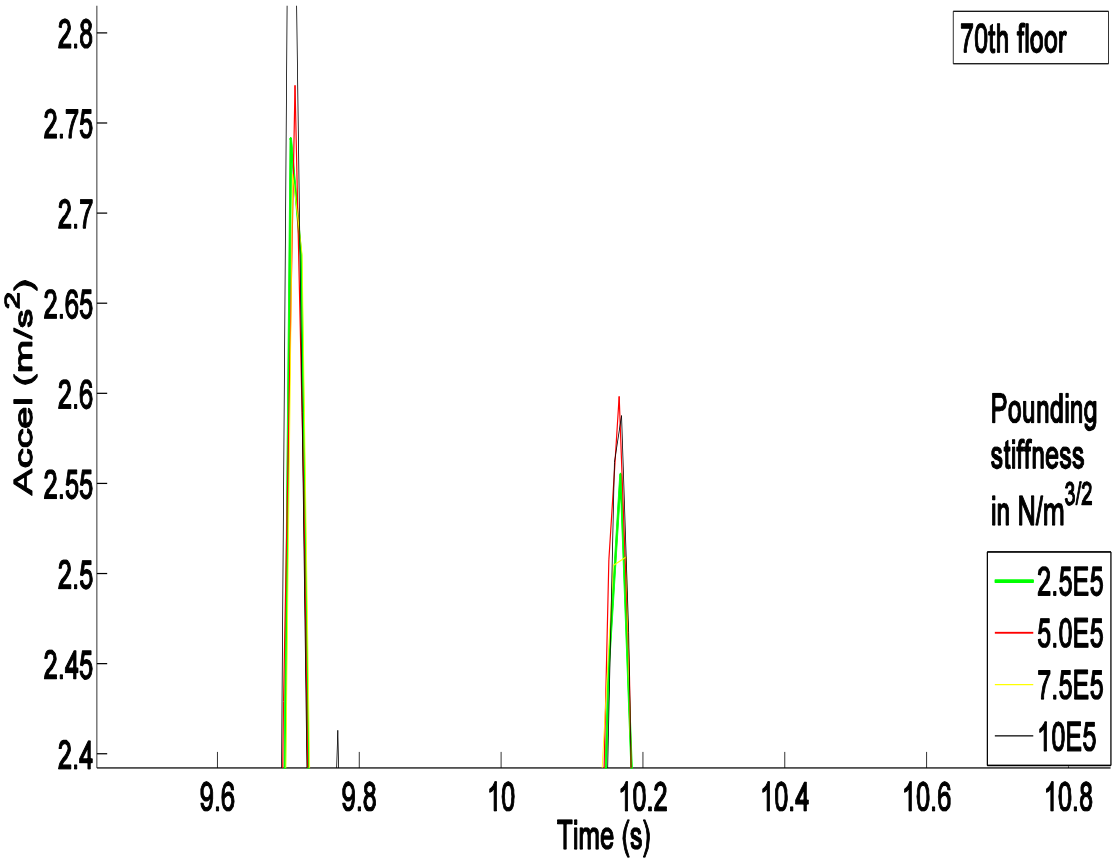

Figure 52 : Acceleration of floor 70 in detail

The responses of the building with PTMD under earthquake loading are obtained for the optimum value of pounding stiffness and other parameters. The maximum and standard deviation of displacement, drift ratios and acceleration of building with PTMD is plotted against uncontrolled and building with TMD as shown in Figure 53 and Figure 55.

From the Figure 53we can see that there is a significant decrease in displacement and drift ratios when TMD is placed on the top floor of the building. The displacement of the top floor is reduced from 0.95m to 0.75m as shown in Figure 53 due to the addition of TMD. But due to the addition of PTMD the displacement of the top floor is not reduced significantly from that of TMD and same goes for drift ratios. The addition of TMD has no effect on the acceleration of the building on the top floor. But due to the addition of PTMD the acceleration of Top floor has reduced more than 2.5m/s² which is very significant as shown in Figure 54.

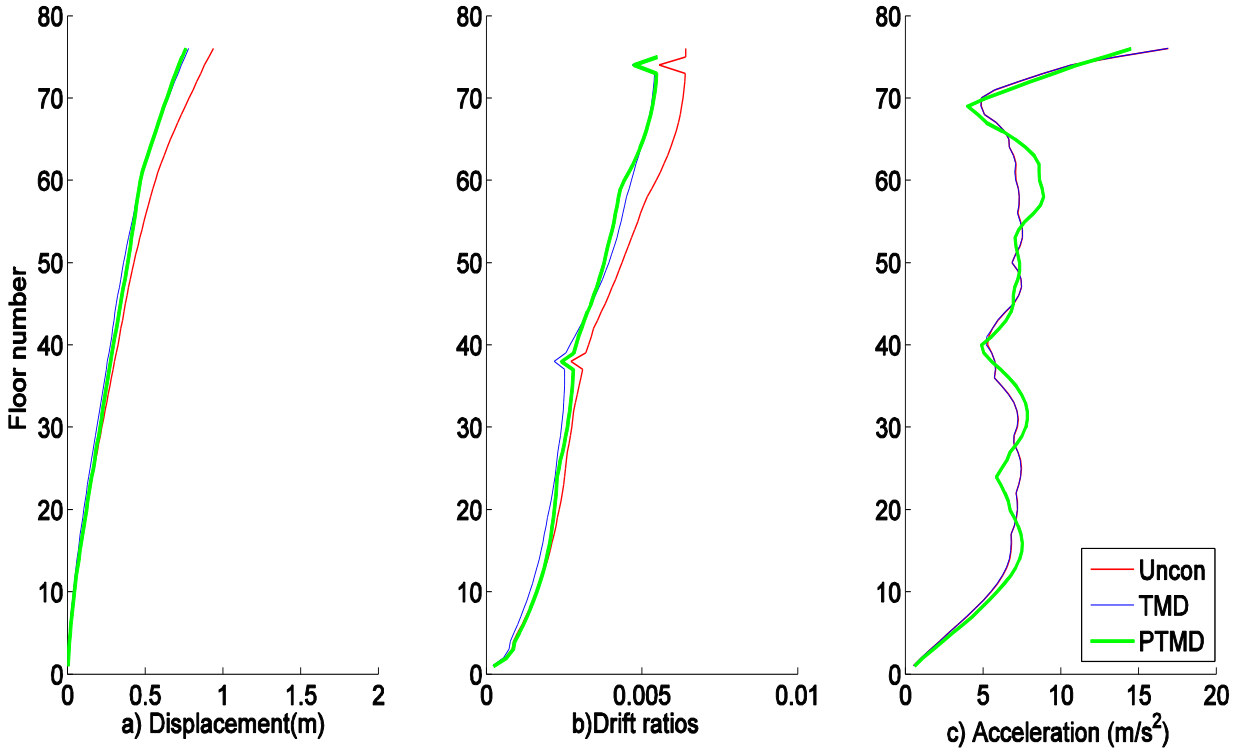

Figure 53: Maximum displacement, drift ratios and acceleration of uncontrolled building and building with PTMD, TMD under earthquake loading

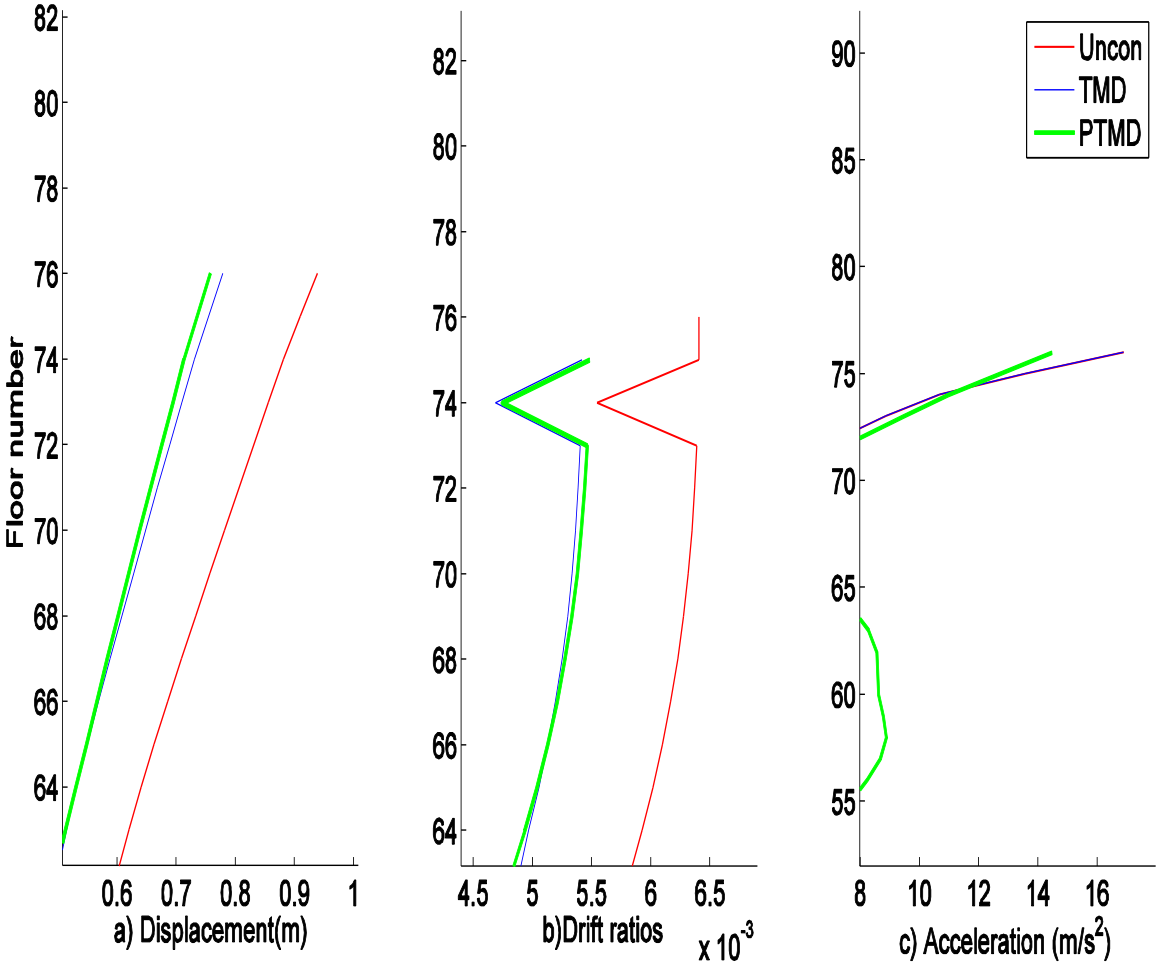

Figure 54: Maximum displacement, drift ratios and acceleration of the top floor of uncontrolled building and building with PTMD, TMD under earthquake loading.

The standard deviation of displacement is reduced from 0.45m to 0.35m of the top Floor due to the addition of TMD and drift ratios are reduced from 2.5E-3 to 2.1E-3 of top floor. Unlike max acceleration there is no change in standard deviation of acceleration due to addition of TMD and PTMD. The values are similar to that of uncontrolled building which can be seen from Figure 55.

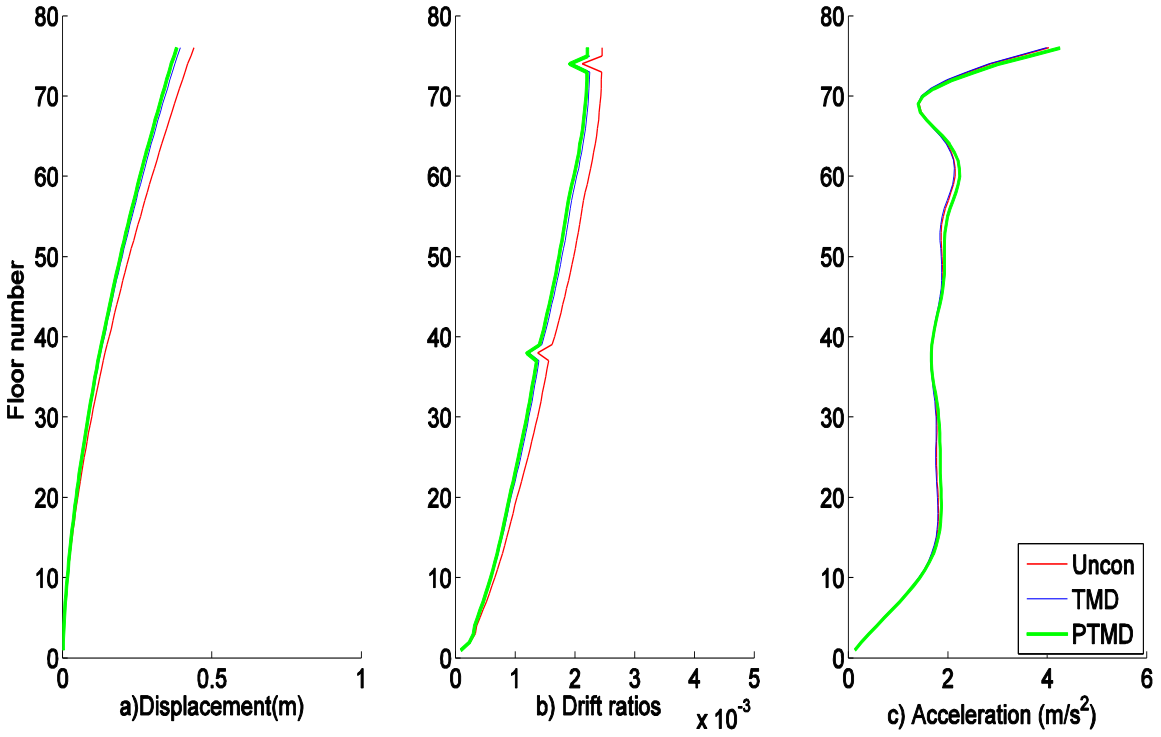

Figure 55: Standard deviation of displacement, drift ratios and acceleration of uncontrolled building and building with PTMD, TMD under earthquake loading

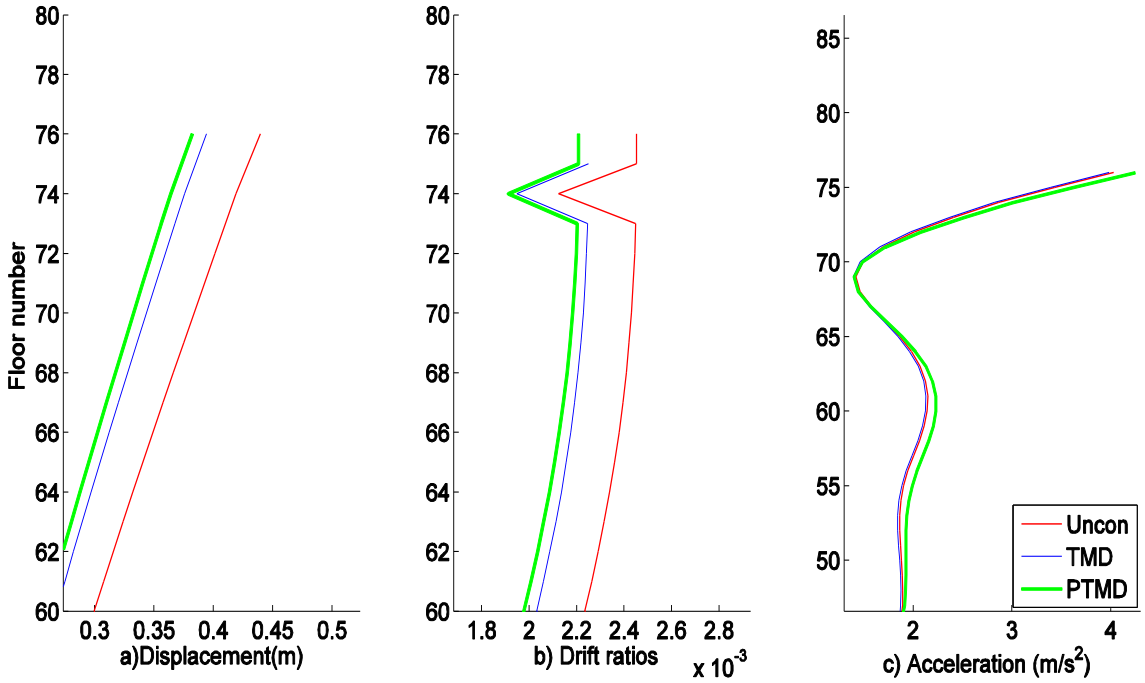

Figure 56: Standard deviation of displacement, drift ratios and acceleration of uncontrolled building and building with PTMD, TMD under earthquake loading

Responses of the building with viscous dampers under earthquake loading

The role of damping:

It was shown that the wind-induced responses of the tower are out of the comfort and security limits. Also the earthquake loading produced relatively high accelerations that can be damaging to the non-structural components of the building. Because of this, it is essential to design a control system that can work for both wind and earthquake loadings. This means that it is important to produce damping in the building in order to reduce its response. Damping is the dissipation of energy from an oscillating system, primarily through friction. The kinetic energy is transformed into heat.

Although, finite element software packages can help to provide mode shapes, modal masses and modal frequencies of the desired modes, it does not provide information about damping in buildings. This is because unlike mass and rigidities that are distributed in a well-known matter along the elements, damping however is related to friction between joints and some hysteresis in the material which is difficult to be modeled. However, there is no convenient mean to refine the predictive capabilities regarding inherent structural damping, owing to its association with a number of complex mechanisms and even non-structural elements.

Unlike the uncertainty in the stiffness, uncertainty in structural damping is comparatively high. However, while the main objective of adding damping via specially engineered components is to reduce building motion and in some cases design loads, a good effect is that the uncertainty in the damping level can also be reduced. Viscous dampers offers an attractive means to directly increase damping in buildings and other types of civil engineering structures.

The challenge in using such devices in tall buildings is related to where to put the device in the building. Unlike short and shear buildings, in which floor rotational angles are relatively

small and there is a significant inter-story drift under dynamic loads, slender tall buildings, however, may behave like a cantilever. Cantilever like behavior of the building hinders the design of an effective internal bracing system. As shown in Figure 57, for shear buildings, internal bracings with viscous dampers are recommended, while for cantilever-like buildings outer bracings with viscous dampers are more effective. Since the displacement across the damper can be relatively small, a lever mechanism is recommended for motions magnification (Aly, 2015; Aly and Abburu, 2015).

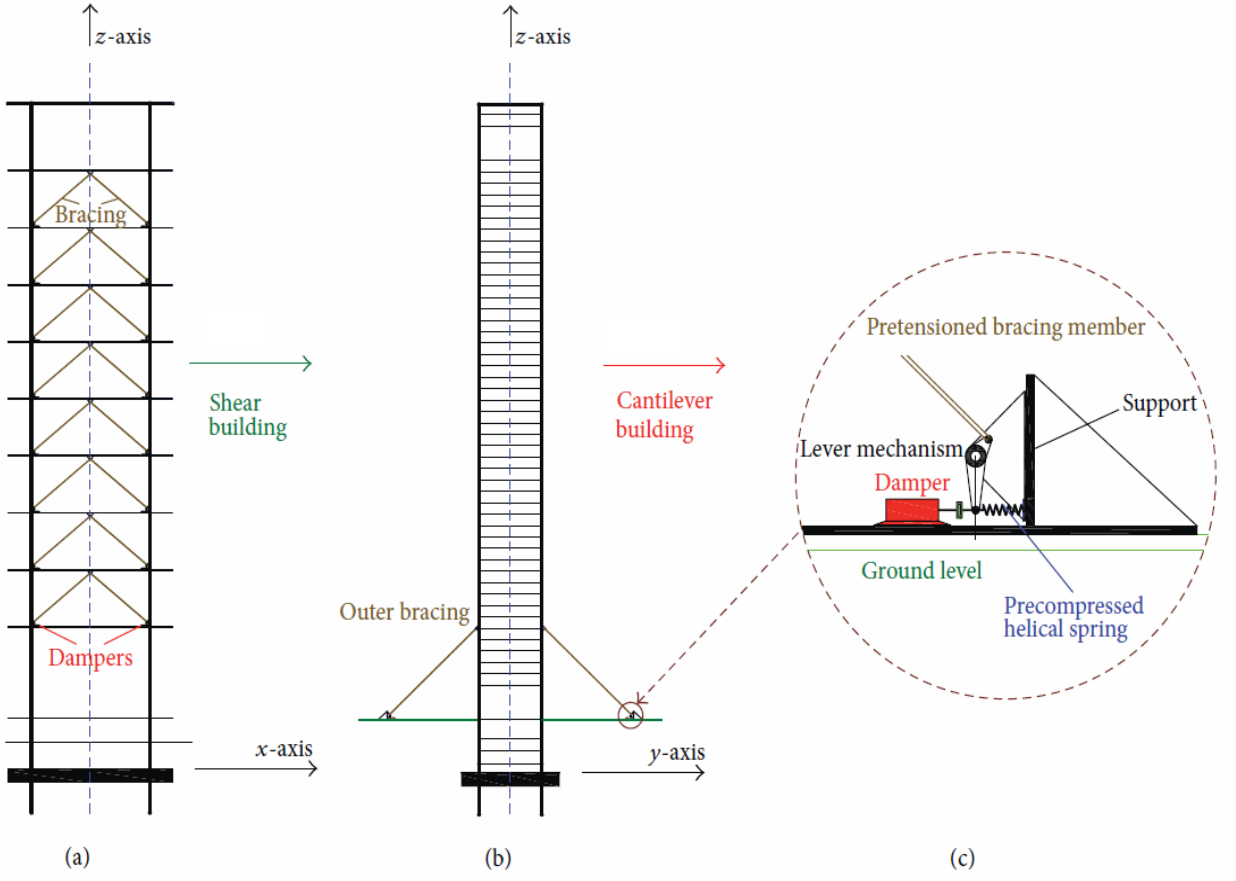

Figure 57: Proposed configuration of viscous dampers with bracing system: (a) bracings with dampers between adjacent floors for shear buildings; (b) outer bracings with dampers for cantilever and slender buildings; (c) damping unit consisting of a viscous damper, helical spring, and a lever mechanism for drift amplification across the damper.

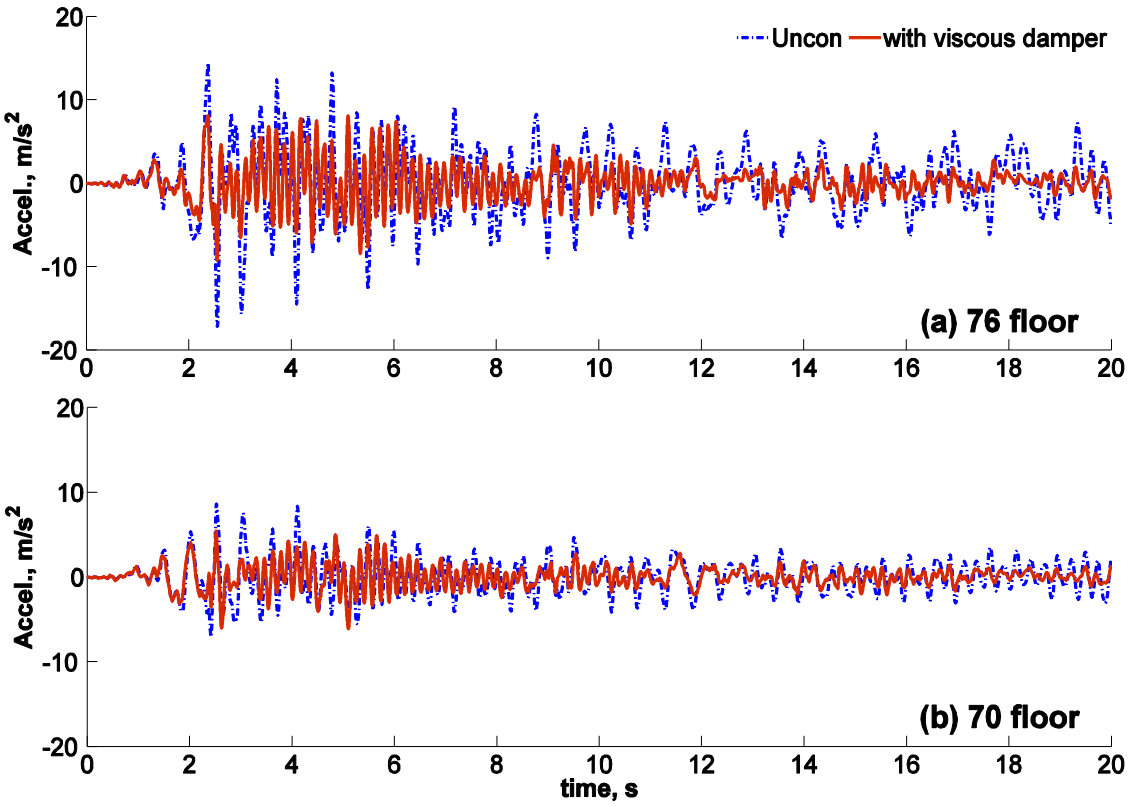

Figure 58: Acceleration response of the building under earthquake loadings for both uncontrolled and with viscous dampers: (a) response of the 76 floor; (b) response of the 70 floor.

Figure 58 shows the acceleration response of the building under earthquake loadings for both uncontrolled and with viscous dampers, with outer bracing connection as shown in Figure 57(b). The bracing system was connected between floor number 20 and the ground. The reason for connecting the bracing system at floor 20 to make the bracing system more efficient. In the Figure 58(a) the reduction in acceleration of 76th floor was throughout the time of earthquake excitation due to the addition of viscous dampers. The impact of the earthquake is very high at the initial stages. The viscous dampers reduced the acceleration of the top floor by 5m/s² at time 2s where the acceleration was very high. Similarly the acceleration of 70th floor is also reduced by nearly 2m/s² by the addition of viscous dampers which is very significant. It promises to build more resilient structures that can resist earthquakes with minimum damage.

Chapter 5
Discussion of Results

The TMD was very effective in reducing the maximum displacements of the top floor of building by 28.6% and acceleration by 31.25% under wind loading. The maximum shear force at ground floor is reduced by 27.2% and standard deviation of shear force by 41.6% with the addition of TMD. Similarly maximum and standard deviation of BM at ground floor is reduced by 20% and 40%, respectively. The TMD proved to be effective in reducing the effects of wind on buildings. Unlike wind, earthquakes vibrates at higher accelerations and high period earthquakes can cause significant damage to the internal members of the building. Under earthquake TMD reduced the maximum displacement of top floor by 25% and standard deviation of displacement by 11%. The TMD has no effect in reducing the absolute acceleration, shear force and bending moment of the building. When the TMD was replaced by a PTMD, under earthquake loadings, there was no significant reduction in the maximum displacement at the top floor, but there was 14.7% reduction in the maximum acceleration of the top floor. However, there was no significant change in the standard deviation of the top floor acceleration. It is worthy to mention that parametric study of the PTMD may help find the optimum parameters that further improve the efficacy of the PTMD. The door is open for researchers to further investigate the performance of the PTMD.

Although the TMD is shown to be effective in the response reduction of tall buildings under wind loads, they are large, heavy, and take up valuable space at the top of the building. Moreover, they are an additional cost to the project. On the other hand, viscous dampers and semi active dampers can be used as alternatives to alleviate these problems. These devices do not require frequency tuning, and while there is an optimum resistance characteristic for each application, the overall damping achieved is usually insensitive to the exact resistance characteristic of the device

(Smith and Willford 2007). It is therefore sometimes possible to damp several modes with one device. The benefits of using dampers in tall buildings under wind loads are discussed in Hart and Jain (2013). Magnetorheological (MR) dampers were used to reduce the accelerations and the design loads of a building tower in the two lateral directions (Aly et al. 2011, Figure 57). MR dampers have received a renewed interst as means by which vibrations can be effectively suppressed in buildings under wind and earthquake loadings (Dyke 1996; Metwally et al. 2006; Aly et al. 2011; Aly 2013b; Aly 2015). Also, as shown in the current study, viscous dampers can be used for vibration mitigation under multi-hazard loading brought by both wind and earthquakes.

It is important to mention that, even if the inter-story drift ratios in tall buildings may be relatively small under earthquakes, with no significant risk issues for the main force resisting system of the structure, nonstructural systems represent a high percentage of loss exposure of buildings to earthquakes. For instance, the *ceiling-piping-partition* system may be exposed to significant damage under earthquakes. Past earthquakes and numerical modeling considering potential earthquake scenarios show that the damage to this system causes the preponderance of the U.S. earthquake related losses (Weiser et al., 2013; Zaghi et al., 2012).

In the last two centuries, some major structural failures due to winds have occurred. Large structures have experienced failures as well – for example, the collapse of the Ferry bridge cooling towers in the U.K. in 1965, and the permanent deformation of the columns of the Great Plains Life Building in Lubbock, Texas, during a tornado (1970). Moreover, many super tall buildings have seen to suffer from wind loads leading to structural annoying vibrations that cause, some time, horrible effects on the occupants. Such phenomenon needs a deep understanding in order to allow for providing adequate solutions.

Structural response prediction and reduction under multi-hazard loadings form an integral part of the building design process, providing architects and design engineers with a comprehensive understanding of the interaction between environmental factors and building design. A proper connotation of this interaction can provide significant cost savings to building owners in terms of developmental, material, and operational costs. To expose them to the methods and procedures for the efficient application of wind studies in designing a building more economically than a similar building designed with more conservative building code provisions.

By so doing, the dynamic response of the building to wind effects (buffeting and vortex shedding) is virtually eliminated; leading to substantially reduced lateral design forces and assured occupant comfort. Substantial reductions in structural member size and construction cost savings can be realized in many cases. This may significantly improve the economic viability and sustainability of a development.

The safety and sustainability of buildings under wind and seismic hazards is a major concern, and it is a challenge for both the government and building owners. There is an argument for developing a decision support tool to assist decision-makers in the mitigation and retrofitting of buildings for multi-hazard environments, to improve the safety and sustainability of buildings. Potential damping solutions, in terms of selecting and implementing strategies to mitigate damages and minimize the consequences of failure are therefore needed. It is envisaged that using a proper mitigation framework, and incorporating real-time data, a decision making tool for resilient and sustainable buildings can be developed. This will lead to sustainable solutions that can improve the performance of buildings under wind/earthquakes, reduce building life cycle costs and increase efficiency in design.

Chapter 6
Conclusion

The performance of high-rise buildings is effected greatly, in terms of resiliency and serviceability, by multi-hazard loadings. Typically, multi-hazard loadings brought by wind and earthquakes lead to significant vibrations in tall buildings. These vibrations can be detrimental to tall buildings, and they can greatly impact their safety and functionality. To reduce these vibrations, in the current study, several vibration suppression devices are investigated. A 76-story bench mark building was occupied by a TMD and its performance under multi-hazard was studied. The TMD is very effective in reducing the maximum displacements of the top the floors of the building by 28.6%, and the acceleration response by 31.25% under wind loadings. The maximum shear force at ground floor is reduced by 27.2% and the standard deviation of shear force was reduced by 41.6%, with the addition of the TMD. Similarly, the maximum and standard deviation of the overall bending moment at the ground floor is reduced by 20% and 40%, respectively. The TMD proved to be effective in reducing the effects of wind on buildings. Unlike wind loadings, which mostly excite lower modes of vibrations, earthquakes tend to excite higher modes, and prolonged earthquakes can cause significant damage to the internal members (non-structural components) of the building. Under earthquake loadings, TMD reduced the maximum displacement of top floor by 25% and the standard deviation of displacement by 11%. The TMD has no significant effect in reducing the absolute acceleration, base shear force, and the overall turning moment of the building. When the TMD was replaced by a PTMD, under earthquake loads, there was no significant reduction in the maximum displacement at the top floor, but there was 14.7% reduction in the top floor acceleration. Unlike maximum the reduction in the acceleration, there was no significant change in the standard deviation of acceleration at the top floor.

This means that the PTMD is may be performing better than a conventional TMD in high-rise buildings, in terms of acceleration reduction. However, due to the high non-linearity nature of the PTMD, the efficiency may be affected if the parameters are not carefully chosen. Future research should focus on finding the optimum pounding stiffness, coefficient of restitution, and the gap lengths to increase its efficiency under earthquakes. The study showed that viscous dampers can significantly reduce the acceleration response of tall buildings under earthquakes, with promises to build more resilient structures that can resist multi-hazard loadings. The main objective of the current study was to further the understanding of the impact of multi-hazard loading, brought by wind and earthquakes, on the behavior of high-rise buildings, in order to apply such knowledge to design.

References

Aly, A.M., Abburu, S. (2015), "On the Design of High-Rise Buildings for Multihazard: Fundamental Differences between Wind and Earthquake Demand," *Shock and Vibration*, **2015**, Article ID 148681, 22 pages.

Aly, A.M., (2015), "Control of wind-induced motion in high-rise buildings with hybrid TM/MR dampers", *Wind and Structures*, **21**(5), 565-595.

Aly, A.M. (2014a), "Proposed robust tuned mass damper for response mitigation in buildings exposed to multidirectional wind," *The Structural Design of Tall and Special Buildings*, **23**(9), 664-691.

Aly, A.M. (2014b), "Vibration control of high-rise buildings for wind: a robust passive and active tuned mass damper," *Journal of Smart Structures and Systems*, **13**(3), 473-500.

Aly, A.M., (2013a), "Pressure Integration Technique for Predicting Wind-Induced Response of a High-rise Building," *Alexandria Engineering Journal*, **52**(4), 717-731.

Aly, A.M. (2013b), "Vibration Control of Buildings Using Magnetorheological Damper: A New Control Algorithm," *Journal of Engineering*, **2013**, Article ID 596078, 10 pages.

Attaway, Matlab: A Practical Introduction to Programming and Problem Solving, Butterworth-Heinemann, Amsterdam, The Netherlands, 2009.

Arnold, C. (2013). EARTHQUAKE EFFECTS ON BUILDINGS 4. *Risk Management Series: Designing for Earthquakes-A Manual for Architects (Fema 454/December 2006)*.

ASCE 7-2010, (2010). Minimum design loads for buildings and other structures, ASCE Standard, ASCE/SEI 7-10, American Society of Civil Engineers, Reston, Virginia.

Bhattacharjee, E., Halder, L., & Sharma, R. P. (2013). An experimental study on tuned liquid damper for mitigation of structural response. *International Journal of Advanced Structural Engineering (IJASE)*, **5**(1), 1-8.

Boggs, D.W. and Peterka, J.A. (1989), "Aerodynamic model tests of tall buildings," *Journal of Engineering Mechanics*, ASCE, **115**(3), 618–635.

Davenport, A.G. (1966), "The treatment of wind loading on tall buildings", *Proceedings of a Symposium on Tall Buildings*, Pergamon Press, Southampton, 1-44.

Djilali, N., Gartshore, I.S. (1992), "Effect of leading-edge geometry on a turbulent separation bubble", *American Institute of Aeronautics and Astronautics Journal*, **30**(2), 559-561.

Dragomirescu, E. and Tun, Y. (2014), "Modular repetitive structures as countermeasure to galloping," *Advances in Wind and Structures* (AWAS14), South Korea, August.

Eurocode 1, 2004. Actions on structures - Part 1-4: General actions - Wind actions. prEN 1991-1-4, European Standard.

Geller, R. J., Jackson, D. D., Kagan, Y. Y., Mulargia, F. (1997), "Enhanced: earthquakes cannot be predicted," *Science*, **275**(5306), 1616-1620.

Gu, M., Cao, H. L. and Quan, Y. (2014), "Experimental study of across-wind aerodynamic damping of super high-rise buildings with aerodynamically modified square cross-sections," *The Structural Design of Tall and Special Buildings*, **23**(16), 1225-1245.

Holmes, J.D. (2007), *Wind Loading of Structures (Second Edition)*, Taylor and Francis Group, New York.

Hosseini, S. S., Ghorbani-Tanha, A. K., and Rahimian, M. (2012), "Performance of Tuned Liquid Dampers with Different Tank Geometries for Vibration Control of Structures," In proceedings of *The 15th World Conference on Earthquake Engineering*, Lisbon, Portugal, September.

Iemura, H., Igarashi, A., and Takahashi, Y. (1999), "Substructured hybrid techniques for actuator loading and shaking table tests," In *Proceedings of the First International Conference on Advances in Structural Engineering and Mechanics* (pp. 821-826).

Igarashi, A., Iemura, H., and Suwa, T. (2000), "Development of sub-structured shaking table test method," In *Proceedings of the 12th World Conference on Earthquake Engineering*, Paper No. 1775, January.

Kanamori, H., Hauksson, E., Heaton, T. (1997), "Real-time seismology and earthquake hazard mitigation," *Nature*, **390**(6659), 461-464.

Kareem, A. (1992), "Dynamic Response of High-rise Buildings to Stochastic Wind Loads," *Journal of Wind Engineering and Industrial Aerodynamics*, **42**(1-3), 1101-1112.

Kareem, A. (1998), "Aerodynamic Response of Structures with Parametric Uncertainties," *Structural Safety*, **5**(3), 205-225.

Kareem, A., and Cermak, J. E. (1979), "Wind tunnel simulation of wind structure interactions," *ISA Transactions*, **18**(4), 23-41.

Kasai, K., Maison, B. F., & Patel, D. J. (1990), "An earthquake analysis for buildings subjected to a type of pounding," In *Proceedings of Fourth US National Conference on Earthquake Engineering*, **2**, 289-298, May.

Kim, B. (2013). Prediction of Wind Loads on Tall Buildings: Development and Applications of an Aerodynamic Database. M.S. Thesis, The University of Western Ontario.

Kim, H., & Adeli, H. (2005), "Wind-induced motion control of 76-story benchmark building using the hybrid damper-TLCD system," *Journal of Structural Engineering*, ASCE, **131**(12), 1794-1802

Lamb, H. (1932). *Hydrodynamics*. Cambridge university press. Pan, P., Nakashima, M., and Tomofuji, H. (2005), "Online test using displacement-force mixed control," *Earthquake Engineering and Structural Dynamics*, **34**(8), 869-888.

Maison, B. F., & Kasai, K. (1990), "Analysis for a type of structural pounding," *Journal of Structural Engineering*, ASCE, **116**(4), 957-977.

Mendis, P., Ngo, T., Haritos, N., Hira, A., Samali, B., & Cheung, J. (2007), "Wind loading on tall buildings," *EJSE Special Issue: Loading on Structures*, **3**, 41-54.

Metwally, H.M., El-Souhily, B.M. and Aly, A. (2006), "Reducing vibration effects on buildings due to earthquake using magneto-rheological dampers," *Alexandria Engineering Journal*, Elsevier, **45**(2), 131-140.

NatHaz. (2015), Aerodynamic Loads Database, http://aerodata.ce.nd.edu, webpage was visited in November.

Ogata, K. 2010. Modern Control Engineering. 5th Edition, Prentice Hall.

Rezaee, M., Aly, A.M. (2015), "Vibration Control in Wind Turbines for Performance Enhancement: A Comparative Study", *Wind and Structures*, **21**(5), in press.

Rosa, L., Tomasini, G., Zasso, A. and Aly, A.M. (2012), "Wind-induced dynamics and loads in a prismatic slender building: modal approach based on unsteady pressure measures," *Journal of Wind Engineering and Industrial Aerodynamics*, **107-108**, 118-130.

Richards, P. and Hoxey, R. (2004), "Quasi-steady theory and point pressures on a cubic building", *Journal of Wind Engineering and Industrial Aerodynamics*, **92**, 1173-1190.

Simiu, E. (1996), *Wind Effects on Structures (Third Edition)*, John Wiley and Sons, Inc., New York.

Smith, R.J. and Willford, M.R. (2007), "The damped outrigger concept for tall buildings," *The Structural Design of Tall and Special Buildings*, **16**, 501-517.

Tait, M.J., Isyumov, N., and El Damatty, A. (2007), "Effectiveness of a 2D TLD and its numerical modeling," *Journal of Structural Engineering*, ASCE, **133**(2), 251-263.

Tait, M. J., Isyumov, N., and El Damatty, A.A. (2008), "Performance of tuned liquid dampers," *Journal of Engineering Mechanics*, ASCE, **134**(5), 417-427.

Takanashi, K., Udagawa, K., and Tanaka, H. (1980), "Inelastic Response of H-Shaped Columns to Two Dimensional Earthquake Motions," *Bulletin of Earthquake Resistant Structure Research Center*, (**13**).

Takanashi, K., Udagawa, K., Seki, M., Okada, T., and Tanaka, H. (1975). Nonlinear earthquake response analysis of structures by a computer-actuator on-line system. *Bulletin of Earthquake Resistant Structure Research Center*, **8**, 1-17.

Taylor, Z., Palombi, E., Gurka, R., Kopp, G.A. (2011), "Features of the turbulent flow around symmetric elongated bluff bodies," *Journal of Fluids and Structures*, **27**, 250-265.

Vranes, K., Pielke Jr, R. (2009), "Normalized earthquake damage and fatalities in the United States: 1900–2005," *Natural Hazards Review*, **10**(3), 84-101.

Weiser, J., Pekcan, G., Zaghi, E., Itani, A., Maragakis, M. (2013), "Floor Acceleration in Yielding SMRF Structures," *Earthquake Spectra*, **29**(3), 987-1002.

Wolf, J. P., and Skrikerud, P.E. (1980), "Mutual pounding of adjacent structures during earthquakes," *Nuclear Engineering and Design*, **57**(2), 253-275.

Yang, J.N., Agrawal, A.K., Samali, B., and Wu, J.C. (2004), "Benchmark problem for response control of wind-excited tall buildings," *Journal of Engineering Mechanics*, ASCE, **130**(4), 437-446.

Zaghi, A. E., Maragakis, E. M., Itani, A., and Goodwin, E. (2012), "Experimental and analytical studies of hospital piping assemblies subjected to seismic loading," *Earthquake Spectra*, **28**(1), 367-384.

Zasso, A., Aly, A.M., Rosa L. and Tomasini, G. (2008), "Wind induced dynamics of a prismatic slender building with 1:3 rectangular section," BBAA VI International Colloquium on Bluff Bodies Aerodynamics & Applications, Milano, Italy, 20-24 July.

Zhang, P., Song, G., Li, H., and Lin, Y. (2013), "Seismic Control of Power Transmission Tower Using Pounding TMD," *Journal of Engineering Mechanics*, ASCE, **139**(10), 1395-1406.

Zhou, Y., Kijewski, T. and Kareem, A. (2003), "Aerodynamic loads on tall buildings: interactive database," *Journal of Structural Engineering*, ASCE, **129**(3), 394-404.

Vita

Srinivasa Adithya Sailesh Abburu is a native of Andhra Pradesh, India. He received his B.S. degree from Acharya Nagarjuna University in 2013. His interest in the field of structural engineering made him enter the graduate program in the Department of Civil and Environmental Engineering, Louisiana State University. He will receive his M.S. degree in December 2015, and plans to work for a structural designing company upon graduation.